

**Human gene array analysis of THP-1 macrophages exposed to lipoprotein hydrolysis
products generated by lipoprotein lipase**

by

©Narmadaa Thyagarajan

A dissertation submitted to the

School of Graduate Studies

in partial fulfillment of the requirements for the degree of

Masters of Science in Biochemistry

Department of Biochemistry

Memorial University of Newfoundland

May 2017

St. John's

Newfoundland and Labrador

Abstract

Macrophage lipoprotein lipase (LPL) contributes to atherogenesis. However, the complete effect of LPL hydrolysis products and its free fatty acid (FFA) component on modifying genes associated with macrophage-derived foam cell formation are not fully understood. I hypothesized that the FFA liberated from lipoproteins by LPL affects the gene expression in macrophages to potentially promote atherogenesis. Human microarray analyses on the RNA isolated from THP-1 macrophages treated with lipoprotein hydrolysis products generated by LPL revealed that selected genes associated with ribosome biogenesis, cell cycling, stress response, type I interferon signaling, and lipid accumulation were affected (at false discovery rate ≤ 0.03 , $n=3$). Testing the effects of either the total FFA component of the hydrolysis products, or individual classes of the FFA component, revealed mixed effects on the gene expression profiles. Overall, LPL hydrolysis products appear to affect gene expression profiles that favor foam cell formation, but it is likely that components other than the FFA differentially affect macrophage gene expression.

Acknowledgements

First and foremost, I wish to thank my supervisor Dr. Robert J. Brown for his valuable guidance and constant support. The office doors of Dr. Sherri L. Christian, one of my committee members, were always open to help me with microarray data analysis and troubleshoot problems in my experiment. I also wish to thank Dr. Phil Davis, a committee member, for providing constructive feedback with my project. Without all your support, my project would have been a nightmare.

Next, I wish to thank all my present and past lab members: Alexander Brannan, Jenika Marshall, Arthur Travis Pickett, Clemens Schumacher, Yanbo Yang, Breanne Coady, Emily Courage, and Danielle Gardiner for their technical assistance in the lab and for their assistance with my thesis. Thank you all for providing a very friendly environment in Dr. Brown's lab.

I wish to thank all my family members and close friends for their love, support and motivation. Lastly, I wish to thank my close friend Ms. Harishni Arumugam for her moral support. Although, she has passed away, the kindness and support she provided will make her presence strongly felt in my heart forever.

Table of Contents

Abstract	ii
Acknowledgements	iii
Table of Contents	iv
List of Figures	viii
List of Tables	x
List of Abbreviations	xi
Chapter 1: Introduction	1
1.1 Atherosclerosis: A Chronic Arterial Disease	1
1.1.1 Cardiovascular disease	1
1.1.2 Overview of atherosclerosis	1
1.2 Overview of Lipoproteins and their Metabolism	6
1.3 The <i>sn</i> -1 lipases: Tissue Profile, Substrate Specificities, and Physiological Roles	12
1.4 Characteristics of LPL	15
1.4.1 LPL genetics and structure	15
1.4.2 Synthesis and secretion of LPL	16
1.4.3 Biological functions of LPL	19
1.4.4 The regulation of LPL expression and activity	20
1.4.4.1 Transcriptional control of LPL	20
1.4.4.2 Translational and post-translational regulation	22
1.5 Macrophage LPL in Atherosclerosis	23
1.6 LPL Hydrolysis Products: FFA Components and their	

Pro-atherogenic Effects	25
1.7 Objectives	27
1.8 Hypothesis	28
1.9 Summary	28
Chapter 2: Materials and Methods	30
2.1 Mammalian Cell Culture	30
2.1.1 HEK-293 cell culture and maintenance	30
2.1.2 THP-1 cell culture and differentiation	30
2.2 HEK-293 Transfection with Recombinant LPL Plasmid	32
2.2.1 Human LPL plasmid generation	32
2.2.2 HEK-293 cell transfection	33
2.3 Qualitative and Quantitative Analysis of LPL	34
2.3.1 Activity assay	34
2.3.2 Immunoblot analysis	34
2.4 Lipoprotein Isolation and Quantification	36
2.4.1 Total lipoprotein isolation	36
2.4.2 Phospholipid quantification in total lipoproteins	37
2.5 Lipoprotein Hydrolysis Product Generation, Quantification, and Incubation with THP-1 Macrophages	37
2.5.1 Lipoprotein hydrolysis by LPL	37
2.5.2 Lipoprotein hydrolysis product quantification	38
2.5.3 THP-1 macrophages treatment with lipoprotein hydrolysis product	38

2.5.3.1 Trypan blue exclusion assay	39
2.6. Incubation of FFA Mixture and Distinct FFA Classes with THP-1 Macrophages	40
2.7 RNA Isolation, Genomic DNA Removal and RNA Clean-up	41
2.8 Microarray and Quantitative PCR	42
2.8.1 Microarray analysis	42
2.8.2 Quantitative PCR analysis	44
2.8.2.1 cDNA synthesis	44
2.8.2.2 Quantitative PCR analysis	44
2.9 Statistical Analysis	47
Chapter 3: Results	48
3.1 Microarray Analyses of THP-1 Macrophages in Response to Lipoprotein Hydrolysis Products	48
3.2 Validation of Expression for Select Genes by Real-Time PCR	61
3.3 Select Gene Expression in Response to FFA	61
Chapter 4: Discussion	91
4.1 Modulation of snoRNA Expression by FFA Components within LPL Hydrolysis Products may Affect Ribosome Biogenesis in Human Macrophages	91
4.2 LPL Hydrolysis Products Alters Select Cell Cycling Gene in THP-1 Macrophages	93
4.3 The Role of LPL Hydrolysis Products and their FFA	

Components in Modulating Select Stress Response Gene in Human Macrophages	94
4.4 The Effects of LPL Hydrolysis Products and the FFA Components in Impairing Macrophage Immune Response	96
4.5 LPL Hydrolysis Products, but not their FFA Components, Induces Lipid Accumulation Genes in Human Macrophages	97
4.6 Study Limitations	101
4.7 Future Perspectives	102
4.8 Overall Conclusion	103
References	105
Appendix I: Supplementary methods	121
Appendix II: Supplementary tables	124

List of Figures

Figure 1: Schematic diagram of the processes leading to atherosclerosis	2
Figure 2: Schematic representation of lipoprotein metabolism	9
Figure 3: Schematic representation of LPL synthesis, processing and transportation	17
Figure 4: LPL protein expression and catalytic activity	49
Figure 5: Hydrolysis of total lipoproteins by heparinized media	51
Figure 6: The effect of LPL hydrolysis products on THP-1 macrophage cell viability	53
Figure 7: The effect of total lipoprotein hydrolysis products generated by LPL on THP-1 RNA integrity	56
Figure 8: Validation of expression of select genes within THP-1 macrophages incubated with total lipoprotein hydrolysis products generated by LPL	63
Figure 9: The influence of the FFA component of total hydrolysis products on <i>SNORA56</i> expression in THP-1 macrophages	69
Figure 10: The influence of the FFA component of total hydrolysis products on <i>DKCI-v3</i> expression in THP-1 macrophages	72
Figure 11: The influence of the FFA component of total hydrolysis products on <i>IFITM1</i> expression in THP-1 macrophages	75
Figure 12: The influence of the FFA component of total hydrolysis products on <i>CD36</i> expression in THP-1 macrophages	78
Figure 13: The influence of the FFA component of total hydrolysis products on <i>PCNA</i> expression in THP-1 macrophages	81
Figure 14: The influence of the FFA component of total hydrolysis products on	

<i>ATF3</i> expression in THP-1 macrophages	84
Figure 15: The influence of the FFA component of total hydrolysis products on	
<i>PLIN2</i> expression in THP-1 macrophages	87
Figure 16: Lipoprotein hydrolysis products generated by LPL modulates	
lipid-associated genes	99

List of Tables

Table 1: List of primer sequences for select genes	45
Table 2: SnoRNA molecules identified by microarray analyses with at least a four-fold increase of expression in THP-1 macrophages in response to total lipoprotein hydrolysis products liberated by LPL	58
Table 3 List of significantly over-represented GO Biological processes and the genes identified within these processes by microarray analyses	60
Table 4: Genes from microarray analyses that were selected for further study	62
Table S1: Product length and amplification efficiencies of select gene-primers	125
Table S2: List of up-regulated transcripts in LPL hydrolysis product treatment	126
Table S3: List of down-regulated transcripts in LPL hydrolysis product treatment	136
Table S4: Enrichment analysis on biological processes modulated by LPL hydrolysis products	143

List of Abbreviations

A/A	Antibiotic/antimycotic
ABCA1	Adenosine triphosphatebinding cassette transporter member 1
ABCG1	Adenosine triphosphate-binding cassette transporter member G
ATF3	Activating transcription factor 3
CAD	Coronary artery disease
CD36	Cluster of differentiation 36
CE	Cholesteryl ester
CETP	Cholesteryl ester transfer protein
CVD	Cardiovascular disease
DKC1-v3	Dyskerin 1, variant 3
DMEM	Dulbecco's Modified Eagle Medium
DMSO	Dimethyl sulfoxide
EDTA	Ethylenediaminetetraacetic acid
EL	Endothelial lipase
FAF-BSA	Fatty acid free-bovine serum albumin
FBS	Fetal bovine serum
FFA	Free fatty acid
GO	Gene ontology
GPIHBP1	Glycosylphosphatidylinositol anchored high-density lipoprotein binding protein 1
HAEC	Human aortic endothelial cells
HDL	High-density lipoprotein

HEK	Human embryonic kidney
HL	Hepatic lipase
HSPG	Heparan sulfate proteoglycan
IDL	Intermediate-density lipoprotein
IFITM1	Interferon inducible transmembrane protein 1
LCAT	Lecithin:cholesterol acyltransferase
LDL	Low-density lipoprotein
LDLR	Low-density lipoproteinreceptor
LPL	Lipoprotein lipase
LXR	Liver-X-receptor
miR	MicroRNA
MUFA	Monounsaturated fatty acid
NCL	Nucleolin
PBS	Phosphate-buffered saline
PCNA	Proliferating cell nuclear antigen
PL	Phospholipid
PLIN2	Perilipin 2
PLTP	Phospholipid transfer protein
PMA	Phorbol-12-myristate-13-acetate
PPAR	Peroxisome proliferator-activated receptor
PUFA	Polyunsaturated fatty acid
RCT	Reverse cholesterol transport
RIN	RNA integrity number

SD	Standard deviation
SDS	Sodium dodecyl sulfate
SMC	Smooth muscle cell
snoRNA	Small nucleolar RNA
Sp	Specificity protein
SR-BI	Scavenger receptor class B member 1
TG	Triglyceride
TNF- α	Tumor necrosis factor- α
UPR	Unfolded protein response
VLDL	Very low-density lipoprotein

Chapter 1: Introduction

1.1 Atherosclerosis: A Chronic Arterial Disease

1.1.1 Cardiovascular disease

Cardiovascular disease (CVD) is a group of disorders, including coronary artery disease (CAD), cerebrovascular disease, rheumatic heart disease, peripheral arterial disease, congenital heart disease, and pulmonary embolism, which all affect the heart and blood vessels. Compared to other diseases, CVD is estimated to contribute a large proportion to worldwide morbidity and mortality rates. In 2008, CVD was reported to cause 17.3 million deaths worldwide, with CAD alone contributing about 7.4 million deaths (1). The number of CVD deaths is expected to rise above 23.6 million by 2030 (2). Two major factors that have been implicated in the development of CVD are behavioral and metabolic risk factors. Behavioral risk factors include unhealthy diet and physical inactivity, whereas metabolic risk factors include increased blood lipids, blood sugar, and blood pressure (1).

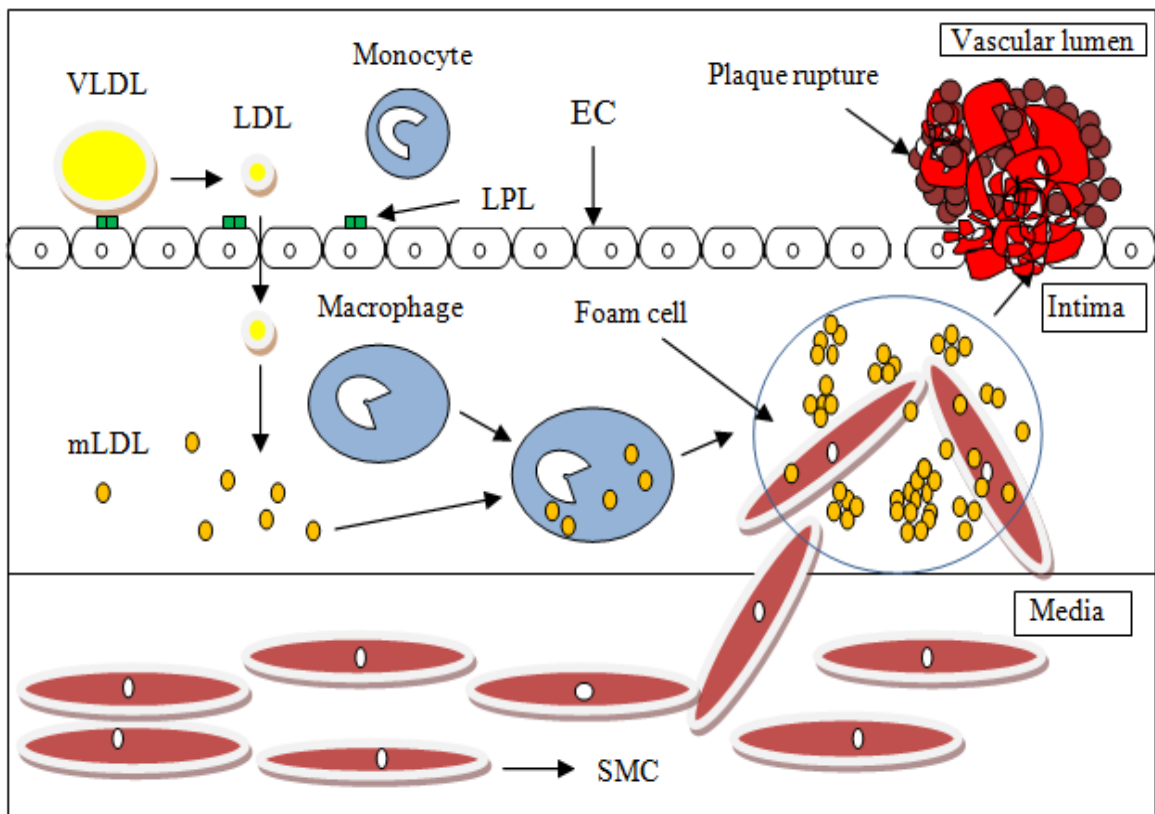
1.1.2 Overview of atherosclerosis

The underlying pathological process occurring in the arterial walls which results in CAD is termed atherosclerosis. Atherosclerosis is an arterial disease where, due to lipid accumulation, a plaque builds up within the arteries and restricts the oxygen-rich blood supply to the heart and other parts of the body (Figure 1). Progression of this disease occurs

Figure 1: Schematic diagram of the processes leading to atherosclerosis

A triglyceride (TG)-rich lipoprotein, such as plasma very low-density lipoprotein (VLDL), is hydrolysed by lipoprotein lipase (LPL) bound to endothelial cells (EC). The hydrolysed lipoproteins tend to lose their lipid moiety and become smaller in size, forming low-density lipoprotein (LDL). This cholesterol-enriched lipoprotein enters the sub-endothelial space where it undergoes modifications, such as oxidation, thus triggering monocyte chemotaxis. The monocyte-derived macrophages in the sub-endothelial space uptake modified LDL (mLDL), leading to macrophage-derived foam cells. The smooth muscle cells (SMC) migrate to intima where they too uptake mLDL forming foam cells. The accumulation of lipid provokes a complex inflammatory response which ultimately leads to plaque rupture.

Figure 1



through a sequence of key steps (3). Notably, three key stages are involved in atherosclerosis: formation of a fatty streak, fibrous lesions, and complex lesions (4). Initially, lipoprotein retention within the sub-endothelial space of the arterial wall triggers various biological responses. Accumulated lipoproteins can become oxidized, thus provoking inflammatory responses, such as monocyte chemotaxis, cytokine production, and T-lymphocyte recruitment (4,5). The monocytes recruited into the sub-endothelial space are differentiated into macrophages, a major immune cell type found in atherosclerotic tissue (4,5). The oxidized lipoproteins and, in particular, the low-density lipoproteins (LDL) in the sub-endothelial space are internalized by macrophages through scavenger receptors (6,7). However, Moore *et al.* (8) have shown that macrophage cells accumulated lipids and promoted atherosclerosis in the absence of scavenger receptors, suggesting that additional mechanisms are also involved in lipid uptake. Subsequent studies by Kruth *et al.* (9,10) have shown that macrophages also accumulate native LDL through a process called macropinocytosis. The internalized lipoproteins are further hydrolysed by lysosomal acid lipase, a lysosomal enzyme present in late endosomes, liberating lipids that can contribute to macrophage foam cell formation that plays an important role in the progression of atherosclerosis (11). The lipid loaded macrophages also trigger the migration of smooth muscle cells into the intima, that leads to the secretion of collagen and matrix proteases (12). In addition, smooth muscle cells also contribute to foam cell progression by their ability to accumulate lipids (12). These lipid laden cells collectively appear as a yellow streak in the arterial wall (4). No chronic symptoms are noticed at this stage (3). Over several years, a fibrous cap covers the smooth muscle cells

and lipid laden macrophage cells, which are susceptible to rupture at later stages (3). In addition, increased thickness of fibrous cap, calcification, microhemorrhage, thrombosis, and fissures were noticed at this complex stage (3-5). Moreover, aggregation of extracellular lipids in the intima results in the progression of atherosclerotic conditions, causing complex lesions. At this stage, an advanced inflammatory response is triggered, resulting in the apoptosis of foam cells, as well as necrosis, which can affect plaque stability. Plaque rupture usually occurs in lipid-rich macrophage-dense regions of the lesion. The apoptotic and necrotic foam cells release proteolytic enzymes that impair the fibrous cap, resulting in release of thrombotic molecules and increased vascular occlusion that further leads to stroke, myocardial infarction, and may even cause death (3-5). However, several fates are possible during all stages of atherosclerosis. For instance, a reduction in plasma cholesterol levels could possibly result in disease regression (13).

Major lipid types that are found in atherosclerotic lesions are cholesterol, cholesteryl esters (CE), and phospholipids (PL) (14). All of these lipids originate from circulating lipoproteins, notably from LDL and remnant lipoproteins (15,16). The retention of lipoproteins in the arterial wall is enhanced by lipolytic enzymes, particularly lipoprotein lipase (LPL) bound to the endothelial cell surface (15,17). The role of LPL in atherosclerosis has been studied for several decades. LPL expression in certain tissues, such as heart, skeletal muscle, and adipose tissue, has been shown to play an atheroprotective role by hydrolyzing triglyceride (TG)-rich lipoproteins and by increasing high-density lipoprotein (HDL) levels in the plasma (18-20). In contrast, several pieces of evidence support the notion that macrophage LPL could promote atherosclerosis (15,21-

24). In addition, Mamputu *et al.* (25) and Obunike *et al.* (26) have shown that LPL anchored to the endothelial cell surface induces monocyte adherence, thus promoting foam cell formation. The LPL bridging function has also been shown to enhance monocyte adhesion to bovine aortic endothelial cells, suggesting a possible pathophysiological role of LPL (25). Furthermore, the lipolytic products generated through lipoprotein hydrolysis by LPL, such as free fatty acids (FFA), can provoke several cytotoxic events involved in plaque formation (27).

1.2 Overview of Lipoproteins and their Metabolism

A lipoprotein is a complex particle that contains both lipid and protein. It plays a crucial role by transporting hydrophobic lipids within the aqueous environment of the circulation to peripheral tissues. Based on their density, lipoproteins are classified into five major classes: chylomicrons ($\rho < 0.94$ g/ml), very low-density lipoproteins (VLDL) ($\rho < 1.006$ g/ml), intermediate-density lipoproteins (IDL) ($\rho = 1.006-1.019$ g/ml), LDL ($\rho = 1.019-1.063$ g/ml), and HDL ($\rho = 1.063-1.21$ g/ml) (28). These complex particles contain TG and CE in their hydrophobic core, surrounded by a PL monolayer embedded with cholesterol and apolipoproteins. Although lipoprotein classes share the same elementary structural traits, each class has a distinct size range, as well as distinct proteins and lipids which further determine the function of each class (29,30).

An apolipoprotein is a protein that combines with lipid to produce lipoproteins. Their distribution plays a crucial role in determining the structure of lipoproteins. Most apolipoproteins have an amphipathic alpha helix structure, where the hydrophilic amino

acid residues are exposed to the aqueous circulation, and the hydrophobic amino acid residues interact with the lipoprotein lipids. Most of the apolipoproteins have the ability to solubilize neutral lipids in the circulation. In addition, some apolipoproteins also have flexible regions that help them to change their conformation according to the lipid composition in the lipoprotein and also according to different lipoprotein transformation forms in the circulation. Furthermore, some apolipoproteins play a key role in receptor recognition and in regulating key enzymes involved in lipoprotein metabolism (30).

Each major class of lipoproteins has an individual role in transporting lipids in the circulation. Exogenous TG obtained from the diet are packed with a truncated apolipoprotein, termed apoB48, cholesterol, CE, and PL to form chylomicrons in the enterocytes of the small intestine (31). Once a chylomicron is synthesized in the intestine, it is transported via the lymphatic system into the circulation, where LPL that is attached to the luminal surfaces of the capillary endothelium can hydrolyse the TG molecules of the chylomicron. On the other hand, endogenous TG synthesized in the liver is packed with apoB100, cholesterol, CE, and PL to synthesize VLDL (31). Similar to chylomicrons, VLDL that is synthesized in the liver also enters the circulation, where LPL anchored to the capillary endothelium hydrolyses molecules on VLDL, thereby liberating fatty acids for tissue utilization. After hydrolysis by LPL, both chylomicron and VLDL particles become smaller and denser in the circulation forming chylomicron remnants and IDL. Chylomicron remnants are removed from the circulation by the liver through a process that is mainly facilitated by the apolipoprotein apoE that is carried by the remnants (32). IDL synthesized in the circulation is mainly hydrolysed by hepatic lipase (HL) to form LDL or

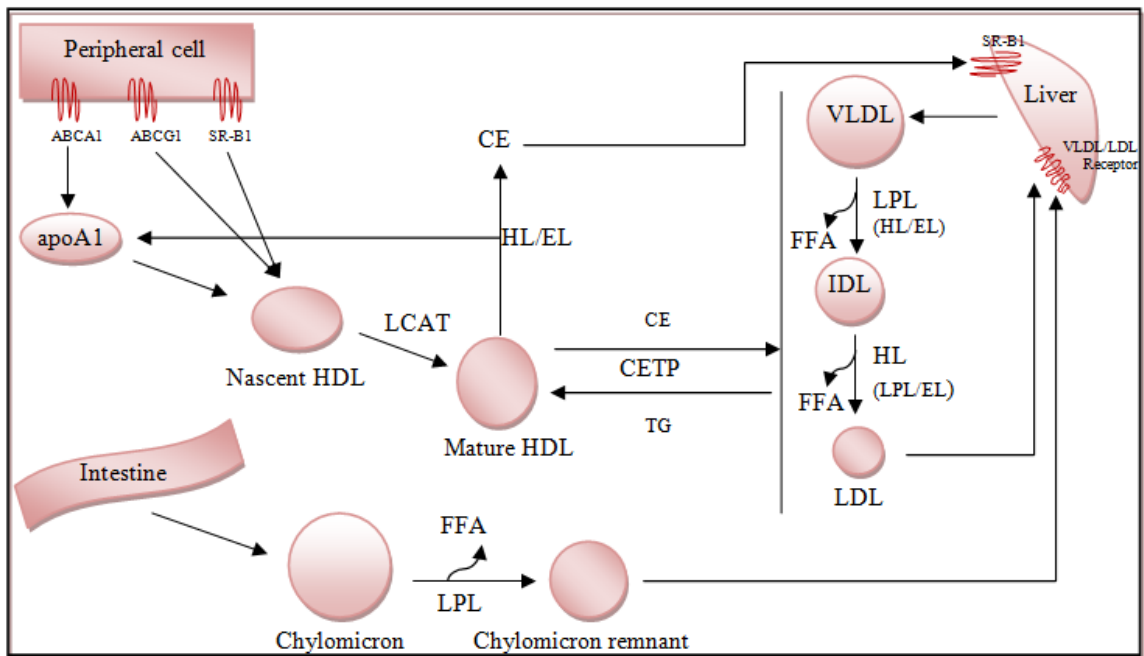
removed from the bloodstream by the liver via receptor-mediated endocytosis (33,34). The LDL particles are taken up by peripheral cells through the LDL receptor (LDLR) where the cholesterol components of the LDL are utilized for the synthesis of steroid hormones and maintenance of cellular membranes. In addition, the liver also removes some LDL particles from the circulation through receptor-mediated endocytosis to prevent excess LDL in the bloodstream. This process of transporting lipoprotein lipids to the peripheral tissue is termed forward lipid transport. Except HDL, all other lipoproteins are involved in this process (Figure 2) (35).

HDL is involved in reverse cholesterol transport (RCT), a process that involves the net movement of cholesterol from non-hepatic tissues to the liver. The mechanism involved in RCT was first postulated by Glomset in 1968 (36). The major apolipoprotein component present in HDL is apoA-I; it is initially synthesized and secreted with little association to lipid from the intestine and the liver. The apoA-I accepts cholesterol and PL extracellularly from the peripheral cells to form pre-beta HDL, which is a HDL precursor that is discoidal in shape (37,38). The cholesterol and PL are transported from peripheral cells by the adenosine triphosphate-binding cassette transporter, sub-family A, member 1 (ABCA1) (39). Aiello *et al.* (40) have shown that the deletion of ABCA1 in macrophages caused severe foam cell accumulation in apoE-null mice. However, the absence of ABCA1 did not affect plasma HDL levels. In addition to ABCA1, adenosine triphosphate-binding cassette transporter, sub-family G, member 1 (ABCG1) and scavenger receptor type-BI (SR-BI) are also involved in transporting cholesterol from peripheral cells to nascent HDL

Figure 2: Schematic representation of lipoprotein metabolism

The exogenous and endogenous triglyceride (TG) molecules are packed into chylomicrons and very low-density lipoproteins (VLDL) in the intestine and the liver. These TG-rich lipoproteins are transported into the circulation where they are preferentially hydrolysed by LPL to yield free fatty acids (FFA) for tissue utilization. Due to the hydrolysis of TG and phospholipid (PL), the chylomicron and VLDL become smaller and denser forming chylomicron remnants and intermediate density lipoprotein (IDL). Chylomicron remnants are cleared from the circulation by the liver where they are utilized for many biological processes, including VLDL synthesis. IDL formed in the circulation are further hydrolysed by hepatic lipase (HL) to liberate FFAs. Due to the loss of TG/PL molecules in IDL, they become smaller in size forming a cholesterol-enriched LDL in the circulation. The cholesterol particles in LDL are taken up by tissues for use in numerous processes. In addition, LDL is cleared from the circulation by the liver through receptor-mediated endocytosis. When excess cholesterol is present in the peripheral cells, apolipoprotein A-I (apoA-I) accepts cholesterol and PL from the cells through adenosine triphosphate-binding cassette transporter, sub-family A, member 1 (ABCA1), forming pre-beta high-density lipoprotein (HDL). In addition, two other lipid transporters namely, adenosine triphosphate-binding cassette transporter, sub-family G, member 1 (ABCG1) and scavenger receptor type-BI (SR-BI), also transport cell cholesterol and PL to pre-beta HDL. The free cholesterol in the nascent HDL is esterified by lecithin:cholesterol acyltransferase (LCAT), forming mature HDL. The cholesteryl ester (CE) of HDL is removed from the bloodstream in two ways: 1) HDL exchanges its CE for TG that is present in VLDL, IDL and LDL with the help of CE transfer protein (CETP), which is ultimately removed from the circulation by VLDL/LDL receptors in the liver; and 2) mature HDL is hydrolysed by HL and endothelial lipase (EL) that are anchored to cell surfaces, thereby liberating apoA-I and CE. The liver also uptakes HDL CE via SR-BI; lipid-poor apoA-I that is generated in this process can be reused for reverse cholesterol transport.

Figure 2



(41,42). These cholesterol transporter expression levels are shown to be regulated by different nuclear receptors. For instance, peroxisome proliferator-activated receptor (PPAR)- γ combined with liver X receptor (LXR)- α have been shown to regulate ABCA1 expression in THP-1 macrophages and inactivating the PPAR- γ gene in macrophages increased atherosclerosis in LDLR-null mice (43).

The cholesterol acquired by pre-beta HDL is initially in an unesterified form. Lecithin:cholesterol acyltransferase (LCAT) binds to the apoA-I component of pre-beta HDL and transfers one acyl group from lecithin (or phosphatidylcholine) to unesterified cholesterol in order to produce CE and lysolecithin (or lysophosphatidylcholine) (36). This catalyzed reaction is vital for accepting more free cholesterol from peripheral cells (36). Newly formed CE moves to the hydrophobic core of the nascent HDL and eventually makes mature HDL. Although LCAT is crucial for mature HDL formation and the increase in plasma HDL levels, an overexpression of LCAT in mice fed a cholesterol-rich diet did not reduce atherosclerosis (44,45). In addition to LCAT, PL transfer protein (PLTP) also plays an important role in mature HDL formation by transferring phospholipids from apoB100-containing lipoproteins to HDL (46). A study showed that C57BL/6 mice overexpressing human PLTP had increased pre-beta HDL formation and decreased plasma HDL cholesterol levels compared to wild-type mice, suggesting potential anti-atherogenic effects of PLTP (47).

The mature HDL removes extrahepatic CE in two different ways. Some of the CE in HDL is transferred to apoB-containing lipoproteins in exchange for TG molecules with

the help of CE transfer protein (CETP). The liver clears CE molecules in apoB-containing lipoproteins through receptor-mediated endocytosis. Although CETP-mediated CE transfer is also a part of RCT, a deficiency of this protein in humans leads to increased HDL levels and reduced catabolism of apoA-I (48). TG-enriched HDL formed by CETP undergoes hydrolysis by HL that is bound to the sinusoidal capillaries of the liver surface and endothelial lipase (EL) that is bound to the vascular endothelium (49,50). The remodeling of HDL by HL and EL liberates HDL remnant particles and lipid-poor apoA-I (49). The HDL remnant particles are internalized and degraded by putative receptors in the liver (37,51). Also, SR-BI expressed on the liver binds to apoA-I of the mature HDL and promotes selective uptake of CE, which can be further processed by the liver into bile for excretion (52). The lipid-poor apoA-I liberated from HDL initiates RCT again by accepting free cholesterol from peripheral cells (37).

1.3 The *sn*-1 Lipases: Tissue Profiles, Substrate Specificities, and Physiological Roles

The key enzymes that constitute the *sn*-1 lipase family are LPL, HL, and EL. These enzymes release fatty acids by hydrolyzing the ester bonds at the *sn*-1 position of the TG and PL components of circulating lipoproteins (53). The *sn*-1 lipases are heparan sulfate proteoglycan-binding enzymes that are usually bound to the endothelial cell surface (53). In addition, these enzymes also possess a bridging function that is independent of their catalytic function (54-56). The bridging function of *sn*-1 lipases allows them to bring plasma lipoproteins very close to cell surface receptors to promote lipoprotein uptake into cells (57). All three enzymes have a common ancestral origin, as they share similar

sequences at both the DNA and protein levels (57). However, *sn*-1 lipases have different substrate specificities and tissue expression profiles, suggesting that the different lipases emerged for unique physiological functions (53).

The *sn*-1 lipases exhibit distinct tissue expression profiles. LPL expression in many species, including humans, has been observed in adipose tissue, mammary glands, spleen, heart, skeletal muscles, and lungs (58-62). HL expression has been previously reported in ovaries, adrenal tissues, and hepatocytes of rat and humans (63-65). EL expression has been reported in the placenta, thyroid, lungs, kidneys, hepatocytes, and macrophages of mice and humans (66). EL is initially synthesized in arterial/venal endothelial cells and is anchored to the luminal surface of the capillary endothelium, exposing itself to the bloodstream to perform its biological function (49,66).

With respect to substrate specificity, LPL predominantly hydrolyses TG and EL preferentially hydrolyses PL in circulating lipoproteins (67). HL shows equal preferences for both TG and PL in lipoproteins (67). LPL principally hydrolyses TG molecules in chylomicrons and VLDL, and reduced LPL activity was reported to induce severe hypertriglyceridemia and cause death in LPL-null mice (68). Also, low levels of LPL have a negative impact on HDL levels (68,69). EL is involved in preferentially hydrolyzing PL from HDL, and this is inversely associated with HDL levels (70,71). Recently, Miksztowicz *et al.* (72) have shown that EL is accountable for low levels of HDL in chronic kidney disease patients. HL is primarily involved in hydrolyzing TG and PL from all

lipoproteins (73,74). HL activity has been shown to positively correlate with small dense LDL levels and negatively correlate with HDL levels (75,76).

Several lines of evidence suggest that *sn*-1 lipases may play a vital role in atherosclerosis. Tissue-specific expression of LPL determines its crucial role in atherosclerosis. For instance, LPL expression in adipose tissue and muscle contribute to apoB-containing lipoprotein clearance, therefore suggesting that LPL has anti-atherogenic properties (18,20). In contrast, compelling evidence from *in vitro* and *in vivo* studies have shown that macrophage LPL exhibits pro-atherogenic properties (15,21-24,77).

Similar to LPL, anti-atherogenic and pro-atherogenic actions of HL could depend on where it is expressed. Hepatic HL increases TG-rich lipoprotein clearance from the bloodstream, suggesting HL could possess anti-atherogenic properties (78,79). However, studies on murine models had shown contradictory results with respect to the role of HL in atherosclerosis (80,81).

A clinical study by Badellino *et al.* (82) reported that EL activity positively correlates with coronary artery calcification. Also, immunohistochemical analysis and double label immunofluorescence confirmed that EL is expressed within human atheromatous plaques (83). These studies suggest that EL might have a unique role in atherosclerosis. However, a study on the loss-of-function and gain-of-function of EL on THP-1 macrophages showed that EL overexpression promoted apoA-I-mediated cholesterol efflux and EL suppression reduced apoA-I-mediated cholesterol efflux (84).

The role of HL and EL in atherosclerosis is not clearly known and requires further clarification.

1.4 Characteristics of LPL

1.4.1 LPL genetics and structure

The human LPL gene is found on chromosome 8p22, spanning about 30,000 base pairs in length with 10 exonic regions and encodes for mature LPL that contains 448 amino acids (85). A putative three-dimensional model of LPL that was proposed based upon crystal structure of pancreatic lipase showed that LPL contains a larger N-terminal domain and a smaller C-terminal domain that are structurally distinct and connected by a flexible linker region (86-88). Studies have shown that the N-terminal domain of human LPL contains a binding site for heparan sulfate at residues 279-282 and 292-304, a highly conserved catalytic triad (Ser¹³², Asp¹⁵⁶, and His²⁴¹), an apoC-II interaction site at Lys¹⁴⁷/Lys¹⁴⁸, and a polypeptide 'lid domain' at residues 216-239 that covers the catalytic cleft and is essential for lipolysis (89-91). In addition, it also contains a β 5 loop that is required for binding lipid substrates (89). The C-terminal domain is necessary for binding lipoprotein substrates (89). Wong *et al.* (92) previously showed that LPL monomers are organized in a head-to-tail orientation to form active homodimers. However, dissociation of native homodimers to monomers has been shown to permanently inactivate LPL catalytic function (93).

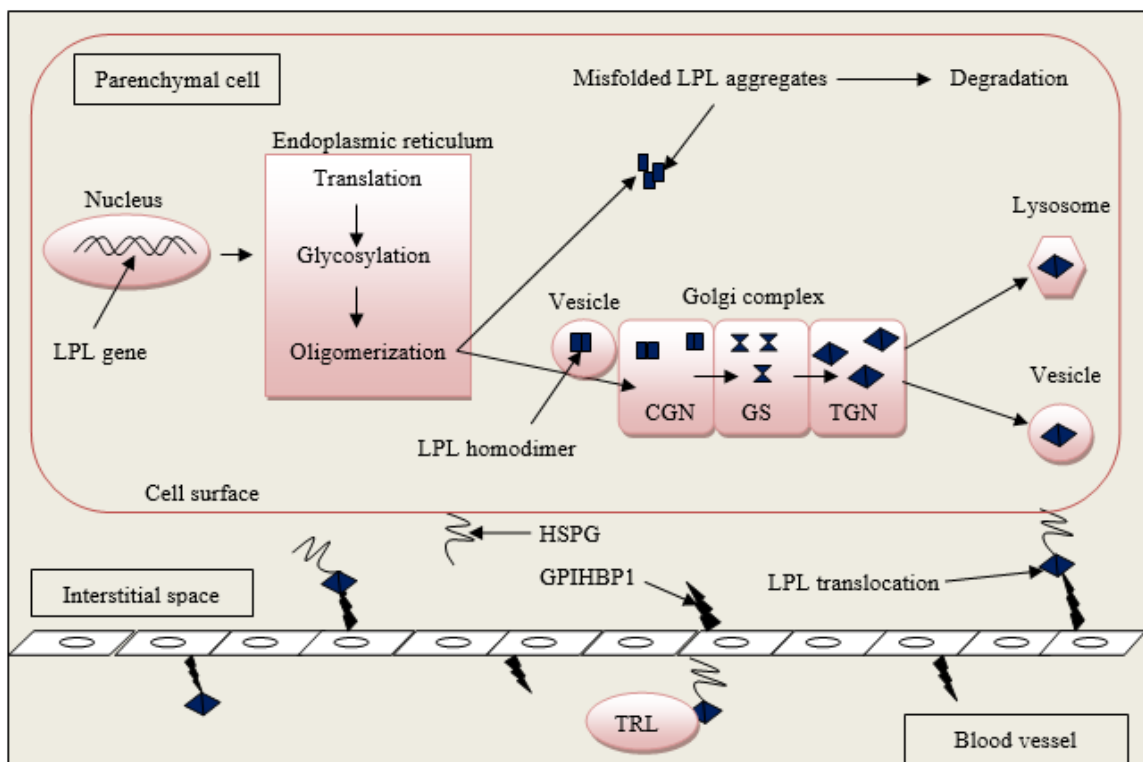
1.4.2 Synthesis and secretion of LPL

The nascent polypeptide chain translated from the LPL mRNA is not catalytically active until it undergoes a sequence of post-translational modifications. Studies have shown that mature LPL can occur as various glycoforms (94-96). The newly synthesized polypeptide chain is subjected to *N*-glycosylation and two important oligosaccharide processing events: 1) trimming of glucose residues by glucosidases; and 2) trimming of high mannose chain by mannosidases, in the endoplasmic reticulum (ER). Ben-Zeev *et al.* (97) have shown that inhibition of glucose trimming in mutant Chinese hamster ovary cells decreased LPL activity and secretion; however, blocking mannose trimming did not affect LPL activity or secretion. Therefore, their results suggest that the trimming of the terminal glucose residues in the *N*-linked oligosaccharide moiety of LPL by glucosidases is responsible for acquisition of LPL catalytic activity. The glycosylated LPL protein becomes an active homodimer in the presence of lipase maturation factor 1, a chaperone that is involved in properly folding and assembling lipases in the ER (98). Overexpression of lipase maturation factor 1 has been shown to increase the LPL activity in adipose and muscle tissues (99). Next, the active LPL is transported from the ER to different compartments of the Golgi complex where it is fully processed. The mature LPL is transported either to lysosomes or heparan sulfate proteoglycans (HSPG) on the cell surface (Figure 3).

Figure 3: Schematic representation of LPL synthesis, processing and transportation

The LPL gene is transcribed in the nucleus of the parenchymal cell. The transcribed LPL undergoes translation and translational modifications, such as *N*-linked glycosylation and oligomerization in the endoplasmic reticulum. Properly folded and assembled active LPL homodimers (■) are transported to the Golgi complex through vesicles. In contrast, inactive and misfolded LPL aggregates are subjected to degradation (100). Inside the Golgi network, the active LPL is received by the *cis*-Golgi network (CGN) which then transports the active LPL to the Golgi stack (GS) where the enzyme is further processed (✕). The active LPL is transported to the *trans*-Golgi network (TGN) where they undergo further processing. The mature LPL (◆) from TGN is either transported to heparan sulfate proteoglycans (HSPG) on the cell surface through vesicles or transported to lysosomes for degradation. LPL anchored to HSPG on the cell surface is further translocated to the luminal surface of capillary endothelium by glycosylphosphatidylinositol anchored high density lipoprotein binding protein 1 (GPIHBP1). LPL on the capillary endothelium hydrolyses triglyceride-rich lipoproteins (TRL).

Figure 3



The active LPL bound to HSPG on the parenchymal cell surface is further translocated through the interstitial space to the luminal surface of the vascular endothelium. However, the mechanism involved in translocating LPL onto the HSPG bound to the luminal surface of the capillary endothelium is not very clear. Glycosylphosphatidylinositol anchored high density lipoprotein binding protein 1 (GPIHBP1), a GPI-anchored protein, has been shown to transport LPL onto the luminal surface of capillary endothelial cells using a GPIHBP1-null mouse model (101). This study clearly showed that the absence of GPIHBP1 protein results in impaired LPL lipolytic activity.

1.4.3 Biological functions of LPL

LPL, previously known as ‘clearing factor’, is an extracellular lipase enzyme that plays a crucial role in lipid metabolism (102). Due to their larger size, chylomicrons and VLDL cannot directly pass through the capillary endothelium in different tissues. Thus, LPL is bound to negatively charged HSPG on the luminal side of capillary endothelial cells and acts to hydrolyse these TG-rich lipoproteins. However, homodimeric LPL has to be initially activated by a cofactor before it can perform its catalytic function. The apoC-II component of chylomicrons and VLDL acts as a specific LPL cofactor that is required for the activation of LPL on the cell surface (103). The active LPL then hydrolyses lipid components of lipoproteins to produce non-esterified fatty acids, which are utilized by tissues for various biological processes.

Eisenberg *et al.* (104) had suggested that lipoprotein lipid hydrolysis by LPL could occur through a series of attachment and detachment events. Moreover, experiments

conducted by Saxena *et al.* (105) and Vilella *et al.* (106) reported that LPL could detach itself from the capillary endothelium cell surface and attach with remnant lipoproteins in the circulation. The displaced LPL is replaced by newly synthesized LPL on the cell surface.

Like other *sn*-1 lipases, LPL also possesses a non-catalytic bridging function independent of its catalytic function. Eisenberg *et al.* (56) reported that LPL binds simultaneously to both lipoproteins and HSPG on the cell surface. In addition, several studies have shown that LPL interacts with members of the LDLR gene family, such as LDLR, the VLDL receptor, the LDLR-related protein 1 and glycoprotein 330 (107). This LPL-receptor interaction allows the cell to uptake lipoproteins effectively.

1.4.4 The regulation of LPL expression and activity

1.4.4.1 Transcriptional control of LPL

Numerous *cis*-acting elements are present in the 5' regulatory region of the LPL gene and these are vital for the regulation of LPL promoter activity. For instance, Yang *et al.* (108) have shown that 5'-CCTCCCCC-3', a conserved sequence motif in the LPL regulatory region, can bind with transcription factors such as specificity protein (Sp) 1 and Sp3, and positively regulate basal promoter activity. Also, Sp1 interacts with sterol regulatory element binding protein-1 to synergistically activate the LPL promoter. In contrast, the same study also showed that a T to G substitution within the LPL regulatory region can suppress the promoter activity (108).

PPAR- α , - δ , and - γ have also been shown to regulate LPL gene expression in a tissue-specific manner by interacting with the PPAR response element site in the LPL promoter. PPAR- α was shown to regulate LPL gene expression in the rat liver, while PPAR- γ was shown to increase the LPL mRNA expression in rat adipose tissue (109). In addition, Blanchard *et al.* (110) reported that PPAR- γ activation induces LPL gene expression in rat adipose tissue through the mammalian target of rapamycin signaling pathways. In contrast, PPAR- δ is a VLDL sensor that increases LPL gene expression and lipid accumulation in murine macrophage cells (111). Numerous chemical compounds, including fatty acids, are reported to activate PPARs and LPL gene transcription (112,113).

With respect to other nuclear receptors, LXR was shown to predominantly induce LPL expression in macrophage cells and the liver of mice fed with high cholesterol diet, but it did not regulate LPL gene expression in adipose tissue or muscle (114). Moreover, cytokines are also involved in regulating LPL transcription. Tengku *et al.* (115) have shown that interferon γ and tumor necrosis factor (TNF)- α synergistically eliminate the LPL mRNA expression in murine macrophage cells. In addition, Morin *et al.* (116) reported that TNF- α inhibits LPL activity in adipocytes by eliminating the binding affinity of organic cation transporter-1 and nuclear factor-Y proteins in the CCAAT site of the LPL promoter. Also, Irvine *et al.* (117) reported that transforming growth factor (TGF)- β negatively regulates the expression of the LPL gene at the transcriptional level.

1.4.4.2 Translational and post-translational regulation

LPL activity is regulated by various factors, including hormones, fatty acids and microRNAs (miR). Several studies have reported a correlation between decreased LPL activity and diabetes. For instance, Kraemer *et al.* (118) showed that LPL activity in rat adipose tissue is controlled by insulin through phosphatidylinositol 3-kinase and ribosomal protein S6 kinase signaling pathways. A subsequent study by Ranganathan *et al.* (119) reported that LPL translation is inhibited in the adipocytes of diabetic rats due to an interaction between a cytoplasmic factor, likely RNA-binding protein, and specific nucleotide sequences of the 3'- untranslated region of LPL. Other hormones, including thyroid hormone and epinephrine, have been shown to regulate LPL activity in rat adipose tissue (120,121). As well, an accumulation of FFA (in particular, unsaturated fatty acids) at the endothelial cell surface was shown to cause LPL dissociation *in vitro*, thereby suggesting the impact of fatty acids in regulating LPL activity (105,122). Recent studies also established the role of miRNAs in regulating LPL activity. For example, inhibiting miR-467b expression in mouse hepatocytes increased LPL mRNA and protein levels, suggesting that miR-467b post-transcriptionally regulates LPL expression (123). Also, Tian *et al.* (124) reported that apoE-null mice injected with a synthetic miR-467b molecule showed inhibition of both LPL mRNA and protein levels in the aorta. In addition, LPL activity is also regulated by several interactive proteins, including angiopoietin-like proteins. For example, Bergo *et al.* (125) and Sukonina *et al.* (126) have previously shown that angiopoietin-like protein 4 inhibits LPL by turning active homodimers into inactive monomers in murine adipose tissue during the fasting state.

1.5 Macrophage LPL in Atherosclerosis

The evidence for a pro-atherogenic role of macrophage LPL was strongly reinforced by rodent studies. Zilversmit *et al.* (15) first reported that aortic LPL activity increases in correlation with cholesterol accumulation and CE influx into the aorta of cholesterol-fed rabbits, suggesting that LPL in the arterial wall may contribute to atherosclerosis. Subsequently, several rodent studies provided strong evidence for a pro-atherogenic role of macrophage LPL. For instance, peritoneal macrophages isolated from inbred murine strains that were susceptible or resistant to atherosclerosis showed that susceptible murine strains have higher LPL expression in comparison to resistant strains (127). Upon being fed a cholesterol-rich diet for three months, C57BL/6 mice transplanted with LPL-null mouse bone marrow showed a reduction in serum cholesterol levels, apoE levels, and aortic lesion area compared to wild-type mice, which suggested that a blockade of macrophage LPL minimizes lesion development in mice (128). Supporting this work, Babaev *et al.* (22) transplanted C57BL/6 mice with either LPL^{-/-} or LPL^{+/+} fetal liver cells, a source of hematopoietic cells, to study the role of macrophage LPL in foam cell formation. Their study reported that recipients of LPL^{-/-} cells fed an atherogenic diet had a 55% decreased mean aortic lesion area compared to mice that received LPL^{+/+} fetal liver cells. In addition, subsequent studies on LDLR-null mice transplanted either with LPL^{-/-} or LPL^{+/+} macrophages also showed that mice that received LPL^{-/-} cells had a 69% reduced *en face* aortic lesion area compared to LPL^{+/+} recipients (21). The transgenic overexpression of LPL in mice also led to increased atherosclerosis: Wilson *et al.* (23) reported that male apoE-null mice expressing macrophage-specific human LPL and fed a Western diet for

eight weeks displayed increased occlusion in the aortic sinus region compared to control mice. Wu *et al.* (129) also showed that the adenoviral expression either catalytically active human LPL or inactive LPL in balloon-injured rabbit carotid arteries enhanced lipid accumulation in arteries, suggesting that even catalytically inactive LPL enhances atherosclerosis lesion formation, likely through its binding ability. In addition to lipid deposition, adenoviral gene transfer of both active and inactive human LPL in endothelial intact-carotid arteries of apoE-null mice enhanced vascular cell adhesion molecule-1 expression (130). Recently, Takahashi *et al.* (131) reported that peritoneal macrophages isolated from macrophage-specific LPL knockout (generated using Cre-loxP gene targeting) and apoE double knockout mice had less accumulation of CE and TG compared to control mice. In addition, the authors also observed low levels of cluster of differentiation 36 (CD36) and carnitine palmitoyltransferase-1 gene expression in double knockout mice macrophages incubated with VLDL in comparison to macrophages from apoE-null mice (131). Together, these *in vivo* studies suggest that arterial wall LPL, likely derived from macrophages, have a pro-atherogenic effect.

In vitro studies also support the notion that LPL expression in macrophages causes foam cell formation. A previous study showed that LPL hydrolyses VLDL (isolated from normolipidemic donors) in a saturable manner and causes accumulation of TG and CE in J774 macrophages (132). LPL has been previously shown to increase the uptake and degradation of LDL in THP-1 macrophages, independent of the LDLR (133). In addition, LPL has been shown to preferentially uptake mildly oxidized LDL and VLDL compared to heavily oxidized lipoproteins in THP-1 macrophages via an unknown mechanism (134).

Recently, Kawashima *et al.* (24) showed that the downregulation of LPL expression in THP-1 macrophages increased ABCA1 gene expression and ABCA1-dependent cholesterol efflux, suggesting an inverse relationship between macrophage LPL and ABCA1 cholesterol transporter expression levels. In support of this, Yang *et al.* (77) showed that hydrolysis products that are generated by LPL downregulate the expression of ABCA1 and cholesterol efflux from THP-1 macrophages. Together, these studies suggest LPL induces lipid accumulation in macrophages and may have a pro-atherogenic effect.

1.6 LPL Hydrolysis Products: FFA Components and their Pro-atherogenic Effects

The LPL-mediated hydrolysis of lipoprotein lipids in macrophages and smooth muscle cells was shown to liberate FFA, which may contribute to atherogenesis. For example, mice overexpressing human LPL in aortic smooth muscle cells were shown to induce FFA generation by 69% compared to their control mice and the FFA liberated by LPL also triggered vascular dysfunction by activating nicotinamide adenine dinucleotide phosphate-oxidase in a protein kinase C-dependent manner (135). Thus, this finding suggests that LPL hydrolysis products, independent of LPL, may also play a role in atherosclerosis. Interestingly, an *in vivo* study also showed that lipoprotein-derived fatty acids are taken up by two different pathways in the heart by using three mice models: CD36-null mice, heart-specific LPL knockout mice, and CD36-null mice without heart LPL (119). Their results showed that VLDL-derived fatty acids are taken up via a CD36-mediated pathway and chylomicron-derived fatty acids are taken up via non-CD36 pathways (136).

In vitro studies had reinforced the notion that the hydrolysis products liberated from lipoprotein lipids by LPL, and in particular the FFA, may potentially trigger foam cell formation. Previously, it was reported that the FFA components within LPL hydrolysis products increase the phosphorylation of Akt in THP-1 macrophages and induces lipid accumulation partly by modulating the phosphatidylinositide 3 kinase signaling pathway (137,138). In addition, Yang *et al.* (77) have previously shown that the FFA components within LPL hydrolysis products impair apoA-I mediated cholesterol efflux by modulating the gene expression levels of nuclear receptors and cholesterol transporters in THP-1 macrophages. Using Raman spectroscopy, Hartigh *et al.* (139) showed that TG-rich lipoprotein hydrolysis by LPL enhances lipid droplet formation in THP-1 monocytes. In particular, the hydrolysis of postprandial VLDL by LPL led to more intense spectroscopic signals for lipid droplets in macrophages compared to hydrolysis products from preprandial VLDL that were generated by LPL. The authors also showed that saturated fatty acids (SFA) within the hydrolysis products induced a greater accumulation of lipid droplets in THP-1 monocytes compared to monounsaturated fatty acids (MUFA) and polyunsaturated fatty acids (PUFA) (139). Taken together, these observations also suggest FFA species liberated by LPL could be potentially pro-atherogenic.

In addition to lipid accumulation, previous studies have also shown that LPL hydrolysis products, and especially the FFA species, may act as an inflammatory mediator, thereby affecting cellular homeostasis. Eiselein *et al.* (140) reported that lipolytic products generated from TG-rich lipoproteins by LPL increased endothelial layer permeability in human aortic endothelial cells (HAEC) by rearranging the actin cytoskeleton organization,

by affecting junction protein localization and by stimulating caspase-3 activity. In their subsequent study, the authors also showed that LPL hydrolysis products enhances a stress response protein, activating transcription factor (ATF) 3, through the transforming growth factor- β 1 signaling pathway in HAEC and, thus, suggesting that the hydrolysis products liberated by LPL enhances pro-inflammatory responses that may contribute to atherogenesis (141). Wang *et al.* (142,143) showed that LPL hydrolysis products generated from TG-rich lipoproteins enhance reactive oxygen species production in HAEC. Furthermore, the authors showed that the FFA components from LPL hydrolysis products stimulated TNF- α and the intracellular adhesion molecule expression level in HAEC (143). Taken together, these studies suggest that LPL hydrolysis products, particularly the FFA, may exert a critical role in atherogenesis. Although some studies have shown that the hydrolysis products liberated by LPL may play a pro-atherogenic role, a recent *in vivo* study reported that loss of fatty acid liberation from lipoprotein lipids by LPL enhances glucose oxidation and impairs cardiac function in the hearts of mice with a deletion of cardiac LPL (144). Thus, more studies are necessary to understand the role of LPL hydrolysis products in atherogenesis. Nonetheless, the effects of LPL hydrolysis products on differentially regulating macrophage gene expression are not yet established.

1.7 Objectives

The FFA liberated from total lipoprotein hydrolysis by LPL may act as bioactive lipids to differentially regulate the transcript profile of macrophages. Thus, the main objectives of my thesis are: 1) to identify differentially regulated genes in macrophages

treated with hydrolysis products generated from total lipoproteins by LPL using a human gene array; and 2) to study the effects of purified FFA or individual FFA classes on modulating the expression of select genes (based on microarray data) that may play a role in foam cell formation. I expect that the hydrolysis products (in particular, the FFA component) liberated from lipoproteins by LPL will increase the expression levels of genes associated with stress response, immune response, and lipid droplet formation.

1.8 Hypothesis

I hypothesize that the total lipoproteins hydrolysed by LPL will affect the gene expression in macrophages in a way that could potentially promote foam cell formation. I also hypothesize that the FFA components of LPL hydrolysis products will be responsible for modulation of select gene expression in macrophages to favor foam cell formation.

1.9 Significance

LPL expression in macrophages promotes atherosclerosis. Previous studies from our laboratory have shown that the FFA components of LPL hydrolysis products detrimentally affect the gene expression profile that is associated with macrophage cholesterol efflux (77). However, the complete effects of LPL hydrolysis products and its FFA components on macrophage gene expression and atherosclerosis are not fully understood. This study will provide new insights into the role of LPL hydrolysis products in altering macrophage transcript levels, and how these differentially regulated genes may contribute to foam cell formation. Understanding the impact of the FFA components of

LPL hydrolysis products on atherosclerosis will potentially highlight macrophage LPL as a therapeutic target in the future.

Chapter 2: Materials and Methods

2.1 Mammalian Cell Culture

2.1.1 HEK-293 cell culture and maintenance

Human embryonic kidney (HEK)-293 cells (American Type Culture Collection, Manassas, VA, USA) were cultured in T75 flasks (BD Biosciences, Mississauga, ON, Canada) with Dulbecco's Modified Eagle Medium (DMEM) containing 4 mM L-glutamine, 4.5 g/L glucose and 110 mg/L sodium pyruvate (#SH30243.01, HyClone, South Logan, UT, USA) and further supplemented with 10% v/v fetal bovine serum (FBS) (#SH30396.03, HyClone) and 1% v/v antibiotic/antimycotic (A/A) (HyClone). HEK-293 cells were maintained at 37°C with 5% CO_{2(g)}. At 80-90% confluency, the cells were washed with 5 mL of DMEM media without both FBS and A/A. After washing, the cells were trypsinized with 2.5 mL of 0.25% (w/v) trypsin-ethylenediaminetetraacetic acid (EDTA) (#25200-056, HyClone) and incubated for 2 minutes at 37°C for the cells to detach from the surface. After incubation, 10 mL of DMEM media supplemented with 10% v/v FBS and 1% v/v A/A was added to the cells and mixed thoroughly. Lastly, 1 mL of cells were added to a new flask containing 14 mL of DMEM media supplemented with 10% FBS and 1% A/A and incubated at 37°C with 5% CO_{2(g)}.

2.1.2 THP-1 cell culture and differentiation

THP-1 monocytic cells (American Type Culture Collection) were cultured in Roswell Park Memorial Institute (RPMI)-1640 media containing 25 mM HEPES and 0.3 mg/L L-glutamine (#SH30255.01, HyClone) which was further supplemented with 10%

FBS and 1% A/A (HyClone), and incubated at 37°C with 5% CO_{2(g)}. After 4 days of incubation, 3 mL of THP-1 cells (8×10^5 cells/mL) were added to a new T75 culture flask containing 12 mL of RPMI-1640 media with 10% v/v FBS and 1% v/v A/A, and maintained at 37°C with 5% CO_{2(g)}.

THP-1 cells were differentiated into macrophages when their concentration reached 8×10^5 cells/mL. The cells were added to 15 mL centrifuge tubes and spun down at 750 rpm for 5 minutes. The supernatant was discarded and 10 mL of RPMI-1640 with 10 % v/v FBS and 1% v/v A/A was added to the pellets and mixed thoroughly. The cells were counted with a hemocytometer and 2.5 mL of 7.72×10^5 cells/mL were added to a 6-well plate with 100 nM of phorbol 12-myristate-13-acetate (PMA) (Sigma, St. Louis, MO, USA). After 48 hours of incubation, the cells were washed three times with RPMI-1640 media without both FBS and A/A, and then incubated with RPMI-1640 media containing 0.2% w/v fatty acid free-bovine serum albumin (FAF-BSA) (Sigma), 1% v/v A/A, 100 nM PMA. After 24 hours of incubation, the cells were washed once with RPMI-1640 media and incubated for 1 hour by supplementing RPMI-1640 media with 0.2 % w/v FAF-BSA, 1% v/v A/A, 100 nM PMA and 25 µg/mL tetrahydrolypstatin (THL) (Sigma) – to inhibit endogenous lipase activity (145). After 1 hour, the THP-1 macrophages were treated with lipoprotein hydrolysis products, or FFA mixtures.

2.2 HEK-293 Transfection with Recombinant LPL Plasmid

2.2.1 Human LPL plasmid generation

Firstly, 100 μL of cultured *Escherichia coli* DH5 α competent cells (Lucigen, Middleton, WI, USA) with transformation efficiency $\geq 1 \times 10^{10}$ colony forming units per μg DNA were mixed with 1 μg of pcDNA3 containing the human LPL cDNA [GenBank: NM_000237] (pcDNA3.LPL, a kind gift from Dr. Daniel Rader, University of Pennsylvania, Philadelphia, PA, USA). The mixture was tapped gently and placed on ice for 30 minutes, then incubated at 42°C for 90 seconds. The mixture was then placed on ice again for 10 minutes. A total of 900 μL of lysogeny broth (LB) (Sigma) was added to the mixture and the mixture was incubated at 37°C in a MaxQ 4000 E-class shaker (Barnstead International, Dubuque, IA, USA) at 200 rpm for 90 minutes. Then, 200 μL of competent cells containing LPL plasmid were spread on 100-mm culture dishes (BD Biosciences) with LB agar (Fisher Scientific, Ottawa, ON, Canada) containing 100 $\mu\text{g}/\text{mL}$ ampicillin (Sigma) and incubated for 18 hours at 37°C. After incubation, a colony from the agar plate was picked and used to inoculate 5 mL of LB broth containing 5 μL of 100 $\mu\text{g}/\text{mL}$ ampicillin in a 17 \times 100 mm culture test tube (ThermoFisher Scientific). The cells were subsequently incubated at 37°C, shaking at 200 rpm for 16 hours. After the incubation, the bacterial culture was centrifuged at 12,000 rpm using Legend Micro 21 R centrifuge (ThermoFisher Scientific) for 5 minutes at room temperature followed by removal of the supernatant. The pcDNA3.LPL plasmid was then extracted from the bacterial pellet using

the GeneJET plasmid miniprep kit (#K0502, ThermoFisher Scientific), according to the manufacturer's instructions. The purified plasmid was stored at -20°C until used.

2.2.2 HEK-293 cell transfection

HEK-293 cells that had grown to 60-70% confluency were first washed with 5 mL of DMEM media and trypsinized (*see section 2.1.1*). After trypsinization, the cells were detached from the surface by incubating them at 37°C with 5% CO₂ (g). After 2 minutes of incubation, 21 mL of DMEM media with 10% v/v FBS and 1% v/v A/A was added to the cells in the T75 flask. The cells were mixed thoroughly and 10 mL of cells were seeded in two 100-mm tissue culture dishes (BD Biosciences), and incubated for 24 hours. After the 24 hours, cells were transfected with Lipofectamine™ (Invitrogen, Burlington, ON, Canada) containing 5.85 µg of pcDNA3.LPL (*see section 2.2.1*) or Lipofectamine™ without LPL plasmid (mock control). After 5 hours, 2X DMEM growth media (DMEM media supplemented with 20% v/v FBS and 2% v/v A/A) was added to the cells. At 24 hours following the start of transfection, the cells were washed with 5 mL of plain DMEM and then treated with 5 mL of DMEM media containing 1% v/v A/A, and 10 U/mL heparin (Organon, Toronto, ON, Canada) to displace LPL from the cell surface. After 23.5 hours of incubation, the cells were further treated with 1 mL of DMEM containing 100 U/mL heparin and 1% v/v A/A, and cells were subsequently incubated for 30 minutes at 37°C with 5% CO₂ (g). After incubation, the heparinized media from both the plates was removed and centrifuged in 15 mL tubes at 1,050 rpm for 5 minutes in an IEC HN-SII centrifuge (International Equipment Company, Nashville, TN, USA) to remove cell debris. The media containing LPL was aliquoted in 1.5 mL tubes and stored at -80°C. The cells were washed

with 1X phosphate-buffered saline (PBS) prepared from 10X PBS containing 5.24g of NaH_2PO_4 , 23 g of Na_2HPO_4 , and 87.68 g of NaCl in 1 L distilled H_2O (pH 7.4) and stored at -80°C for immunoblot analysis.

2.3 Qualitative and Quantitative Analysis of LPL

2.3.1 Activity assay

LPL activity was measured using 1,2-O-dilauryl-rac-3-glutaric-resorufin ester (#D7816-10MG, Sigma) as the substrate, as previously described by Lehner *et al.* (146). Briefly, a resorufin ester stock was prepared by dissolving 2 mg of resorufin ester in 1 mL of dioxane (Sigma) and stored at 4°C until use. In a 96 well plate (ThermoFisher Scientific), in triplicate wells, 15 μL of heparinized media containing LPL or mock obtained from HEK transfection (*see section 2.2.2*) was added with 165 μL of lipase assay buffer (20 mM Tris, 1 mM EDTA, pH 8.0). Next, 20 μL of 0.3 mg/mL resorufin ester, freshly prepared by diluting resorufin stock with lipase assay buffer, was added to each well containing LPL or mock samples. A Synergy fluorescent plate reader (Bio-Tek, Terrebonne, QC, Canada) was used to measure the absorbance at 572 nm over 60 minutes at 25°C . The concentration of resorufin released was determined by using a standard curve, prepared by diluting 400 μM resorufin ester stock to 0, 1, 2, 3, 4, 6, 10, 15, 20, 40 μM in 200 μL lipase assay buffer.

2.3.2 Immunoblot analysis

Transfected HEK-293 cells in 100-mm dishes were scraped with 1 mL of a 2X sample buffer (20% v/v glycerol, 0.125 M Tris-HCl, 5% v/v β -mercaptoethanol, 0.01% v/v bromophenol blue, 4% w/v sodium dodecyl sulfate (SDS), pH 6.8). Heparinized media (50

μL) from the transfected cells was mixed with equal volume of 2X sample buffer. Cell and media samples were then incubated for 5 minutes at 100°C. After incubation, proteins from 20 μL of each sample were separated on a 10% SDS-polyacrylamide gel, using a Tris-glycine-SDS buffer (25 mM Tris, 192 mM glycine, 0.1% w/v SDS, pH 8.3) (Bio-Rad, Mississauga, ON, Canada). Proteins were transferred onto a nitrocellulose membrane (Bio-Rad) using a transfer buffer of Tris-glycine-SDS with 20 % v/v methanol (ThermoFisher Scientific). The transfer was carried out at 300 mA for 3 hours at 4°C. After transfer, the membrane was incubated with a blocking solution of 5% bovine serum albumin (Sigma), 0.05% v/v Tween-20 (Sigma), and 0.05% w/v NaN₃ (ThermoFisher Scientific) in PBS on a rocking platform at room temperature. After 2 hours of blocking, the membrane was subsequently incubated with a polyclonal anti-human LPL antibody (#sc-32885, Santa Cruz Biotechnology, Santa Cruz, CA, USA) in a 1:1,000 dilution with 5% bovine serum albumin (Sigma) for 3 hours at room temperature with rocking. After primary antibody incubation, the membrane was washed 4 times for every 10 minutes with PBS while rocking. Next, the membrane was incubated for 2 hours with a horseradish peroxidase-conjugated anti-rabbit IgG in a 1:1,000 dilution with 5% bovine serum albumin (Sigma) (#SA1-200, Pierce Biotechnology, Rockford, IL, USA) at room temperature with rocking. Subsequently, the membrane was washed 4 times with PBS for 10 minutes with rocking. Finally, the membrane was developed with the ECLTM Prime chemiluminescent reagent (GE Healthcare, Baie d'Ufre, QC, Canada) according to manufacturer's instructions, and chemiluminescence was detected using an ImageQuant 4000 gel imager (GE Healthcare).

2.4 Lipoprotein Isolation and Quantification

2.4.1 Total lipoprotein isolation

As previously described, the total lipoproteins ($\rho < 1.21$ g/mL) were isolated from the fasted plasma of healthy donors (by Dr. Robert Brown (Department of Biochemistry, Memorial University of Newfoundland), approval #11-109 by the Human Investigation Committee of Memorial University of Newfoundland). The blood (50-70 mL) was drawn in a 50 mL tubes and 0.2 M EDTA stock solution was added to each tube in order to have a final EDTA concentration of 2 mM. The blood was centrifuged at 2,800 rpm using a Heraeus™ Multifuge™ X1R centrifuge (ThermoFisher Scientific) for 15 minutes at 4°C. After centrifugation, the plasma in the supernatant was pooled and the overall volume of plasma was measured. The density of plasma was exactly adjusted to 1.21 g/mL using a high density gradient solution prepared with 38.25 g of NaCl, 88.5 g of KBr, and 2.5 mL of 0.2 M EDTA. The adjusted plasma was transferred to ultracentrifuge tubes and subjected to ultracentrifugation using a Beckman L90K centrifuge with a 70.1Ti rotor (Beckman, Mississauga, ON, Canada) at 50,000 rpm for 44 hours at 4°C. After 44 hours, the top layer that contains total lipoprotein (yellow in color) was pipetted out into another tube and placed on ice. Meanwhile, cellulose dialysis tubing (ThermoFisher Scientific) was boiled in a beaker containing 500 mL of distilled water with 2% w/v NaHCO₃ and 1 mM EDTA for 30 minutes. Next, the total lipoproteins were transferred into 13 cm cellulose membrane tubing and dialyzed against PBS for 24 hours (with PBS being changed every 6 hours) at 4°C. In order to avoid oxidation, the lipoproteins were stored under N_{2(g)} at 4°C after dialysis.

2.4.2 Phospholipid quantification in total lipoproteins

The total lipoproteins were quantified using the Phospholipid C assay (Wako Diagnostics, Richmond, VA, USA) in a 96 well plate according to manufacturer's instructions. Briefly, in triplicate, 5 μ L of total lipoproteins were added to a well containing 15 μ L of PBS. A standard curve was created from a 300 mg/dL solution stock of phospholipid; using the stock, diluted working solutions (of 200 μ L) of 5 mg/dL, 10 mg/dL, 25 mg/dL, 50 mg/dL, 100 mg/dL, and 150 mg/dL were prepared using PBS. Then, 20 μ L of each diluted concentration was added per well in the 96 well plate. Both lipoprotein samples and standard solutions were mixed with 200 μ L of reagent and incubated for 5 minutes at 37°C. The absorbance of these samples was measured at 600 nm using a Synergy fluorescent plate reader (Bio-Tek).

2.5 Lipoprotein Hydrolysis Product Generation, Quantification, and Incubation with THP-1 Macrophages

2.5.1 Lipoprotein hydrolysis by LPL

Lipoprotein hydrolysis products were generated as previously described (137,147). Briefly, the total lipoproteins, at a concentration of 3.5 mM (assessed using a phospholipid assay, *see section 2.4.2*), were mixed with in a 1:1 dilution ratio with either heparinized media containing LPL or heparinized media containing no LPL (mock) (obtained from HEK-293 transfections, *see section 2.2.2*) in 1.5 mL Eppendorf tubes. The mixtures were incubated at 37°C for 4 hours. After incubation, the samples were put on ice immediately.

The FFA liberated were quantified (*see section 2.5.2*). The hydrolysis products were used immediately to incubate THP-1 macrophages (*see section 2.5.3*).

2.5.2 Lipoprotein hydrolysis product quantification

FFAs liberated from the total lipoprotein hydrolysis by LPL were measured using the NEFA-HR(2) commercial kit (Wako). Firstly, 4 μL of LPL hydrolysis products or non-hydrolysis products were added per well (in triplicate) to 96-well plates. Using a multichannel pipette, 225 μL of Solvent A from the kit was added to the samples and incubated for 10 minutes at 37°C. After 10 minutes, 75 μL of Solvent B was added to the samples and incubated at 37°C for 10 minutes. The absorbance was measured at 550 nm at 37°C using the Synergy plate reader. The concentration of FFA in each sample was determined by creating a standard curve from a stock solution containing 1 mM oleic acid; a total of 0, 0.5, 0.75, 1, 1.5, 2, or 4 μL of the stock solution was added into each well, and the volume in each well was brought to a final volume of 4 μL using distilled H₂O.

2.5.3 THP-1 macrophages treatment with lipoprotein hydrolysis product

The LPL hydrolysis products (*see section 2.5.1*) were diluted to a concentration 0.68 mM (which is a concentration that is comparable to those observed in the bloodstream in normophysiological conditions (148)) with RPMI-1640 media supplemented with 0.2% FAF-BSA, 1% A/A, 100 nM PMA, and 25 $\mu\text{g}/\text{mL}$ THL. Similar to LPL hydrolysis product volume, the non-hydrolysis products (0.03 mM) generated from mock transfection were also mixed with conditioned RPMI-1640 media. Following a 1 hour pre-treatment of THP-1 macrophages with THL (*see section 2.1.2*), the spent media from the cells was

removed and 930 μ L of diluted LPL hydrolysis products or non-hydrolysis products were added to the THP-1 macrophage cells. After 18 hours of incubation, the media was removed and 1 mL of TRIzol[®] (ThermoFisher Scientific) was added to each well. The cells were mixed thoroughly in TRIzol[®] and transferred to 1.5 mL Eppendorf tubes, and stored at -80°C.

2.5.3.1 Trypan Blue exclusion assay

The viability of cells, following treatment with LPL hydrolysis or non-hydrolysis products, was assessed using Trypan Blue. Briefly, the macrophage cells that were subjected to the two different treatments were trypsinized using 500 μ L of 0.25% (w/v) trypsin and incubated for 2 minutes at 37°C to detach the cells from the tissue culture dish surface. The detached cells were further mixed with 1 mL of RPMI media supplemented with 10% FBS and 1% A/A, and then pipetted up and down several times to mix. In a separate tube, 30 μ L of cell sample was mixed with 30 μ L of 0.4% (w/v) Trypan Blue (Corning, NY, USA). The cells were loaded into a hemocytometer and both dead and live cells were counted in a defined area under the microscope. The following formula was used to calculate cell viability percentage:

$$\text{Cell viability \%} = \frac{\text{Average of viable cells per treatment}}{\text{Average of total cells per treatment}} \times 100 \quad (\text{equation 1})$$

where, a total cell per square is the sum of viable and dead cells.

2.6. Incubation of FFA Mixture and Distinct FFA Classes with THP-1 Macrophages

The concentrations of individual FFA species that are present in LPL hydrolysis products from total lipoproteins were previously quantified by our group (137). As previously described (77,137), a FFA mixture was prepared according to the amount of FFA liberated by LPL from the hydrolysis of total lipoprotein lipids. Palmitate (16:0), myristate (14:0), palmitoleate (16:1), oleate (18:1), stearate (18:0), linoleate (18:2), arachidonate (20:4) and docosahexaenoate (22:6) (all reagents from Nu-Chek Prep, Elysian, MN, USA) were dissolved to a concentration of 10 mg/ml using high performance liquid chromatography grade methanol and stored under $N_{2(g)}$ at $-20^{\circ}C$ until use. The total FFA mixture was prepared by removing 275.0 nmol of 16:0, 18.6 nmol of 14:0, 23.7 nmol of 16:1, 241.8 nmol of 18:1, 45.4 nmol of 18:0, 70.0 nmol of 18:2, 0.9 nmol of 20:4 and 0.4 nmol of 22:6 from the stock solution. The methanol in the total FFA mixture was evaporated under $N_{2(g)}$ at $35^{\circ}C$ and resuspended with 10 μ L of dimethyl sulfoxide (DMSO). THP-1 macrophage cells, pre-treated with THL (*see section 2.1.2*), were further incubated with 990 μ l of RPMI containing 0.2% w/v FAF-BSA, 1% A/A, 100 nM PMA, 25 μ g/ml THL, and either the total FFA mixture or 10 μ L of DMSO (vehicle control). The FAF-BSA concentration was chosen because it is within the range observed within the aortic intima (149). FFA mixtures in DMSO, containing only the SFA (275.0 nmol 16:0, 18.6 nmol 14:0, and 45.4 nmol of 18:0), MUFA (23.7 nmol 16:1, and 241.8 nmol 18:1), and PUFA (70.0 nmol 18:2, 0.9 nmol 20:4, and 0.4 nmol 22:6), were also prepared. To make 1 ml of tissue culture media with each FFA mixture, the fatty acid/DMSO mixture or 10 μ l DMSO (as vehicle control) was added at a rate of 1 μ l/min to 990 μ l RPMI-1640 containing

0.2% w/v FAF-BSA, 1% v/v A/A, 100 nM PMA, and 25 µg/ml THL while continuously vortexing. The media containing FFA were immediately incubated with THP-1 macrophages. After 18 hours of incubation, the RNA was isolated using TRIzol® LS reagent (ThermoFisher Scientific) and the samples were stored at -80°C until use.

2.7 RNA Isolation, Genomic DNA Removal and RNA Clean-up

RNA was isolated from the samples stored with 1 mL of TRIzol® (*see section 2.5.3 and 2.6*) as previously described (150). The samples with TRIzol® were mixed thoroughly with 200 µL of chloroform, then they were centrifuged at 12,000 rpm in a Legend Micro 21 R centrifuge (ThermoFisher Scientific) for 15 minutes at 4°C. The centrifugation yields three phases: an upper aqueous phase containing RNA, an interphase containing DNA, and a lower organic phase containing protein. The upper aqueous phase was collected and added to 500 µL of isopropanol in a 1.5 mL microfuge tube, then it was incubated at room temperature for 10-15 minutes. After incubation, the tube was centrifuged at 12,000 rpm in Legend Micro 21 R centrifuge (ThermoFisher Scientific) for 10 minutes at 4°C. The supernatant was discarded and 1 mL of 75% ethanol was added to each tube containing RNA pellets to remove any impurities. The tubes containing RNA samples were then centrifuged at 8,800 rpm for 5 minutes at 4°C. After centrifugation, the supernatant was discarded. The ethanol was evaporated completely, then 20 µL of nuclease-free water was added to the RNA pellet and the tube was tapped gently to dissolve and mix the RNA. The concentration of RNA was measured using a NanoDrop 2000 spectrophotometer (ThermoFisher Scientific). To remove trace genomic DNA contamination, the isolated RNA was treated with the TURBO® DNA-free DNase kit (Invitrogen), as per the

manufacturer's instructions. The concentration of the RNA was measured again using a NanoDrop 2000 spectrophotometer and the quality of RNA, both before and after DNase treatment, was assessed using a 1% agarose gel. The RNA was further cleaned using RNeasy[®] Mini kit (#74104, Qiagen, Toronto, ON, Canada), according to the manufacturer's instructions. The quality of cleaned RNA was checked again using a 1% agarose gel and stored at -80°C until further use.

2.8 Microarray and Quantitative PCR

2.8.1 Microarray analysis

The RNA isolated from macrophages incubated with either LPL hydrolysis products or non-hydrolysis products from three independent experiments were shipped to The Centre for Applied Genomics (Toronto, ON, Canada) to obtain raw data from analyses using the Human gene 2.0 ST GeneChip (Affymetrix, Santa Clara, CA, USA). For each sample, the RNA integrity was assessed at The Centre for Applied Genomics using an Agilent Bioanalyzer 2100; RNA integrity numbers (RIN) for all the samples were above eight.

Raw microarray data received from The Centre for Applied Genomics were processed using Bioconductor 3.1 (151) in R 3.2.0 (152). Data were normalized with the RMA algorithm (153) using the Oligo package (154). Once the data were pre-processed, the differentially expressed genes were obtained using LIMMA (155). The model matrix was designed for data obtained from LPL hydrolysis product and non-hydrolysis product treated macrophages. The function *eBayes* was used to rank the differentially expressed

genes. Further, a top list of differentially expressed genes was obtained using the function *topTable* by adjusting the *P* value for false discovery rate (FDR), a multiple testing correction method that controls false discoveries. (Detailed line commands are provided in *Appendix I methods*).

Lastly, gene annotation was performed using biomaRT (156,157) and confirmed by using NetAffx™ Affymetrix Analysis Center (Affymetrix), that provides the official gene symbol for each Affymetrix probe ID (158).

Next, the functional interaction between the genes was visualized and gene ontology (GO) analyses were performed using geneMANIA database (159). GeneMANIA database provides the function of different gene sets and performs enrichment analysis to determine what were the biological processes that were significantly enriched. The list of genes (query genes) that were differentially regulated (at $FDR \leq 0.03$) were uploaded onto the website in order to obtain GO biological functions associated with query genes. Finally, enriched biological processes (at $FDR < 0.05$) and their associated genes were chosen, and select genes associated with different biological processes were validated using real-time PCR.

The processed microarray data were submitted to Gene Expression Omnibus, according to the minimum information about microarray experiments regulations (160). The GEO accession number associated with our data is GSE84791.

2.8.2 Quantitative PCR analysis

2.8.2.1 cDNA synthesis

To synthesize cDNA, 500 ng of RNA samples (*see section 2.5.3 and 2.6*) were added to nuclease-free H₂O (4.5 µL) in PCR tubes and placed on ice. Two different master mixes were prepared in 1.5 mL Eppendorf tubes, where master mix 1 contains 1 µL of random primers (3 µg/µL) (#48190-011, ThermoFisher Scientific) and 0.5 µL of deoxyribonucleotide triphosphates (10 mM) (#R0191, ThermoFisher Scientific) and master mix 2 contains 2 µL of 5X First-Strand Buffer (#Y02321, ThermoFisher Scientific), 1 µL of 0.1 M dithiothreitol and 0.5 µL of 40 U/µL RNaseOut™ (#10777-019, ThermoFisher Scientific). The master mixes were freshly prepared for each set of samples that were assessed at any given time. A total of 1.5 µL of master mix 1 was added to each tube containing RNA samples and incubated for 5 minutes at 65°C in an Eppendorf PCR machine (Eppendorf, Mississauga, ON, Canada). After 5 minutes, 3.5 µL of master mix 2 was added to each tube and further incubated for 2 minutes at 37°C. Lastly, 0.5 µL of 200 U/µL M-MLV reverse transcriptase (#28025013, ThermoFisher Scientific) was added to each tube and mixed thoroughly. The RNA sample mixture was then incubated at the following conditions: 25°C for 10 minutes, 37°C for 50 minutes, 72°C for 10 minutes, and 4°C for infinity (optional). The cDNA samples (at a concentration of 500 ng in 10 µL reaction volume) were further diluted to 5 ng/µL and stored at -20°C until use.

2.8.2.2 Quantitative PCR analysis

The relative gene expression of select genes was measured in THP-1 macrophages incubated with LPL hydrolysis products (biological replicates, $n=3$), FFA mixture

(biological replicates, $n=3$), and distinct FFA classes (biological replicates, $n=3$). Gene expression was quantified using iQ SYBR Green Supermix (Bio-Rad) or SsoAdvanced SYBR Green Supermix (Bio-Rad), according to manufacturer's instructions. Primers were designed and used to quantify the genes encoding β -actin, small nucleolar RNA (snoRNA) 56, snoRNA 75, dyskerin 1 variant 3, proliferating cell nuclear antigen (PCNA), ATF3, interferon-induced transmembrane protein 1 (IFITM1), CD36, and perilipin 2 (Integrated DNA Technologies, Coralville, IA, USA) (**Table 1**) in a CFX96TM Real-Time PCR system (Bio-Rad). Real-time PCR cycle conditions were 1 cycle of 95°C for 3 minutes, and 40 cycles of 95°C for 15 seconds, 59.5°C for 15 seconds, and 72°C for 20 seconds.

Amplification efficiencies of select genes (Table S1) were calculated as previously described by Pfaffl *et al.* (161). Briefly, cDNA synthesized from LPL hydrolysis product- and non-hydrolysis product-treated THP-1 macrophages were pooled together. Different amounts of pooled cDNA (50 ng, 10 ng, 2 ng, 0.4 ng, 0.08 ng, and 0.016 ng) were added to 1 μ L of 500 nM select gene primers (both forward and reverse primers), 10 μ L of iQ SYBR Green Supermix, and an appropriate volume of nuclease-free H₂O (Thermo Fisher Scientific) to adjust the final volume to 20 μ L. Threshold cycle (C_t) values were obtained by performing qPCR following the above cycle conditions. Log cDNA inputs were plotted against C_t values obtained for each select genes. The slope obtained from the graph was used in the following equation to obtain amplification efficiency:

$$E = 10^{-1/\text{slope}} \quad (\text{equation 2})$$

Table 1: List of primer sequences for select genes

Gene	Forward Primer	Reverse Primer
<i>ACTB</i> <u>NC 000007.13</u>	5'- ACC TTC TAC AAT GAG CTG CG- 3' Template: 349368	5'- CCT GGA TAG CAA CGT ACA TGG -3' Template: 537.....517
<i>ATF3</i> <u>XM 011509579.1</u>	5'- AGT GAG TGC TTC TGC CAT CG- 3' Template: 228.....247	5'- GCA GAG GTG CTT GTT CTG GA- 3' Template: 354.....335
<i>ADRP</i> <u>XM 017014259.1</u>	5'- TAA CAA CAC GCC CCT CAA CT-3' Template: 1301.....1320	5'- GAG GAC AGG GCC ATT AGC AT- 3' Template: 1439.....1420
<i>CD36</i> <u>XM 011516707.1</u>	5'-TTG ATG TGC AAA ATC CAC AGG-3' Template: 323.....343	5'-TGT GTT GTC CTC AGC GTC CT- 3' Template: 453.....434
<i>PCNA</i> <u>NM 002592.2</u>	5'- GGC GTG AAC CTC ACC AGT AT- 3' Template: 444.....463	5'- TTC TCC TGG TTT GGT GCT TC- 3' Template: 568.....549
<i>IFITM1</i> <u>NM 003641.3</u>	5'- GAC AGG AAG ATG GTT GGC GA- 3' Template: 373.....392	5'- GGT AGA CTG TCA CAG AGC CG- 3' Template: 517.....498
<i>SNORA75</i> <u>NR 002921.1</u>	5'- TCT TCT CAT TGA GCT CCT TTC T- 3' Template: 2.....23	5'-AAT GTC TCA CAA TAC AGC TAA A- 3' Template: 136.....115
<i>SNORA56</i> <u>NM 001288747.1</u>	5'- TTC TAG TCT GGC TCG TGG GA-3' Template: 1794.....1813	5'- TGG CAA GTC TAA AGC CAC CA -3' Template: 1897.....1878
<i>DKC1-v3</i> <u>NM 001288747.1</u>	5'- GTA GAG ACG GCA CAC TTG CT- 3' Template: 1515.....1534	5'- ACA ACC TCC ATG CTC ACC TG -3' Template: 1650.....1631

The primer sequences for target genes and a reference genes are listed above. *ACTB* encodes β -actin. *ADPF*, an alternate symbol for *PLIN2*, encodes perilipin 2. Melting curve analysis of forward and reverse primers of each respective gene showed that primers amplified only one product (data not shown).

where E denotes amplification efficiency in equation 2. All qPCR reactions were performed in duplicate to measure efficiency. Melting curves (not shown) were assessed to ensure only one product was amplified. Next, the gene expression analysis for select genes was performed by calculating the relative expression ratio as previously described (161). Briefly, 25 μL of reaction mixture was prepared by adding 5 μL of 5 ng/ μL cDNA or non-template control to 1.25 μL of 500 nM select gene primers (both forward and reverse), 12.5 μL of IQ SYBR Green Supermix, and 5 μL of nuclease-free H_2O . All reactions were performed in triplicate and target genes were normalized to β -actin (reference gene).

The relative expression ratio was measured using the following mathematical model:

$$\text{Ratio} = \frac{(E_{\text{target}})^{\Delta\text{CP}_{\text{target}}(\text{control-sample})}}{(E_{\text{ref}})^{\Delta\text{CP}_{\text{ref}}(\text{control-sample})}} \quad (\text{equation 3})$$

where E_{target} and E_{ref} represents the amplification efficiency of select target gene and β -actin, respectively. $\Delta\text{CP}_{\text{target}}$ and $\Delta\text{CP}_{\text{ref}}$ refers to the difference in C_t values between the control versus the treated target genes or the reference gene, respectively. Data are presented as mean percentage relative to control treatments.

2.9 Statistical Analysis

Unless otherwise stated, an unpaired student's *t*-test was performed to determine statistical significance and the standard deviation (SD).

Chapter 3: Results

3.1 Microarray Analyses of THP-1 Macrophages in Response to Lipoprotein Hydrolysis Products

The immunoblot analyses of heparinized media from LPL expressing cells showed that the heparinized media contained full length LPL protein, as well as significant lipase activity versus heparinized media from mock-transfected cells (Figure. 4). We incubated 3.5 mM (by PL) of total lipoproteins, isolated from normolipidemic subjects, with heparinized media from HEK-293 cells expressing human LPL. As expected, after a 4 hours incubation at 37°C, the amount of FFA liberated by LPL was significantly higher versus the amount of FFA observed following incubation with heparinized media from control cells (Figure. 5). The lipoprotein hydrolysis products generated by LPL were diluted to a FFA concentration of 0.68 mM; the diluted lipoprotein hydrolysis products were incubated with THP-1 macrophages for 18 hours, and RNA was isolated for microarray analyses. The total lipoproteins treated with control media were comparably diluted to yield a FFA concentration of 0.03 mM; these control samples were also incubated with THP-1 macrophages for 18 hours. Both treatments did not affect cell viability, based on Trypan Blue exclusion assays (Figure. 6).

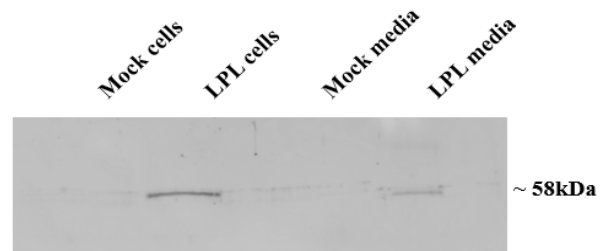
Although the RNA integrity number was consistently above eight from all of the samples, the integrity of the THP-1 RNA that was isolated following incubations with total lipoprotein hydrolysis products was consistently lower versus control cells (8.45 ± 0.26 versus 9.45 ± 0.058 , respectively – $P < 0.001$).

Figure 4: LPL protein expression and catalytic activity

HEK-293 cells were transfected either with pcDNA3 containing the human LPL cDNA or no pcDNA3 (Mock). Heparinized media and cell lysates were collected. (A) Immunoblot analysis for LPL of cell lysates from transfected cells and heparinized media from the transfected cells. (B) Catalytic activity of heparinized media from non-transfected (Mock) or transfected cells toward a resorufin ester substrate. Data are presented as the mean \pm SD from triplicate experiments.

Figure 4

A)



B)

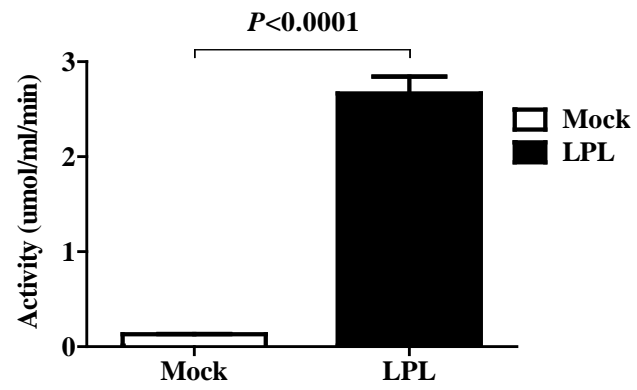


Figure 5: Hydrolysis of total lipoproteins by heparinized media

HEK-293 cells were transfected either with pcDNA3 containing the human LPL cDNA or no pcDNA3 (Mock). Heparinized media from these cells, collected as described under *section 2.2.2*, were incubated with total lipoproteins (Lipo; $d < 1.21$ g/mL, 3.5 mM by PL) for 4 h, as described under *section 2.5.1*. The FFA generated were quantified and data represent the mean \pm SD from triplicate experiments.

Figure 5

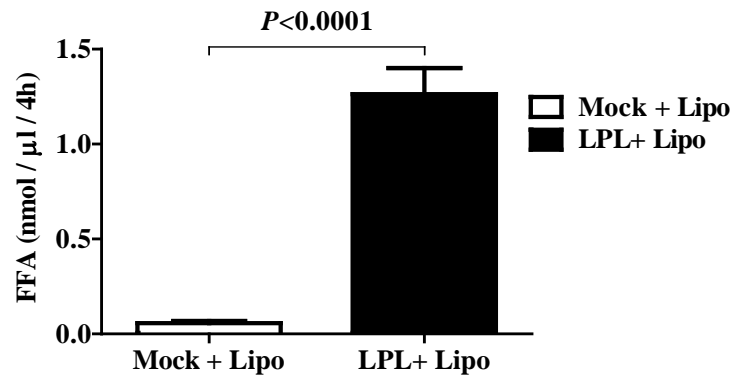
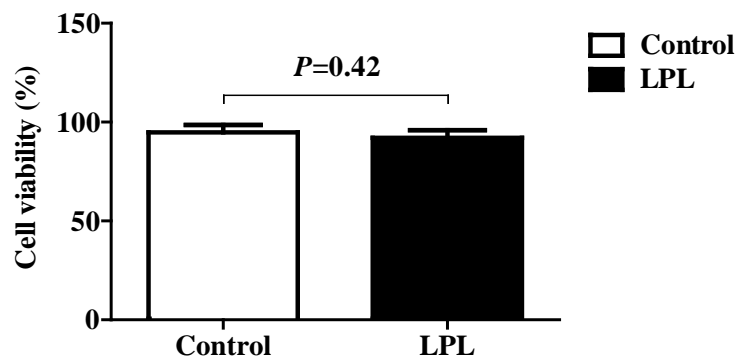


Figure 6: The effect of LPL hydrolysis products on THP-1 macrophage cell viability

THP-1 macrophages were incubated for 18 hours with total lipoprotein hydrolysis products that were generated by LPL or control heparinized media. After 18 hours, cells were incubated with Trypan Blue and counted, as described under *section 2.5.3.1*. Data are presented as a percent of control \pm SD from triplicate experiments.

Figure 6



Our RNA integrity data showed that the levels of both 28S and 18S ribosomal RNA was reduced in response to total lipoprotein hydrolysis products, concomitantly with an unusual appearance of small RNA bands (Figure 7).

Microarray analyses of transcripts from THP-1 macrophages incubated in the absence or presence of total lipoprotein hydrolysis products generated by LPL revealed that 316 transcripts were differentially regulated at a $FDR \leq 0.03$. Out of the 316 differentially regulated transcripts, 183 transcripts (with 145 unique genes and 16 uncharacterized transcripts) were upregulated in response to lipoprotein hydrolysis products, while 133 transcripts (with 118 unique genes and 6 uncharacterized transcripts) were downregulated (Appendix II, Table S2; and Appendix II, Table S3). Of note, 63 of the upregulated transcripts were snoRNAs. Fourteen of the 63 snoRNAs we identified exhibited a fold change of four or greater (Table 2).

A total of 157 differentially regulated transcripts encode functional proteins. Using the GeneMANIA database, an enrichment analysis of the gene ontologies associated with these transcripts showed that eight GO biological processes were significantly influenced by total lipoprotein hydrolysis products generated by LPL ($p < 0.05$). These processes include DNA replication (16 transcripts, GO:0006260), chromosome segregation (10 transcripts, GO:0007059), unfolded protein response (8 transcripts, GO:0006986), ER stress response (7 transcripts, GO:0034976), type I interferon signaling response (8 transcripts, GO:0071357), sterol metabolism (6 transcripts, GO:0016125), cellular metal ion homeostasis (11 transcripts, GO:0006875), and regulation of nuclease activity (9

Figure 7: The effect of total lipoprotein hydrolysis products generated by LPL on THP-1 RNA integrity

Total lipoproteins ($d < 1.21$ g/ml, 3.5 mM by PL) were incubated for 4 h at 37°C with either heparinized media from non-transfected HEK-293 cells, or heparinized media from HEK-293 cells expressing human LPL. THP-1 cells were incubated for 18 hours with the hydrolysis products (Control, 0.03 mM; LPL, 0.68 mM by FFA), and RNA were isolated. RNA were separated in an Affymetrix Bioanalyzer. All samples had an RNA integrity number value above eight. Data are representative of four biological replicates.

Figure 7

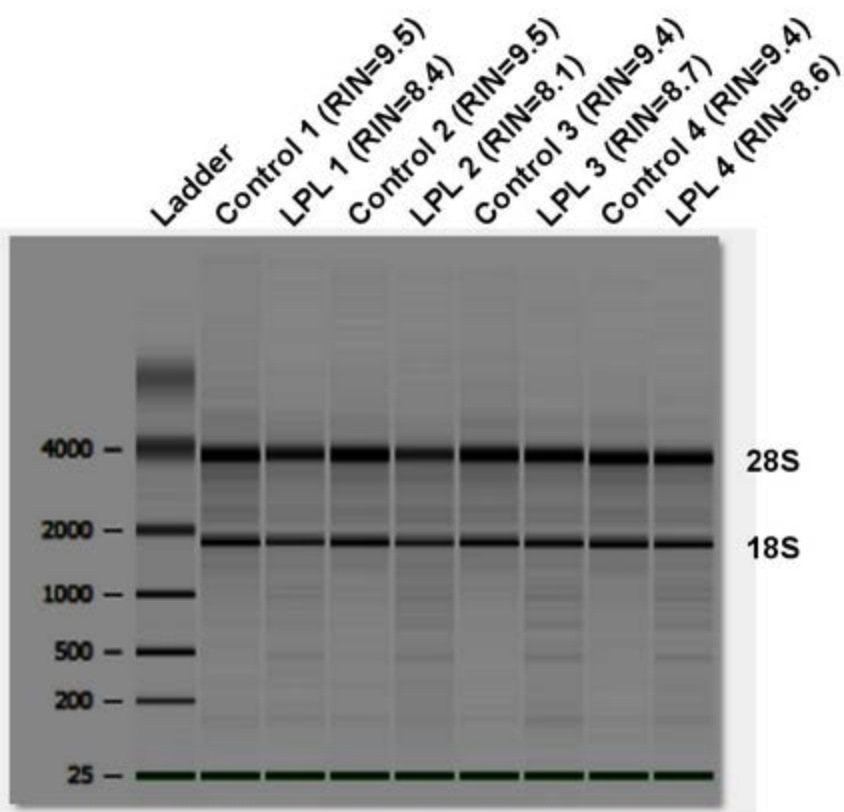


Table 2: SnoRNA molecules identified by microarray analyses with at least a four-fold increase of expression in THP-1 macrophages in response to total lipoprotein hydrolysis products liberated by LPL

Gene	Description	Host Gene*	Target RNA*	Fold Change
<i>SNORA60</i>	small nucleolar RNA, H/ACA box 60	<i>SNHG11</i>	18S rRNA U1004	12.01
<i>SNORA75</i>	small nucleolar RNA, H/ACA box 75	<i>NCL</i>	18S rRNA U93	6.59
<i>SNORA14B</i>	small nucleolar RNA, H/ACA box 14B	<i>TOMM20</i>	18S rRNA U966	6.45
<i>SNORA80E</i>	small nucleolar RNA, H/ACA box 80E	<i>KIAA0907</i>	18S rRNA U572 and U109	6.30
<i>SNORA76C</i>	small nucleolar RNA, H/ACA box 76C	<i>SNHG25</i>	18S rRNA U34 and U105	5.19
<i>SNORA11</i>	small nucleolar RNA, H/ACA box 11	<i>MAGED2</i>	Nil	5.11
<i>SNORA2A</i>	small nucleolar RNA, H/ACA box 2A	<i>FLJ20436</i>	28S rRNA U4263 and U4282	4.84
<i>SNORA42</i>	small nucleolar RNA SNORA42/SNORA80 family	<i>KIAA0907</i>	18S rRNA U572 and 18S rRNA U109	4.77
<i>SNORA33</i>	small nucleolar RNA, H/ACA box 33	<i>RPS12</i>	28S rRNA U4966	4.69
<i>SCARNA8</i>	small Cajal body-specific RNA 8	<i>FAM29A</i>	U2 spliceosome	4.46
<i>SNORA56</i>	small nucleolar RNA, H/ACA box 56	<i>DKC1</i>	28S rRNA U1664	4.23
<i>SCARNA4</i>	small Cajal body-specific RNA 4	<i>KIAA0907</i>	U2 snRNA U41 and U39	4.12
<i>SNORA71B</i>	small nucleolar RNA, H/ACA box 71B	<i>SNHG17</i>	18S rRNA U406	4.02
<i>SNORD92</i>	small nucleolar RNA, C/D box 92	<i>D26488</i>	28S rRNA A3846	4.00

* Information on host genes and target RNA obtained from the snoRNA-LBME-db database (162)

transcripts, GO:0032069) (Table 3). The GO biological processes of DNA replication and chromosome segregation are sub-categories of the cell cycle. Interestingly, with the exception of *DKC1* variant 3 (*DKC1-v3*), the expression of all genes identified from these sub-categories were downregulated. The expression of all genes that were identified within the GO biological process of type I interferon signaling response were also downregulated. On the other hand, the expression of all genes identified within the GO biological process of unfolded protein response was upregulated. Description on enrichment analysis (Table S4) and fold change of genes associated with each selected processes (Table S5) are provided in Appendix II.

We identified genes within the GO biological process of sterol metabolism that were either upregulated or downregulated in response to total lipoprotein hydrolysis products. However, we did not identify other GO biological processes associated with lipid metabolism. This is likely due to the lack of over-representation of genes associated with lipid metabolism following multiple corrections. However, the manual analysis of the top differentially expressed genes (at $FDR \leq 0.03$) showed that the treatment of THP-1 macrophages with total lipoprotein hydrolysis products generated by LPL altered the expression of *FABP4* (5.4-fold increase), *ACAT2* (2.0-fold decrease), *LDLR* (1.7-fold decrease), *FASN* (2.0-fold decrease), *FADS1* (1.7-fold decrease), *FADS2* (2.1-fold decrease), *CD36* (2.9-fold increase), *PLIN2* (2.9-fold increase), and *CPT1A* (3-fold increase) (Appendix II, Table S2; and Appendix II, Table S3).

Table 3: List of significantly over-represented GO Biological processes and the genes identified within these processes by microarray analyses

GO Biological Process	Number of Genes Identified from Microarray Analyses	Genes in Genome	List of Genes Identified from Microarray Analyses	Enriched <i>P</i> Value
DNA replication (GO: 0006260)	16	222	<i>DKC1-v3, CDC25A, MCM7, POLQ, CHEK1, PCNA, MCM4, E2F8, MCM3, MCM6, RAD51, MCM8, DSCC1, ESCO2, TYMS, TOP2A</i>	7.3×10^{-7}
Chromosome segregation (GO: 0007059)	10	128	<i>CENPE, NUSAP1, SKA3, DSCC1, BUB1, NCAPH, CASC5, TOP2A, NCAPG, SKA1</i>	3.0×10^{-4}
Response to unfolded protein (GO: 0006986)	8	106	<i>HSPA1A, ATF3, HSP90B1, HSPA5, KDEL3, DNAJB1, ACADVL, HYOU1</i>	3.1×10^{-3}
Response to ER stress (GO: 0034976)	7	113	<i>ATF3, HSP90B1, HSPA5, KDEL3, ACADVL, HYOU1, CHAC1</i>	2.2×10^{-2}
Response to type 1 interferon (GO: 0071357)	8	74	<i>IFI27, IFIT1, OAS1, MX2, OAS3, XAF1, OAS2, IFITM1</i>	3.6×10^{-4}
Sterol metabolic process (GO: 0016125)	6	80	<i>CYP27A1, ACADVL, FDPS, HMGCS1, DHCR24, DHCR7</i>	2.4×10^{-2}
Cellular metal ion homeostasis (GO: 0006875)	11	264	<i>ATP6V0D2, ABCG2, HSP90B1, CD52, TPT1, HMOX1, C3AR1, P2RX7, PTK2B, CCL1, CXCL10</i>	9.9×10^{-3}
Regulation of nuclease activity (GO: 0032069)	9	73	<i>ATF3, HSP90B1, HSPA5, KDEL3, ACADVL, HYOU1, PCNA, OAS1, OAS3</i>	6.8×10^{-5}

3.2 Validation of Expression for Select Genes by Real-Time PCR

We treated THP-1 macrophages for 18 hours with total lipoprotein hydrolysis products that were generated by LPL, as above, for the purpose of validating the expression of select genes by real-time PCR that we identified in the microarray analyses (Table 4). We chose to validate the expression of two snoRNA genes that were increased in response to lipoprotein hydrolysis products generated by LPL: *SNORA56* and *SNORA75*. We also chose to validate *DKC1-v3* and *PCNA* (both from the GO biological process of cell cycle), *ATF3* (from the GO biological process of stress response), and *IFITM1* (from the GO biological process of type I interferon signaling); genes from each of these processes were chosen because these GO biological processes appear to play a role in atherosclerosis (163-165). Lastly, we also assessed the expression of the lipid metabolism genes *CD36* and *PLIN2* – both of which were found to be significantly upregulated ($FDR \leq 0.03$) in response to total lipoprotein hydrolysis products. Overall, with the exception of *SNORA75*, which showed no difference between the absence or presence of hydrolysis products (Figure 8A), the changes of expression for the remaining seven genes were significant and similar to the microarray data (Figure 8B-H).

3.3 Select Gene Expression in Response to FFA

We previously reported the molar amounts of FFA that were liberated by LPL from total lipoproteins; based on these data, we have previously prepared and tested a mixture of purified FFA (that represents the FFA component of total lipoprotein hydrolysis products) on its influence on cell signaling nodes and cholesterol efflux (77,137). We

Table 4: Genes from microarray analyses that were selected for further study

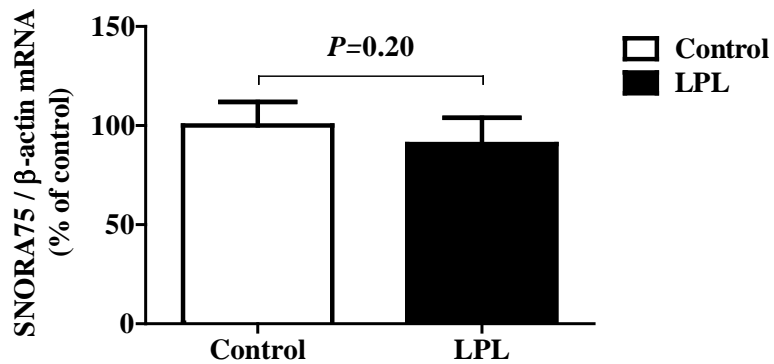
Affymetrix Transcript ID	Gene Symbol	Description	Fold Change in Microarray	Microarray P Value (at FDR \leq 0.03)
16909520	<i>SNORA75</i>	Small nucleolar RNA 75	6.6	0.006
17119802	<i>SNORA56</i>	Small nucleolar RNA 56	4.2	0.006
17119802	<i>DKC1-v3</i>	Dyskerin (variant 3)	4.2	0.006
16720085	<i>IFITM1</i>	Interferon-induced transmembrane protein 1	4	0.005
17047795	<i>CD36</i>	Cluster of differentiation 36	2.9	0.006
16916958	<i>PCNA</i>	Proliferating cell nuclear antigen	1.99	0.02
16677278	<i>ATF3</i>	Activating transcription factor 3	2.9	0.007
17092712	<i>PLIN2</i>	Perilipin 2	2.9	0.006

Figure 8: Validation of expression of select genes within THP-1 macrophages incubated with total lipoprotein hydrolysis products generated by LPL

Total lipoproteins ($d < 1.21$ g/ml, 3.5 mM by phospholipid) were incubated for 4 h at 37°C with either heparinized media from non-transfected HEK-293 cells, or heparinized media from HEK-293 cells expressing human LPL. THP-1 cells were incubated for 18 hours with the hydrolysis products (Control, 0.03 mM; LPL, 0.68 mM by FFA), and RNA were isolated for the quantitative real-time PCR analyses of (A) *SNORA75*; (B) *SNORA56*; (C) *DKC1-v3*; (D) *IFITM1*; (E) *CD36*; (F) *PCNA*; (G) *ATF3*; and (H) *PLIN2*. All data were normalized to the expression of β -actin, and data are presented as a percent of control \pm SD from three biological replicates.

Figure 8

(A)



(B)

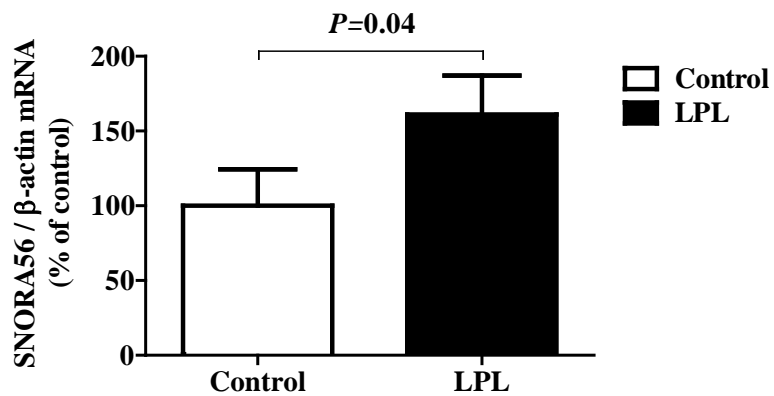
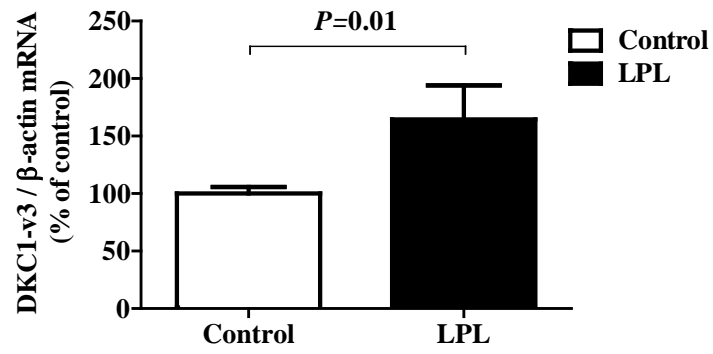


Figure 8 (cont.)

(C)



(D)

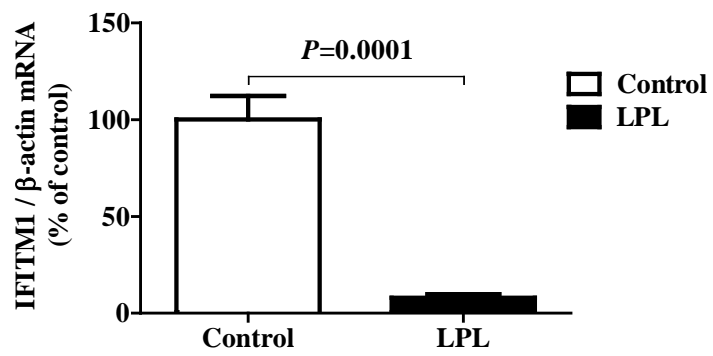
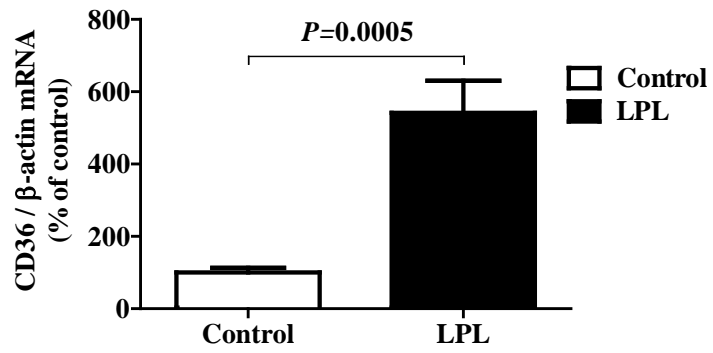


Figure 8 (cont.)

(E)



(F)

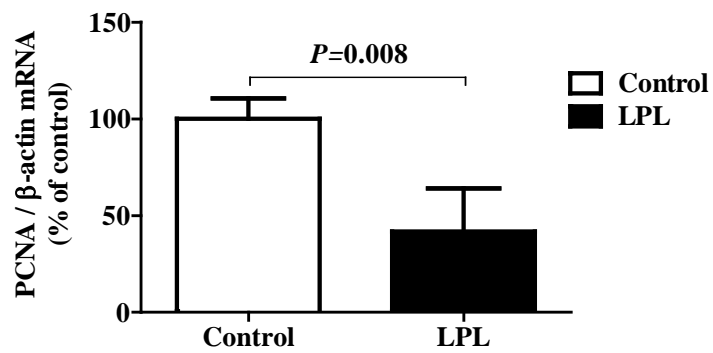
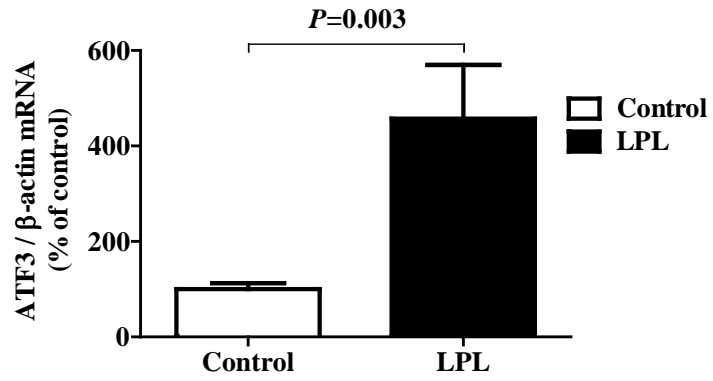
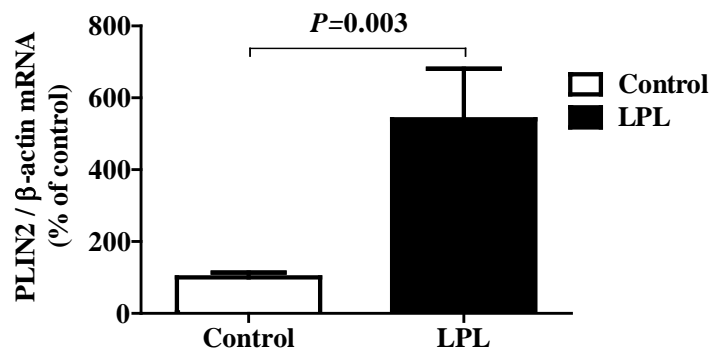


Figure 8 (cont.)

(G)



(H)



prepared a 0.68 mM FFA mixture, to match the concentration of FFA within our hydrolysis products, and we incubated THP-1 macrophages with the mixture for 18 hours in an attempt to determine the role of the FFA component of hydrolysis products on the expression of our seven validated genes. Real-time PCR analyses showed that no significant changes were observed for the expression of *SNORA56* (Figure 9A), *DKC1-v3* (Figure 10A), *IFITM1* (Figure 11A), and *CD36* (Figure 12A). However, the FFA mixture significantly reduced the gene expression of *PCNA* by 20% (Figure 13A), *ATF3* by 37% (Figure 14A), and *PLIN2* by 25% (Figure 15A).

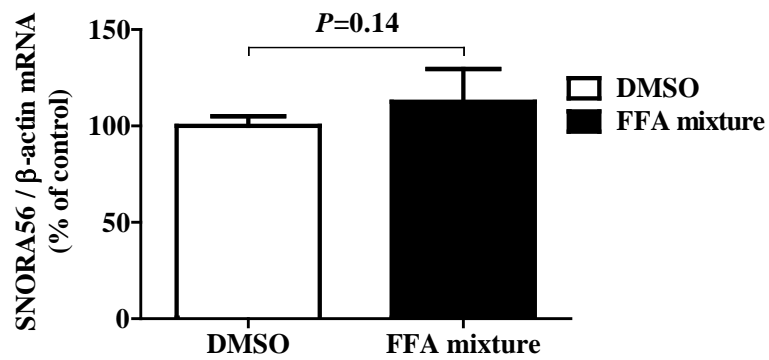
Lastly, to further assess how the FFA component influences the expression of our seven validated genes, we prepared and tested FFA mixtures that only contained the SFA, MUFA, or PUFA components of the total lipoprotein hydrolysis products. These mixtures were incubated with THP-1 macrophages for 18 hours, and gene expression levels were quantified by real-time PCR. The expression of *SNORA56* significantly decreased by 36% in response to SFA (Figure 9B), but it did not change in response to MUFA (Figure 9C) or PUFA (Figure 9D). Similarly, the expression of *DKC1-v3* significantly decreased by 31% in response to SFA (Figure 10B), but it did not change in response to MUFA (Figure 10C) or PUFA (Figure 10D). Similar to what was observed for the total FFA mixture, the gene expression for *IFITM1* was unaffected by the SFA, MUFA, or PUFA mixtures (Figure 11B-D). Our data show that the gene expression of *CD36* was significantly reduced by 34% in the presence of MUFA (Figure 12C), however, the SFA and PUFA mixtures had no significant effect on expression (Figure 12B and 12D, respectively). While the total

Figure 9: The influence of the FFA component of total hydrolysis products on *SNORA56* expression in THP-1 macrophages

THP-1 macrophages were incubated for 18 hours with a vehicle control (DMSO) or with (A) a 0.68 mM total FFA mixture representing the FFA component of total lipoprotein hydrolysis products liberated by LPL; (B) the saturated fatty acid (SFA) component of the total FFA mixture; (C) the monounsaturated fatty acid (MUFA) component of the total FFA mixture; and (D) the polyunsaturated fatty acid (PUFA) component of the total FFA mixture. RNA were isolated following incubations and used to quantify *SNORA56* by quantitative real-time PCR. All data were normalized to the expression of β -actin, and data are presented as a percent of control \pm SD from three biological replicates.

Figure 9

(A)



(B)

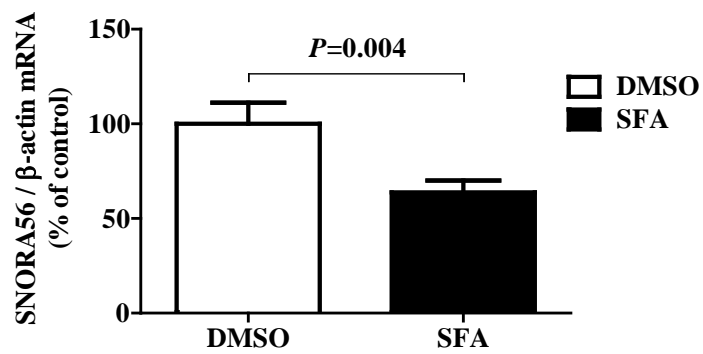
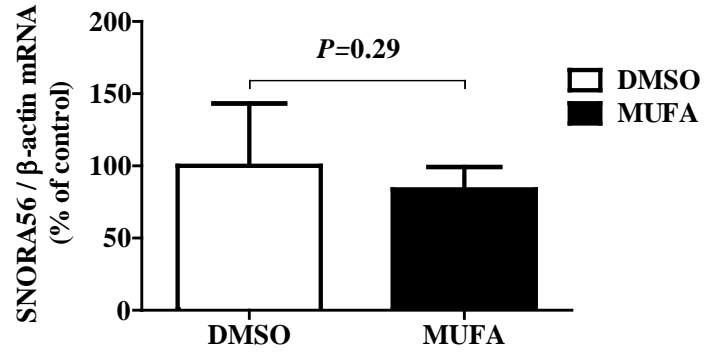


Figure 9 (cont.)

(C)



(D)

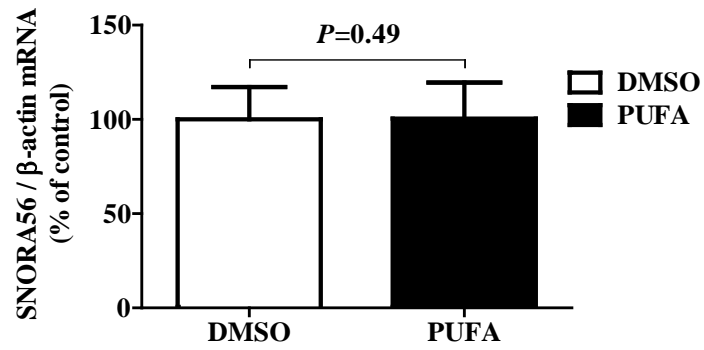
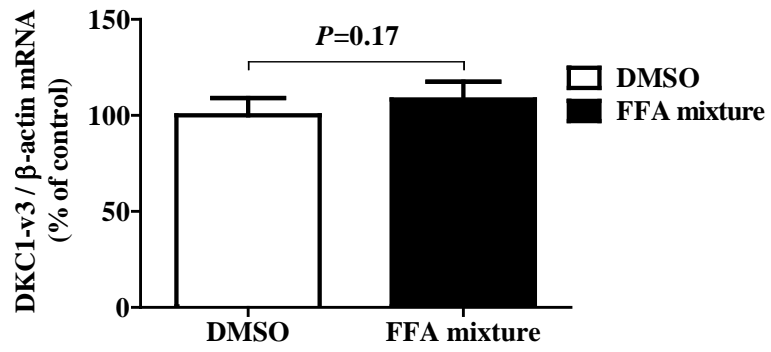


Figure 10: The influence of the FFA component of total hydrolysis products on *DKC1-v3* expression in THP-1 macrophages

THP-1 macrophages were incubated for 18 hours with a vehicle control (DMSO) or with (A) a 0.68 mM total FFA mixture representing the FFA component of total lipoprotein hydrolysis products liberated by LPL; (B) the saturated fatty acid (SFA) component of the total FFA mixture; (C) the monounsaturated fatty acid (MUFA) component of the total FFA mixture; and (D) the polyunsaturated fatty acid (PUFA) component of the total FFA mixture. RNA were isolated following incubations and used to quantify *DKC1-v3* by quantitative real-time PCR. All data were normalized to the expression of β -actin, and data are presented as a percent of control \pm SD from three biological replicates.

Figure 10

(A)



(B)

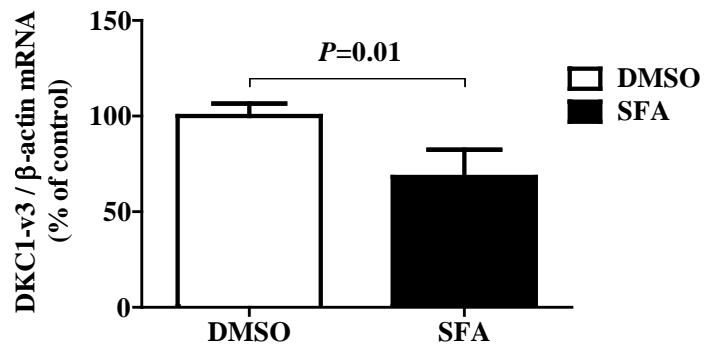
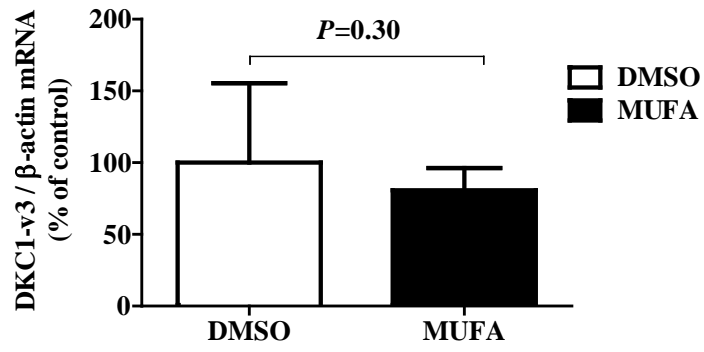


Figure 10 (cont.)

(C)



(D)

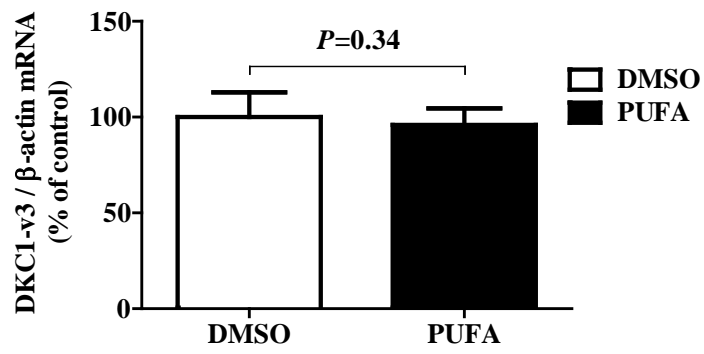
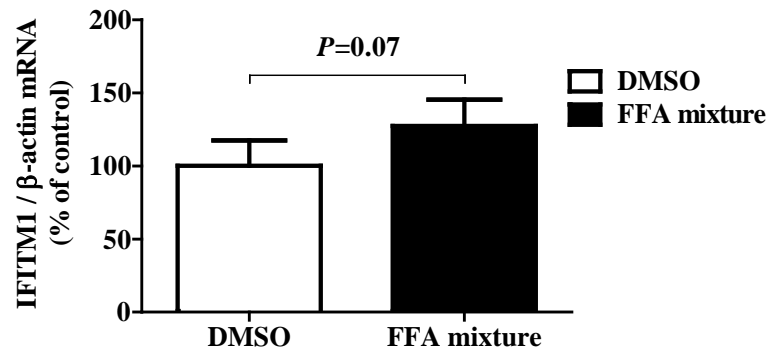


Figure 11: The influence of the FFA component of total hydrolysis products on *IFITM1* expression in THP-1 macrophages

THP-1 macrophages were incubated for 18 hours with a vehicle control (DMSO) or with (A) a 0.68 mM total FFA mixture representing the FFA component of total lipoprotein hydrolysis products liberated by LPL; (B) the saturated fatty acid (SFA) component of the total FFA mixture; (C) the monounsaturated fatty acid (MUFA) component of the total FFA mixture; and (D) the polyunsaturated fatty acid (PUFA) component of the total FFA mixture. RNA were isolated following incubations and used to quantify *IFITM1* by quantitative real-time PCR. All data were normalized to the expression of β -actin, and data are presented as a percent of control \pm SD from three biological replicates.

Figure 11

(A)



(B)

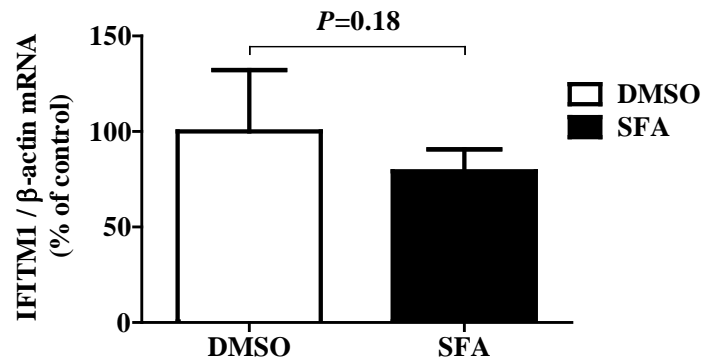
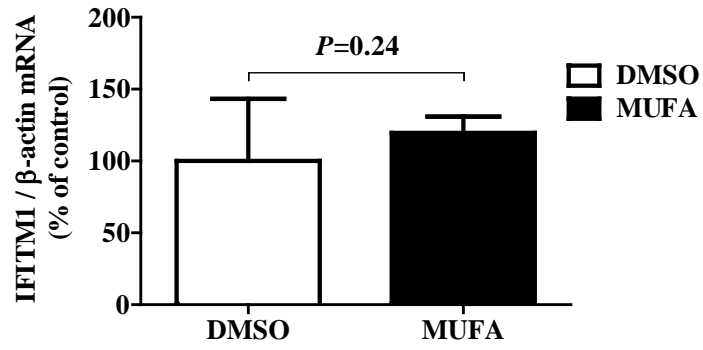


Figure 11 (cont.)

(C)



(D)

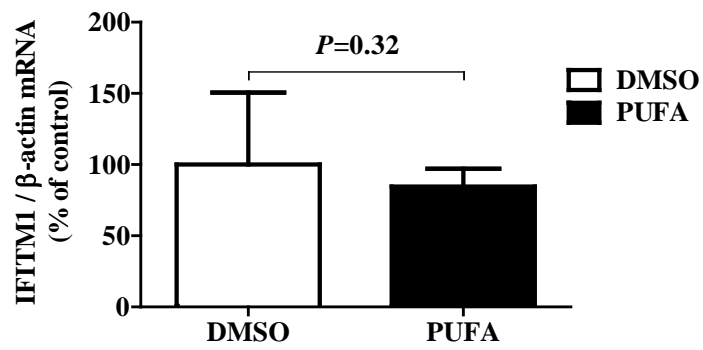
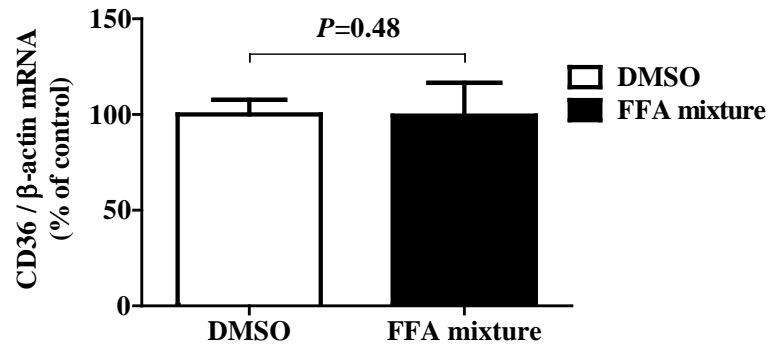


Figure 12: The influence of the FFA component of total hydrolysis products on *CD36* expression in THP-1 macrophages

THP-1 macrophages were incubated for 18 hours with a vehicle control (DMSO) or with (A) a 0.68 mM total FFA mixture representing the FFA component of total lipoprotein hydrolysis products liberated by LPL; (B) the saturated fatty acid (SFA) component of the total FFA mixture; (C) the monounsaturated fatty acid (MUFA) component of the total FFA mixture; and (D) the polyunsaturated fatty acid (PUFA) component of the total FFA mixture. RNA were isolated following incubations and used to quantify *CD36* by quantitative real-time PCR. All data were normalized to the expression of β -actin, and data are presented as a percent of control \pm SD from three biological replicates.

Figure 12

(A)



(B)

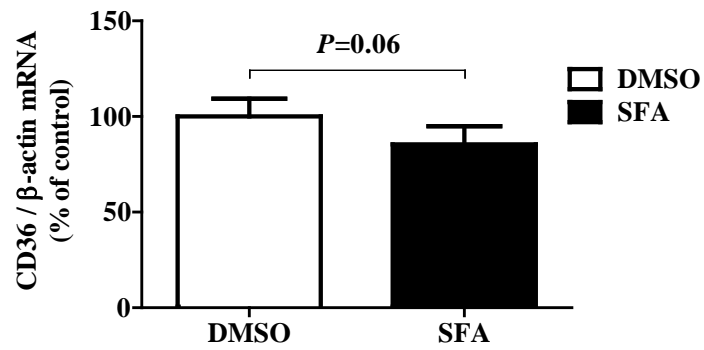
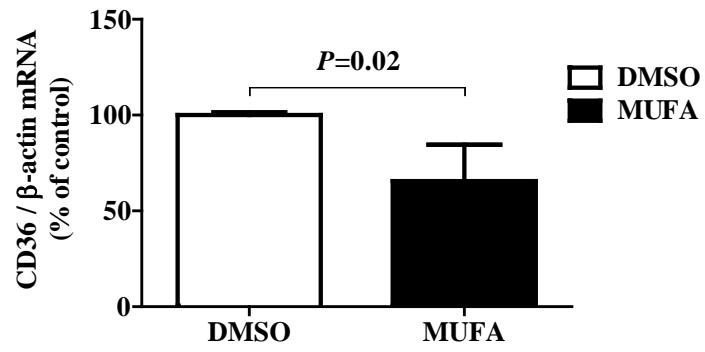


Figure 12 (cont.)

(C)



(D)

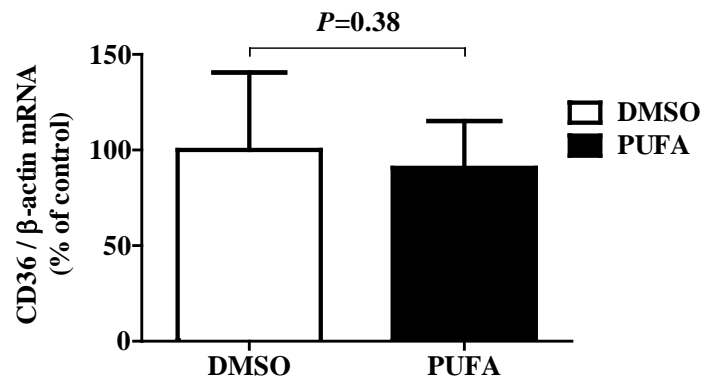
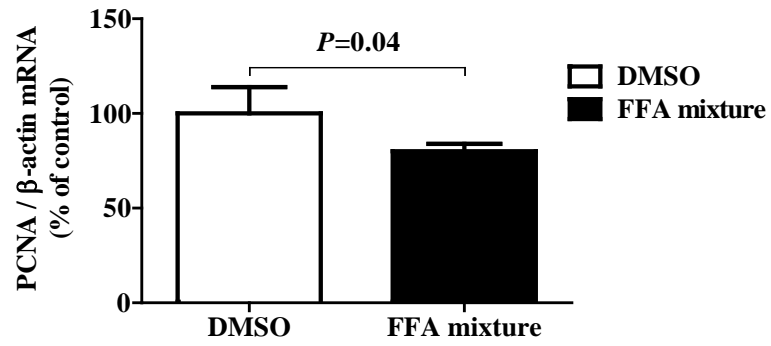


Figure 13: The influence of the FFA component of total hydrolysis products on *PCNA* expression in THP-1 macrophages

THP-1 macrophages were incubated for 18 hours with a vehicle control (DMSO) or with (A) a 0.68 mM total FFA mixture representing the FFA component of total lipoprotein hydrolysis products liberated by LPL; (B) the saturated fatty acid (SFA) component of the total FFA mixture; (C) the monounsaturated fatty acid (MUFA) component of the total FFA mixture; and (D) the polyunsaturated fatty acid (PUFA) component of the total FFA mixture. RNA were isolated following incubations and used to quantify *PCNA* by quantitative real-time PCR. All data were normalized to the expression of β -actin, and data are presented as a percent of control \pm SD from three biological replicates.

Figure 13

(A)



(B)

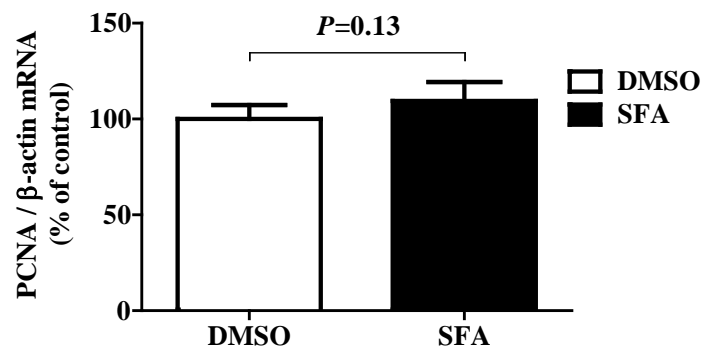
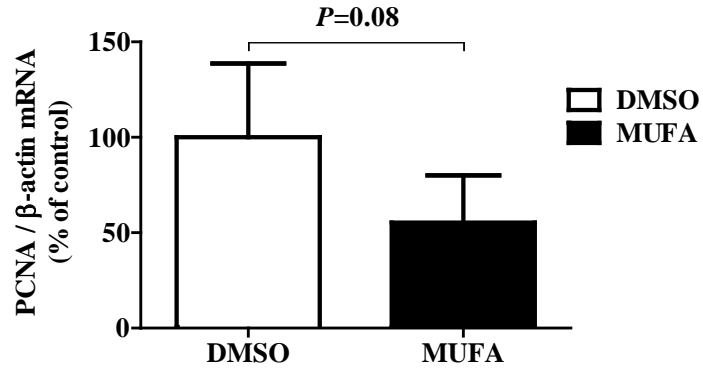


Figure 13 (cont.)

(C)



(D)

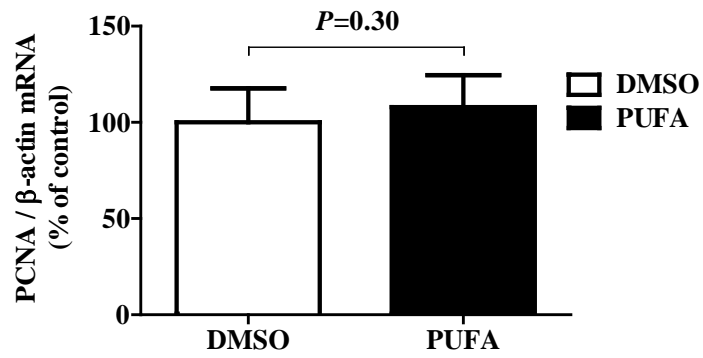
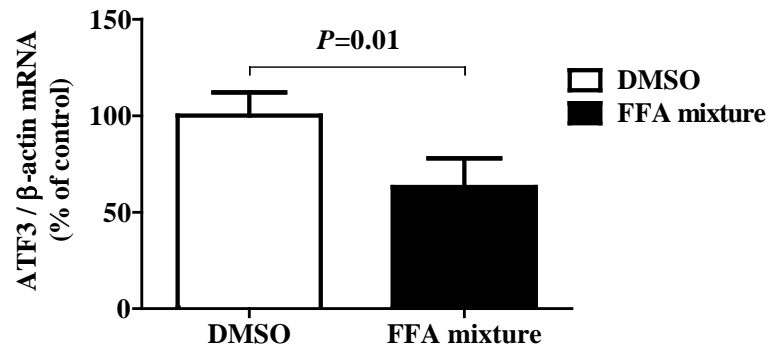


Figure 14: The influence of the FFA component of total hydrolysis products on *ATF3* expression in THP-1 macrophages

THP-1 macrophages were incubated for 18 hours with a vehicle control (DMSO) or with (A) a 0.68 mM total FFA mixture representing the FFA component of total lipoprotein hydrolysis products liberated by LPL; (B) the saturated fatty acid (SFA) component of the total FFA mixture; (C) the monounsaturated fatty acid (MUFA) component of the total FFA mixture; and (D) the polyunsaturated fatty acid (PUFA) component of the total FFA mixture. RNA were isolated following incubations and used to quantify *ATF3* by quantitative real-time PCR. All data were normalized to the expression of β -actin, and data are presented as a percent of control \pm SD from three biological replicates.

Figure 14

(A)



(B)

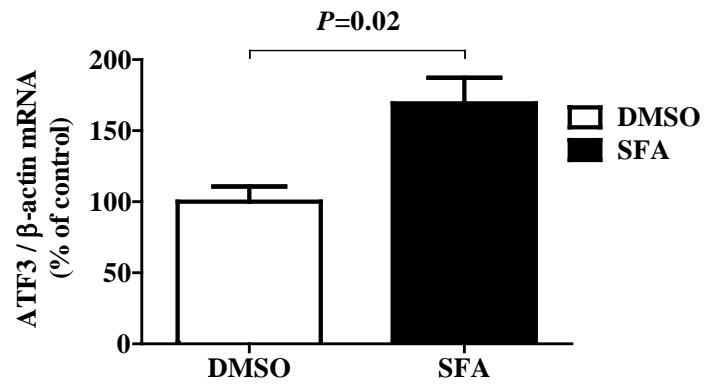
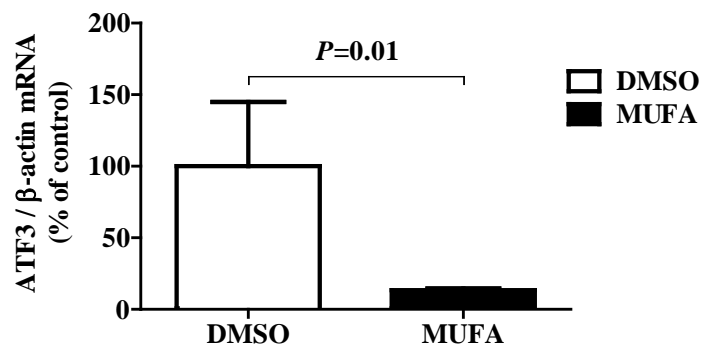


Figure 14 (cont.)

(C)



(D)

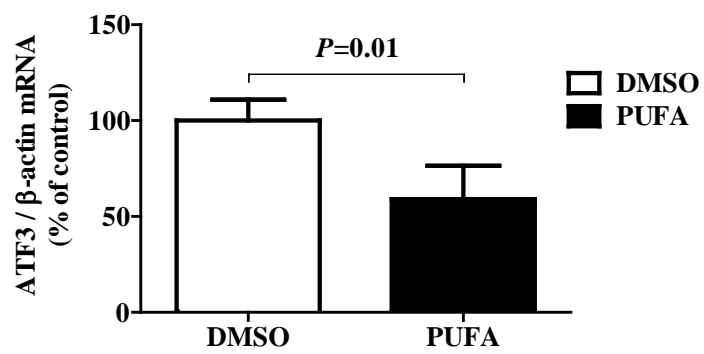
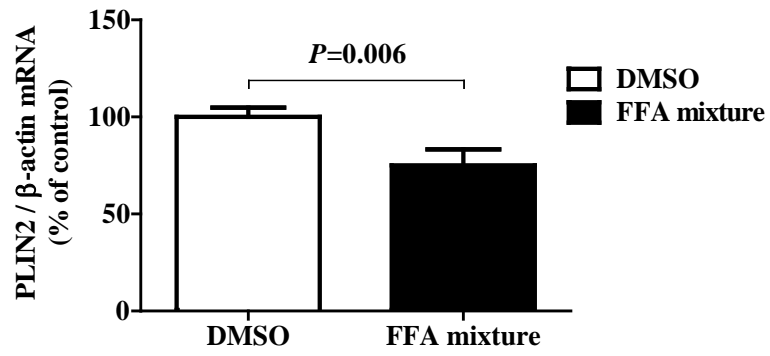


Figure 15: The influence of the FFA component of total hydrolysis products on *PLIN2* expression in THP-1 macrophages

THP-1 macrophages were incubated for 18 hours with a vehicle control (DMSO) or with (A) a 0.68 mM total FFA mixture representing the FFA component of total lipoprotein hydrolysis products liberated by LPL; (B) the saturated fatty acid (SFA) component of the total FFA mixture; (C) the monounsaturated fatty acid (MUFA) component of the total FFA mixture; and (D) the polyunsaturated fatty acid (PUFA) component of the total FFA mixture. RNA were isolated following incubations and used to quantify *PLIN2* by quantitative real-time PCR. All data were normalized to the expression of β -actin, and data are presented as a percent of control \pm SD from three biological replicates.

Figure 15

(A)



(B)

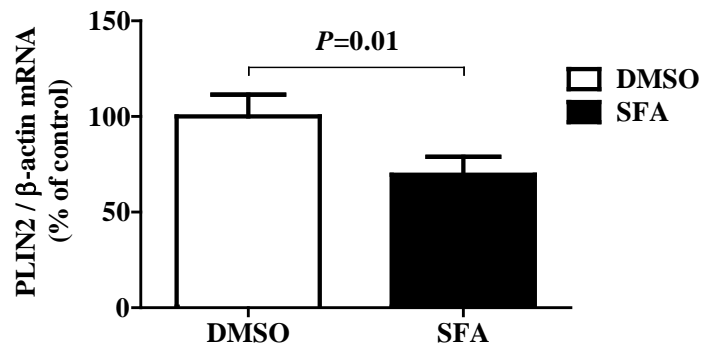
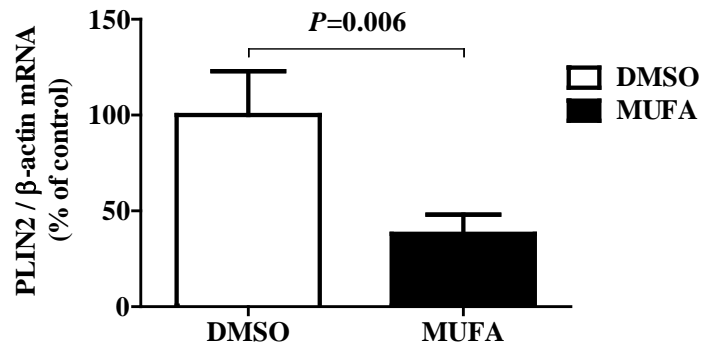
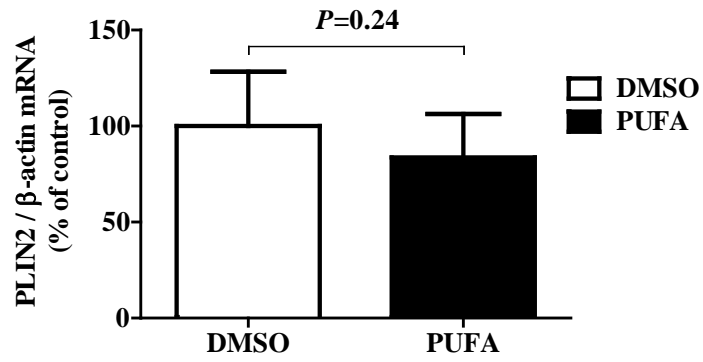


Figure 15 (cont.)

(C)



(D)



FFA mixture reduced the expression of *PCNA*, each class of FFA did not affect its expression (Figure 13). *ATF3* was the only gene from our validated genes that responded to each class of FFA: SFA treatment increased expression by 69%, MUFA treatment reduced expression by 87%, and PUFA treatment reduced expression by 41% (Figure 14B-D). The expression of *PLIN2* significantly decreased by 30% in response to SFA (Figure 14B) and significantly decreased by 62% in response to MUFA (Figure 15C), but no differences were observed in response to PUFA (Figure 15D).

Chapter 4: Discussion

4.1 Modulation of snoRNA Expression by FFA Components within LPL Hydrolysis Products may Affect Ribosome Biogenesis in Human Macrophages

In this study, we performed a transcriptomic analysis to assess changes in gene expression by THP-1 macrophages when exposed to the hydrolysis products that were liberated from total lipoproteins by LPL. The most interesting result, though the most difficult to decipher, was the increased expression of several snoRNA molecules. These non-coding small RNA molecules play a central role in guiding chemical modifications, particularly in ribosomal RNA, transfer RNA, and small nuclear RNA. The snoRNAs are classified as either H/ACA box-type or C/D box-type, based on their sequence recognition motifs; H/ACA box-type snoRNAs guide pseudouridylation and C/D box-type snoRNAs guide methylation (166). The integrity of the THP-1 RNA that was isolated following incubations with total lipoprotein hydrolysis products was consistently lower versus control cells. Liu *et al.* (167) previously reported that mistargeted chemical modifications can also induce ribosomal RNA degradation and impair cell growth. The roles and targets of most snoRNAs are not known, although recent studies have established an emerging role of snoRNAs in other cellular functions, such as roles in unfolded protein responses (168) and regulating cholesterol transport between the plasma membrane and ER (169). It is possible that snoRNAs play a direct role in the differentiation of macrophages into foam cells, possibly by modifying ribosomal RNA and leading to an arrest of cell growth. While this is an attractive hypothesis, a significant amount of work is needed to decipher which

snoRNA, or combination of snoRNAs, may be involved. In the present study, the expression of two H/ACA box-type snoRNAs, *SNORA56* and *SNORA75* were evaluated, within THP-1 macrophages in response to total lipoprotein hydrolysis products, as well as in response to the FFA component of hydrolysis products. *SNORA75* is encoded within the 12th intron of *NCL*, the gene encoding nucleolin. *SNORA75* has been reported to guide pseudouridylation in 18S ribosomal RNA (170,171). Our quantitative real-time PCR data failed to validate any change in *SNORA75* expression, and together with a lack of change to the expression of *NCL* (based on microarray data) within THP-1 macrophages in response to total lipoprotein hydrolysis products. *SNORA56* is encoded within the 12th intron of *DKC1*, and it has been reported to guide pseudouridylation in 28S ribosomal RNA (171,172). Intriguingly, a specific variant of *DKC1*, variant 3, has been shown to retain the sequence of *SNORA56* in its mature mRNA (173), and thus in addition to *SNORA56*, *DKC1-v3* expression was also evaluated; its function is not well understood. The total lipoprotein hydrolysis products generated by LPL increased the expression of *DKC1-v3* and *SNORA56*, but the total FFA component had no influence on their expression. This suggests that other components of LPL hydrolysis products play a role in regulating their expression. However, the SFA component of the total FFA did alter the expression of selected snoRNA genes. Michel *et al.* (174) had previously shown that SFA can induce the expression of three C/D box snoRNAs that are encoded in the *RPL13A* gene in Chinese hamster ovary cells, and a knockdown of these snoRNAs using antisense oligonucleotides protected cells against palmitate-induced cell lipotoxicity. While the functions of *SNORA75* and *DKC1-v3/snoRNA56* remain to be clearly elucidated, it is possible that

total lipoprotein hydrolysis products from dyslipidemic subjects with high levels of plasma SFA would alter their function by altering expression. SFAs are well known to induce lipotoxicity and pro-inflammatory responses in cells. High levels of plasma SFAs could not only induce metabolic stress in cells, but it could also possibly affect the regulation of DNA binding transcription factors, that in turn will modify gene expression levels. However, the mechanisms by which SFAs control the activity of transcription factors remains to be elucidated.

4.2 LPL Hydrolysis Products Alter Select Cell Cycling Gene in THP-1 Macrophages

Using immunocytochemistry studies, Gordon *et al.* (163) reported that smooth muscle cell (SMC) and macrophage cell proliferation occur at low rates in the atherosclerotic plaques of human arteries and carotid balloon catheter injured rat arteries, suggesting that the cell cycling process may be altered in foam cells. In this study, enrichment analyses results showed that the genes associated with select cell cycle processes were all down-regulated except *DKC1-v3*, which indicates that the LPL hydrolysis products may hinder macrophage cell proliferation and may be triggering them to form foam cells. Among the differentially regulated cell cycle genes, *PCNA* was selected as this gene plays a substantial role in DNA replication and repair, and serves as a marker for cell proliferation across different cell cycle stages, such as G1, S, and G2 phases (175). In our study, we observed a reduced expression of *PCNA* mRNA in THP-1 macrophages treated with total lipoprotein hydrolysis products generated by LPL, as well as with the total FFA component of the hydrolysis products. Previously, Artwohl *et al.* (176)

established the effects of individual fatty acids on impairing different cell cycle stages in human umbilical vein endothelial cells. Their results showed that individual species of FFA did arrest the cell cycle of human umbilical vein endothelial cells at concentrations of up to 300 μ M, demonstrating that distinct FFA species do affect cell proliferation; however, it is likely in our study that either the concentrations of FFA within our incubations with SFA, MUFA, or PUFA did not achieve a minimum threshold to affect *PCNA* expression, or the correct combination of these FFA, as present in the total FFA mixture, was not present in the SFA, MUFA, and PUFA mixtures.

4.3 The Role of LPL Hydrolysis Products and their FFA Components in Modulating Select Stress Response Gene in Human Macrophages

Previously, studies have established a correlation between ER stress in macrophages and atherogenesis. For instance, Zhou *et al.* (177) observed that unfolded protein response (UPR) activation occurs at both the early-lesion stage and advanced-lesion stage in apoE-null mice fed with chow diet. However, UPR stimulation and cholesterol accumulation did not correlate with macrophage apoptotic cell death in the early-lesion stage. A previous study showed that ER stress stimulated lipid accumulation in macrophages and regulated macrophage phenotype differentiation (178). The authors also showed that the suppression of ER stress shifted the M2 macrophage phenotype toward an M1 phenotype, which promoted HDL and apoA-I-mediated cholesterol efflux in macrophages (178). In addition, Myoishi *et al.* (179) studied ER stress in coronary artery segments from autopsied patients and atherectomy specimens from patients with unstable

angina pectoris; the authors reported that ER stress and apoptosis were increased in macrophages and SMCs found in the thin-cap of atheroma and ruptured plaques. The genes involved in stress responses were another biological process that was of intrigue, since all genes involved in this process were significantly up-regulated.

ATF3, a transcription factor that belongs to the cyclic AMP responsive element-binding protein family, and participates in the stress response (180) was selectively validated. Aung *et al.* (181) previously showed that LPL lipolytic products increase the expression of *ATF3* in aortic endothelial cells. My data are in agreement with this study, such that *ATF3* expression was increased in THP-1 macrophages in the presence of total lipoprotein hydrolysis products generated by LPL. It is worth noting that *ATF3*-null mice were shown to be resistant to vascular apoptosis (181), thus my data augment the *in vivo* study, by suggesting that LPL and likely its hydrolysis products are pro-atherogenic in nature within macrophages, in part through its influence on *ATF3* expression. However, the attempt to dissect how FFA affects *ATF3* expression revealed a complex story, such that the total FFA mixture, as well as the MUFA and PUFA mixtures, reduced the expression of *ATF3*, while the SFA mixture raised the levels of *ATF3*. Consistent with the latter observation, Krogmann *et al.* (182) and Suganami *et al.* (183) also reported that SFA treatments induce *ATF3* expression in HAECs and in RAW264 macrophage cells. However, unsaturated fatty acids did not significantly change *ATF3* expression in their studies, but significant reduction in *ATF3* mRNA expression was noticed upon unsaturated fatty acid treatment in my study. This controversy emphasizes the need for further study in the future.

4.4 The Effects of LPL Hydrolysis Products and the FFA Components in Impairing Macrophage Immune Response

Previous studies have shed some light on the role type I interferon signaling in atherosclerosis. Although the effect of type I interferon signaling in cellular antiviral responses is well established, the absence of type I interferon signaling in myeloid cells had been shown to reduce atherosclerosis in LDLR- and apoE-null mice (184). All genes associated with type I interferon signaling were downregulated in my study, which indicates that the LPL hydrolysis products may negatively affect immune function of macrophages. *IFITM1*, which showed a maximum fold-change compared to other genes in this process, was selected for analysis. The *IFITM1* gene is regulated by type 1 interferon and is involved in immune response signaling (185). A recent microarray study assessing monocyte-derived macrophages from human subjects with systemic lupus erythematosus and atherosclerosis showed decreases in many signal transduction genes, including *IFITM1* (165). This study suggested that macrophage-derived foam cells likely have compromised immune responses (165). However, the siRNA-mediated inhibition of *IFITM1* has been shown to inhibit cell proliferation and to increase cell death in estrogen receptor-positive human breast cancer cell lines (186) – two processes that occur during the differentiation of macrophages into foam cells, ultimately contributing to atherosclerosis development. My validation data confirmed a decrease in *IFITM1* expression in response to total lipoprotein hydrolysis products generated by LPL; however, mixtures of purified FFA did not affect its expression. Thus, it is likely that components other than FFA within the total lipoprotein hydrolysis products are involved modulating the expression of *IFITM1*.

4.5 LPL Hydrolysis Products, but not their FFA Components, Induce Lipid Accumulation Genes in Human Macrophages

In my study, I verified the microarray data and showed by quantitative real-time PCR that the expression of *CD36* was increased in THP-1 macrophages treated with total lipoprotein hydrolysis products generated by LPL. CD36 is a well-known class B scavenger receptor that has been reported to uptake lipids into macrophages, but its roles are still not well understood, as evidenced by conflicting studies that showed its deletion in mouse models to either reduce atherosclerosis or have no effect (187). My data showing that the expression of CD36 in response to FFA adds to this controversy. Vallvé *et al.* (188) previously reported that treating THP-1 macrophages with 10 μM MUFA or PUFA increased the expression of CD36, whereas no changes were observed with SFA at as high as 100 μM . The latter observation is consistent with those in my study, however, I observed that only the MUFA component of total lipoprotein hydrolysis products liberated by LPL affected CD36 expression, though negatively. A possible explanation behind these differences would be differences of FFA concentration, as the total MUFA and PUFA concentrations used in my study, which match those observed in total lipoprotein hydrolysis products generated by LPL, were 335.5 μM and 1.3 μM , respectively. The total FFA concentrations in my study were within physiological levels that are seen within the bloodstream (148), and thus it is possible that my data reflect some of the *in vivo* controversies of CD36.

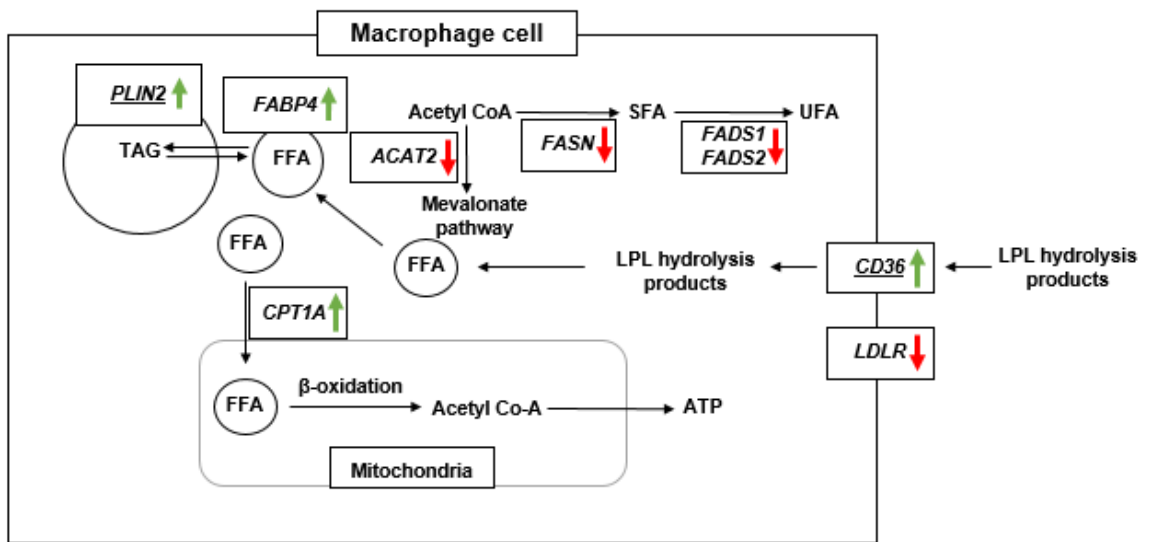
I showed that the expression of *PLIN2*, which encodes the lipid droplet-associated protein perilipin 2, is decreased in the presence of the FFA component of LPL hydrolysis products, as well as in the presence of its SFA and MUFA components. However, this is in contrast to the effect of total lipoprotein hydrolysis products, which significantly increased the expression of *PLIN2* in THP-1 macrophages. These data are comparable to those by Varela *et al.* (189), who showed that TG-rich lipoproteins increased the perilipin 2 protein in THP-1 macrophages. It is very likely that hydrolysis products other than FFA, specifically one or more molecular species of diacylglycerol and lysophospholipid, contribute to the expression of *PLIN2*; these expression remain to be identified.

In addition to the expression of both *CD36* and *PLIN2* being upregulated in THP-1 macrophages in response to total lipoprotein hydrolysis products generated by LPL, my microarray data also show an increased expression of *CPT1A* (which encodes carnitine palmitoyltransferase 1A) and *FABP4* (which encodes fatty acid binding protein 4). In addition, the data show a decreased expression of *ACAT2* (which encodes acetyl-CoA acetyltransferase 2), *FASN* (which encodes fatty acid synthase), and both *FADS1* and *FADS2* (which encode fatty acid desaturase 1 and 2, respectively). It was previously reported that lipoprotein hydrolysis products generated by LPL decrease the expression of *FASN* in THP-1 macrophages (77). Overall, the data for these other lipid metabolism genes suggest that THP-1 macrophages are attempting to process the excess lipid, likely by increasing intracellular fatty acid transport and increasing transfer of fatty acids into mitochondria for oxidation, while likely reducing lipid synthesis (Figure. 13). However,

Figure 16: Lipoprotein hydrolysis products generated by LPL modulates lipid-associated genes

Differentially expressed lipid metabolism genes in THP-1 macrophages in response to LPL hydrolysis products. Our microarray data showed that LPL hydrolysis products enhanced the expression levels of *CD36*, *FABP4*, *PLIN2*, and *CPT1A* in THP-1 macrophages. This suggests that some of the total lipoprotein hydrolysis products that are generated by LPL may be brought into the cells via CD36, the FFA component within the hydrolysis products may be shuttled within the cells by FABP4, and the FFA may be either brought to the mitochondria, where increased β -oxidation may be occurring (as suggested with the increase of *CPT1A* expression), or to be re-esterified into TG and stored in lipid droplets (as suggested with the increase of *PLIN2* expression). On the other hand, our microarray data showed that genes associated with intracellular FFA synthesis (*FASN*, *FADS1*, and *FADS2*), isoprenoid biosynthesis (*ACAT2*), and low-density lipoprotein-cholesterol endocytosis (*LDLR*) were downregulated in response to LPL hydrolysis products. Up arrow (green) denotes an upregulated gene, whereas a down arrow (red) denoted a downregulated gene. The expression levels of genes that were also assessed in separate experiments via quantitative real-time PCR are underlined; the PCR data were similar to those from the microarray data. The quantitative real-time PCR analysis of *FASN* in response to LPL hydrolysis products was previously reported.

Figure 16



the cells continue to accumulate lipid (possibly via CD36 uptake) and store lipid (which accounts for an increase of *PLIN2* expression), ultimately resulting in pathogenic foam cell formation.

4.6 Study Limitations

In this study, the array data showed increases in *SNORA56/DKCI-v3* expression levels. To assess the gene expression using real-time PCR, primer sequences specific for both *SNORA56* and *DKCI-v3* were designed. Although the sequences did not overlap, it is hard to distinguish the effects of our treatment in modulating *SNORA56* or *DKCI-v3* alone, as *SNORA56* sequences are retained within exon 12 of *DKCI-v3*. In my study, the relative expression levels of both these genes were comparable. This suggests that the observed effects of total lipoprotein hydrolysis products or FFA was only reflecting *DKCI-v3* expression. However, there is also a possibility that the expression of intronic *SNORA56* from other *DKCI* variants was influenced.

Microarray analyses were performed on THP-1 macrophages exposed to 0.68 mM LPL hydrolysis products, based on FFA content. However, the hydrolysis products incubated with macrophages is a complex mixture that contains wide range of lipids including cholesterol, CE, TG, monoglycerides, diglycerides, lysophospholipids, in addition to FFAs. Thus, the effects of LPL hydrolysis products in modulating macrophage transcript levels may not necessarily mimic the effects of FFA components within the hydrolysis products. Moreover, it is very hard to confirm which components in the hydrolysis products are responsible for altering each and every gene. Although the effects

of a purified FFA mixture or individual FFA classes in altering select genes were quantified, it does not provide a solid basis to understand the impact of FFA components within LPL hydrolysis products in foam cell formation.

The use of microarrays provides a complete mRNA expression profile and they can cover non-coding RNA transcripts that may affect mRNA expression. However, they only provide information at the transcriptional level. The changes seen in mRNA expression may not necessarily mean that a similar trend will be observed with regards to protein translation and function. The gene expression is regulated post-transcriptionally and post-translationally at different levels, and the half-lives of mRNA and protein vary. Thus, caution must be taken with the interpretations behind the transcriptomic data from THP-1 macrophages in response to LPL hydrolysis products and FFA.

4.7 Future Perspectives

Recent studies have identified the emerging new non-canonical functions of snoRNA in addition to their role in ribosome synthesis (169). Interestingly, some snoRNA species have also shown to possess microRNA capabilities (190). Thus suggesting that snoRNAs can play a role in post-transcriptional modifications. My array data suggested that LPL hydrolysis products modulate several snoRNAs. The effects of the select snoRNAs could be studied in the context of atherosclerosis. Antisense oligonucleotides could be used to inhibit select snoRNA expression in macrophages and high-throughput sequencing, such as RNA sequencing, could be performed on macrophages exposed to purified FFA mixtures to comprehensively study their role in affecting genes associated with foam cell formation.

My study showed that the LPL hydrolysis products affect *SNORA56/DKC1-v3* expression in macrophages. The function of this specific variant is not yet clearly understood. Intron retention in *DKC1-v3* suggests that this specific variant may also have a unique function. Studying the loss-of-function and the gain-of-function of *DKC1-v3* in human macrophages in the presence of LPL hydrolysis products will provide us with insights on the role of these hydrolysis products in macrophage-derived foam cell formation.

Suganami *et al.* (183) showed that the overexpression of ATF3 in RAW264 macrophages suppresses the expression of the pro-inflammatory cytokine TNF- α . This suggests that the increased expression of this transcriptional repressor in LPL hydrolysis product-treated macrophages may be a feedback mechanism to suppress the expression of pro-inflammatory cytokines. Quantifying the protein levels of both ATF3 and TNF- α in macrophages exposed to LPL hydrolysis products is of future interest. Understanding how ATF3 controls the expression pro-inflammatory cytokines in macrophages will make it a therapeutic target in future. *In vitro* knockdown of ATF3 in human macrophages and then exposing to either LPL hydrolysis products or purified FFA mixture will help us unravel the underlying mechanisms in foam cell formation.

4.8 Overall Conclusion

This study has shown for the first time that LPL hydrolysis products may impair ribosome biogenesis by affecting non-coding snoRNA expression levels in human macrophages and, thus, opening windows for new perspectives into how LPL functions in

atherosclerosis. My data suggest that LPL hydrolysis products affect genes associated with cell cycling, stress response, and interferon type I signaling in THP-1 macrophages. The hydrolysis products that are generated by LPL from total lipoprotein lipids appear to positively affect processes in THP-1 macrophages that are associated with atherosclerosis. This is consistent with the known promotion of atherosclerosis by macrophage LPL, but my data provide some insight into the molecular mechanisms behind this process in the early stages of macrophage to foam cell conversion. Although the effects of total lipoprotein hydrolysis products generated by LPL appeared to not exclusively be the act of the FFA components in hydrolysis products, the FFA nonetheless did influence the expression of select genes in THP-1 macrophages.

References

1. Mendis, S., Puska, P., and Norrving, B. (2011) *Global atlas on cardiovascular disease prevention and control*, World Health Organization, Geneva
2. Mozaffarian, D., Benjamin, E. J., Go, A. S., Arnett, D. K., Blaha, M. J., Cushman, M., de Ferranti, S., Despres, J.-P., Fullerton, H. J., and Howard, V. J. (2015) Heart disease and stroke statistics-2015 update: a report from the American Heart Association. *Circulation* **131**, e29
3. Stary, H. C. (2000) Natural history and histological classification of atherosclerotic lesions an update. *Arteriosclerosis, Thrombosis, and Vascular Biology* **20**, 1177-1178
4. Ross, R. (1995) Cell biology of atherosclerosis. *Annual Review of Physiology* **57**, 791-804
5. Williams, K. J., and Tabas, I. (1995) The response-to-retention hypothesis of early atherogenesis. *Arteriosclerosis, Thrombosis, and Vascular Biology* **15**, 551-561
6. Goldstein, J. L., Ho, Y., Basu, S. K., and Brown, M. S. (1979) Binding site on macrophages that mediates uptake and degradation of acetylated low density lipoprotein, producing massive cholesterol deposition. *Proceedings of the National Academy of Sciences of the United States of America* **76**, 333-337
7. Brown, M. S., Basu, S. K., Falck, J., Ho, Y., and Goldstein, J. L. (1980) The scavenger cell pathway for lipoprotein degradation: Specificity of the binding site that mediates the uptake of negatively-charged LDL by macrophages. *Journal of Supramolecular Structure* **13**, 67-81
8. Moore, K. J., Kunjathoor, V. V., Koehn, S. L., Manning, J. J., Tseng, A. A., Silver, J. M., McKee, M., and Freeman, M. W. (2005) Loss of receptor-mediated lipid uptake via scavenger receptor A or CD36 pathways does not ameliorate atherosclerosis in hyperlipidemic mice. *The Journal of Clinical Investigation* **115**, 2192-2201
9. Kruth, H. S., Huang, W., Ishii, I., and Zhang, W.-Y. (2002) Macrophage foam cell formation with native low density lipoprotein. *The Journal of Biological Chemistry* **277**, 34573-34580
10. Kruth, H. S., Jones, N. L., Huang, W., Zhao, B., Ishii, I., Chang, J., Combs, C. A., Malide, D., and Zhang, W.-Y. (2005) Macropinocytosis is the endocytic pathway that mediates macrophage foam cell formation with native low density lipoprotein. *The Journal of Biological Chemistry* **280**, 2352-2360
11. Hakala, J. K., Oksjoki, R., Laine, P., Du, H., Grabowski, G. A., Kovanen, P. T., and Pentikäinen, M. O. (2003) Lysosomal enzymes are released from cultured human macrophages, hydrolyze LDL in vitro, and are present extracellularly in human atherosclerotic lesions. *Arteriosclerosis, Thrombosis, and Vascular Biology* **23**, 1430-1436
12. Yanagi, H., Sasaguri, Y., Sugama, K., Morimatsu, M., and Nagase, H. (1991) Production of tissue collagenase (matrix metalloproteinase 1) by human aortic smooth muscle cells in response to platelet-derived growth factor. *Atherosclerosis* **91**, 207-216

13. Small, D. M. (1988) George Lyman Duff memorial lecture. Progression and regression of atherosclerotic lesions. Insights from lipid physical biochemistry. *Arteriosclerosis, Thrombosis, and Vascular Biology* **8**, 103-129
14. Katz, S., Shipley, G. G., and Small, D. (1976) Physical chemistry of the lipids of human atherosclerotic lesions. Demonstration of a lesion intermediate between fatty streaks and advanced plaques. *The Journal of Clinical Investigation* **58**, 200-211
15. Zilversmit, D. B. (1979) Atherogenesis: a postprandial phenomenon. *Circulation* **60**, 473-485
16. Navab, M., Berliner, J. A., Subbanagounder, G., Hama, S., Lusis, A. J., Castellani, L. W., Reddy, S., Shih, D., Shi, W., and Watson, A. D. (2001) HDL and the inflammatory response induced by LDL-derived oxidized phospholipids. *Arteriosclerosis, Thrombosis, and Vascular Biology* **21**, 481-488
17. Tabas, I., Li, Y., Brocia, R. W., Xu, S. W., Swenson, T. L., and Williams, K. J. (1993) Lipoprotein lipase and sphingomyelinase synergistically enhance the association of atherogenic lipoproteins with smooth muscle cells and extracellular matrix. A possible mechanism for low density lipoprotein and lipoprotein (a) retention and macrophage foam cell formation. *The Journal of Biological Chemistry* **268**, 20419-20432
18. Shimada, M., Shimano, H., Gotoda, T., Yamamoto, K., Kawamura, M., Inaba, T., Yazaki, Y., and Yamada, N. (1993) Overexpression of human lipoprotein lipase in transgenic mice. Resistance to diet-induced hypertriglyceridemia and hypercholesterolemia. *The Journal of Biological Chemistry* **268**, 17924-17929
19. Shimada, M., Ishibashi, S., Inaba, T., Yagyu, H., Harada, K., Osuga, J.-I., Ohashi, K., Yazaki, Y., and Yamada, N. (1996) Suppression of diet-induced atherosclerosis in low density lipoprotein receptor knockout mice overexpressing lipoprotein lipase. *Proceedings of the National Academy of Sciences of the United States of America* **93**, 7242-7246
20. Tsutsumi, K., Inoue, Y., Shima, A., Iwasaki, K., Kawamura, M., and Murase, T. (1993) The novel compound NO-1886 increases lipoprotein lipase activity with resulting elevation of high density lipoprotein cholesterol, and long-term administration inhibits atherogenesis in the coronary arteries of rats with experimental atherosclerosis. *The Journal of Clinical Investigation* **92**, 411-417
21. Babaev, V. R., Patel, M. B., Semenkovich, C. F., Fazio, S., and Linton, M. F. (2000) Macrophage lipoprotein lipase promotes foam cell formation and atherosclerosis in low density lipoprotein receptor-deficient mice. *The Journal of Biological Chemistry* **275**, 26293-26299
22. Babaev, V. R., Fazio, S., Gleaves, L. A., Carter, K. J., Semenkovich, C. F., and Linton, M. F. (1999) Macrophage lipoprotein lipase promotes foam cell formation and atherosclerosis in vivo. *The Journal of Clinical Investigation* **103**, 1697-1705
23. Wilson, K., Fry, G. L., Chappell, D. A., Sigmund, C. D., and Medh, J. D. (2001) Macrophage-specific expression of human lipoprotein lipase accelerates atherosclerosis in transgenic apolipoprotein e knockout mice but not in C57BL/6 mice. *Arteriosclerosis, Thrombosis, and Vascular Biology* **21**, 1809-1815

24. Kawashima, R. L., and Medh, J. D. (2014) Down-regulation of lipoprotein lipase increases ABCA1-mediated cholesterol efflux in THP-1 macrophages. *Biochemical and Biophysical Research Communications* **450**, 1416-1421
25. Mamputu, J., Desfaits, A., and Renier, G. (1997) Lipoprotein lipase enhances human monocyte adhesion to aortic endothelial cells. *Journal of Lipid Research* **38**, 1722-1729
26. Obunike, J. C., Paka, S., Pillarisetti, S., and Goldberg, I. J. (1997) Lipoprotein lipase can function as a monocyte adhesion protein. *Arteriosclerosis, Thrombosis, and Vascular Biology* **17**, 1414-1420
27. Den Hartigh, L. J., Altman, R., Norman, J. E., and Rutledge, J. C. (2014) Postprandial VLDL lipolysis products increase monocyte adhesion and lipid droplet formation via activation of ERK2 and NFκB. *American Journal of Physiology-Heart and Circulatory Physiology* **306**, H109-H120
28. Skipski, V. P. (1972) Lipid composition of lipoproteins in normal and diseased states. *Blood Lipids and Lipoproteins: Quantitation, Composition and Metabolism*, 471-583
29. Nilsson-Ehle, P., Garfinkel, A. S., and Schotz, M. C. (1980) Lipolytic enzymes and plasma lipoprotein metabolism. *Annual Review of Biochemistry* **49**, 667-693
30. Jonas, A., and Phillips, M. C. (2008) Lipoprotein structure. *Biochemistry of Lipids, Lipoproteins and Membranes* 5 ed., Elsevier, The Netherlands
31. Hussain, M. M., Kancha, R. K., Zhou, Z., Luchoomun, J., Zu, H., and Bakillah, A. (1996) Chylomicron assembly and catabolism: role of apolipoproteins and receptors. *Biochimica et Biophysica Acta (BBA)-Lipids and Lipid Metabolism* **1300**, 151-170
32. Sherrill, B., Innerarity, T., and Mahley, R. (1980) Rapid hepatic clearance of the canine lipoproteins containing only the E apoprotein by a high affinity receptor. Identity with the chylomicron remnant transport process. *The Journal of Biological Chemistry* **255**, 1804-1807
33. Soutar, A., Myant, N., and Thompson, G. (1982) The metabolism of very low density and intermediate density lipoproteins in patients with familial hypercholesterolaemia. *Atherosclerosis* **43**, 217-231
34. Zambon, A., Bertocco, S., Vitturi, N., Polentarutti, V., Vianello, D., and Crepaldi, G. (2003) Relevance of hepatic lipase to the metabolism of triacylglycerol-rich lipoproteins. *Biochemical Society Transactions* **31**, 1070-1074
35. Fielding, C. J., and Phoebe, E. F. (2008) Dynamics of lipoprotein transport in the circulatory system. *Biochemistry of Lipids, Lipoproteins and Membranes* 5 ed., Elsevier, The Netherlands
36. Glomset, J. A. (1968) The plasma lecithin: cholesterol acyltransferase reaction. *Journal of Lipid Research* **9**, 155-167
37. Lewis, G. F., and Rader, D. J. (2005) New insights into the regulation of HDL metabolism and reverse cholesterol transport. *Circulation Research* **96**, 1221-1232
38. Kunitake, S. T., La Sala, K., and Kane, J. P. (1985) Apolipoprotein AI-containing lipoproteins with pre-beta electrophoretic mobility. *Journal of Lipid Research* **26**, 549-555

39. Oram, J. F., Lawn, R. M., Garvin, M. R., and Wade, D. P. (2000) ABCA1 is the cAMP-inducible apolipoprotein receptor that mediates cholesterol secretion from macrophages. *The Journal of Biological Chemistry* **275**, 34508-34511
40. Aiello, R. J., Brees, D., Bourassa, P.-A., Royer, L., Lindsey, S., Coskran, T., Haghpassand, M., and Francone, O. L. (2002) Increased atherosclerosis in hyperlipidemic mice with inactivation of ABCA1 in macrophages. *Arteriosclerosis, Thrombosis, and Vascular Biology* **22**, 630-637
41. Kennedy, M. A., Barrera, G. C., Nakamura, K., Baldán, Á., Tarr, P., Fishbein, M. C., Frank, J., Francone, O. L., and Edwards, P. A. (2005) ABCG1 has a critical role in mediating cholesterol efflux to HDL and preventing cellular lipid accumulation. *Cell Metabolism* **1**, 121-131
42. Rothblat, G. H., de la Llera-Moya, M., Atger, V., Kellner-Weibel, G., Williams, D. L., and Phillips, M. C. (1999) Cell cholesterol efflux: integration of old and new observations provides new insights. *Journal of Lipid Research* **40**, 781-796
43. Chawla, A., Boisvert, W. A., Lee, C.-H., Laffitte, B. A., Barak, Y., Joseph, S. B., Liao, D., Nagy, L., Edwards, P. A., and Curtiss, L. K. (2001) A PPAR γ -LXR-ABCA1 pathway in macrophages is involved in cholesterol efflux and atherogenesis. *Molecular Cell* **7**, 161-171
44. Mehlum, A., Muri, M., Hagve, T. A., Solberg, L. Å., and Prydz, H. (1997) Mice overexpressing human lecithin: cholesterol acyltransferase are not protected against diet-induced atherosclerosis. *Acta Pathologica, Microbiologica, et Immunologica, Scandinavica* **105**, 861-868
45. Zannis, V. I., Chroni, A., and Krieger, M. (2006) Role of apoA-I, ABCA1, LCAT, and SR-BI in the biogenesis of HDL. *Journal of Molecular Medicine* **84**, 276-294
46. Albers, J. J., Tollefson, J. H., Chen, C.-H., and Steinmetz, A. (1984) Isolation and characterization of human plasma lipid transfer proteins. *Arteriosclerosis, Thrombosis, and Vascular Biology* **4**, 49-58
47. van Haperen, R., van Tol, A., Vermeulen, P., Jauhiainen, M., van Gent, T., van den Berg, P., Ehnholm, S., Grosveld, F., van der Kamp, A., and de Crom, R. (2000) Human plasma phospholipid transfer protein increases the antiatherogenic potential of high density lipoproteins in transgenic mice. *Arteriosclerosis, Thrombosis, and Vascular Biology* **20**, 1082-1088
48. Inazu, A., Brown, M. L., Hesler, C. B., Agellon, L. B., Koizumi, J., Takata, K., Maruhama, Y., Mabuchi, H., and Tall, A. R. (1990) Increased high-density lipoprotein levels caused by a common cholesteryl-ester transfer protein gene mutation. *The New England Journal of Medicine* **323**, 1234-1238
49. Jaye, M., Lynch, K. J., Krawiec, J., Marchadier, D., Maugeais, C., Doan, K., South, V., Amin, D., Perrone, M., and Rader, D. J. (1999) A novel endothelial-derived lipase that modulates HDL metabolism. *Nature Genetics* **21**, 424-428
50. Clay, M. A., Newnham, H. H., and Barter, P. J. (1991) Hepatic lipase promotes a loss of apolipoprotein AI from triglyceride-enriched human high density lipoproteins during incubation in vitro. *Arteriosclerosis, Thrombosis, and Vascular Biology* **11**, 415-422

51. Wang, N., Arai, T., Ji, Y., Rinninger, F., and Tall, A. R. (1998) Liver-specific overexpression of scavenger receptor BI decreases levels of very low density lipoprotein ApoB, low density lipoprotein ApoB, and high density lipoprotein in transgenic mice. *The Journal of Biological Chemistry* **273**, 32920-32926
52. Varban, M. L., Rinninger, F., Wang, N., Fairchild-Huntress, V., Dunmore, J. H., Fang, Q., Gosselin, M. L., Dixon, K. L., Deeds, J. D., and Acton, S. L. (1998) Targeted mutation reveals a central role for SR-BI in hepatic selective uptake of high density lipoprotein cholesterol. *Proceedings of the National Academy of Sciences of the United States of America* **95**, 4619-4624
53. Miksztowicz, V., Schreier, L., McCoy, M., Lucero, D., Fassio, E., Billheimer, J., Rader, D. J., and Berg, G. (2014) Role of SN1 lipases on plasma lipids in metabolic syndrome and obesity. *Arteriosclerosis, Thrombosis, and Vascular Biology* **34**, 669-675
54. Kobayashi, J., Applebaum-Bowden, D., Dugi, K. A., Brown, D. R., Kashyap, V. S., Parrott, C., Duarte, C., Maeda, N., and Santamarina-Fojo, S. (1996) Analysis of Protein Structure-Function in Vivo Adenovirus-mediated transfer of lipase lid mutants in hepatic lipase-deficient mice. *The Journal of Biological Chemistry* **271**, 26296-26301
55. Strauss, J. G., Marianne, H., Zechner, R., Levak-Frank, S., and Frank, S. (2003) Fatty acids liberated from high-density lipoprotein phospholipids by endothelial-derived lipase are incorporated into lipids in HepG2 cells. *Biochemical Journal* **371**, 981-988
56. Eisenberg, S., Sehayek, E., Olivecrona, T., and Vlodavsky, I. (1992) Lipoprotein lipase enhances binding of lipoproteins to heparan sulfate on cell surfaces and extracellular matrix. *The Journal of Clinical Investigation* **90**, 2013-2021
57. Hide, W., Chan, L., and Li, W. (1992) Structure and evolution of the lipase superfamily. *Journal of Lipid Research* **33**, 167-178
58. Blanchette-Mackie, E. J., Masuno, H., Dwyer, N. K., Olivecrona, T., and Scow, R. (1989) Lipoprotein lipase in myocytes and capillary endothelium of heart: immunocytochemical study. *American Journal of Physiology-Endocrinology And Metabolism* **256**, E818-E828
59. Camps, L., Reina, M., Llobera, M., Vilaro, S., and Olivecrona, T. (1990) Lipoprotein lipase: cellular origin and functional distribution. *American Journal of Physiology-Cell Physiology* **258**, C673-C681
60. Camps, L., Reina, M., Llobera, M., Bengtsson-Olivecrona, G., Olivecrona, T., and Vilaro, S. (1991) Lipoprotein lipase in lungs, spleen, and liver: synthesis and distribution. *Journal of Lipid Research* **32**, 1877-1888
61. Stein, O., Stein, Y., Schwartz, S. P., Reshef, A., Chajek-Shaul, T., Ben-Naim, M., Friedman, G., and Leitersdorf, E. (1991) Expression of lipoprotein lipase mRNA in rat heart is localized mainly to mesenchymal cells as studied by in situ hybridization. *Arteriosclerosis, Thrombosis, and Vascular Biology* **11**, 857-863
62. Mead, J. R., Irvine, S. A., and Ramji, D. P. (2002) Lipoprotein lipase: structure, function, regulation, and role in disease. *Journal of Molecular Medicine* **80**, 753-769

63. Verhoeven, A., and Jansen, H. (1996) The rat hepatic lipase gene is expressed into two different proteins in liver, adrenals and ovaries. *Zeitschrift für Gastroenterologie* **34**, 54-55
64. Schoonderwoerd, K., Hom, M., Luthjens, L., Vieira, v. B. D., and Jansen, H. (1996) Functional molecular mass of rat hepatic lipase in liver, adrenal gland and ovary is different. *Biochemistry Journal* **318**, 463-467
65. Perret, B., Mabile, L., Martinez, L., Tercé, F., Barbaras, R., and Collet, X. (2002) Hepatic lipase structure/function relationship, synthesis, and regulation. *Journal of Lipid Research* **43**, 1163-1169
66. Hirata, K.-i., Dichek, H. L., Cioffi, J. A., Choi, S. Y., Leeper, N. J., Quintana, L., Kronmal, G. S., Cooper, A. D., and Quertermous, T. (1999) Cloning of a unique lipase from endothelial cells extends the lipase gene family. *The Journal of Biological Chemistry* **274**, 14170-14175
67. McCoy, M. G., Sun, G.-S., Marchadier, D., Maugeais, C., Glick, J. M., and Rader, D. J. (2002) Characterization of the lipolytic activity of endothelial lipase. *Journal of Lipid Research* **43**, 921-929
68. Weinstock, P. H., Bisgaier, C. L., Aalto-Setälä, K., Radner, H., Ramakrishnan, R., Levak-Frank, S., Essenburg, A., Zechner, R., and Breslow, J. (1995) Severe hypertriglyceridemia, reduced high density lipoprotein, and neonatal death in lipoprotein lipase knockout mice. Mild hypertriglyceridemia with impaired very low density lipoprotein clearance in heterozygotes. *The Journal of Clinical Investigation* **96**, 2555
69. Coleman, T., Seip, R. L., Gimble, J. M., Lee, D., Maeda, N., and Semenkovich, C. F. (1995) COOH-terminal disruption of lipoprotein lipase in mice is lethal in homozygotes, but heterozygotes have elevated triglycerides and impaired enzyme activity. *The Journal of Biological Chemistry* **270**, 12518-12525
70. Ishida, T., Choi, S., Kundu, R. K., Hirata, K.-i., Rubin, E. M., Cooper, A. D., and Quertermous, T. (2003) Endothelial lipase is a major determinant of HDL level. *The Journal of Clinical Investigation* **111**, 347-355
71. Ehnholm, C., Shaw, W., Greten, H., and Brown, W. (1975) Purification from human plasma of a heparin-released lipase with activity against triglyceride and phospholipids. *The Journal of Biological Chemistry* **250**, 6756-6761
72. Miksztowicz, V., McCoy, M. G., Schreier, L., Cacciagiú, L., Elbert, A., Gonzalez, A. I., Billheimer, J., Eacho, P., Rader, D. J., and Berg, G. (2012) Endothelial Lipase Activity Predicts High-Density Lipoprotein Catabolism in Hemodialysis Novel Phospholipase Assay in Postheparin Human Plasma. *Arteriosclerosis, Thrombosis, and Vascular Biology* **32**, 3033-3040
73. Nicoll, A., and Lewis, B. (1980) Evaluation of the roles of lipoprotein lipase and hepatic lipase in lipoprotein metabolism: in vivo and in vitro studies in man. *European Journal of Clinical Investigation* **10**, 487-495
74. Connelly, P. W. (1999) The role of hepatic lipase in lipoprotein metabolism. *Clinica Chimica Acta* **286**, 243-255
75. Berg, G. A., Siseles, N., González, A. I., Ortiz, O. C., Tempone, A., and Wikinski, R. W. (2001) Higher values of hepatic lipase activity in postmenopause:

- relationship with atherogenic intermediate density and low density lipoproteins. *Menopause* **8**, 51-57
76. Miksztowicz, V., Lucero, D., Zago, V., Cacciagiu, L., Lopez, G., Gonzalez Ballerga, E., Sordá, J., Fassio, E., Schreier, L., and Berg, G. (2012) Hepatic lipase activity is increased in non-alcoholic fatty liver disease beyond insulin resistance. *Diabetes/Metabolism Research and Reviews* **28**, 535-541
 77. Yang, Y., Thyagarajan, N., Coady, B. M., and Brown, R. J. (2014) Cholesterol efflux from THP-1 macrophages is impaired by the fatty acid component from lipoprotein hydrolysis by lipoprotein lipase. *Biochemical and Biophysical Research Communications* **451**, 632-636
 78. Freeman, L., Amar, M. J., Shamburek, R., Paigen, B., Brewer, H. B., Santamarina-Fojo, S., and González-Navarro, H. (2007) Lipolytic and ligand-binding functions of hepatic lipase protect against atherosclerosis in LDL receptor-deficient mice. *Journal of Lipid Research* **48**, 104-113
 79. González-Navarro, H., Nong, Z., Amar, M. J., Shamburek, R. D., Najib-Fruchart, J., Paigen, B. J., Brewer, H. B., and Santamarina-Fojo, S. (2004) The ligand-binding function of hepatic lipase modulates the development of atherosclerosis in transgenic mice. *The Journal of Biological Chemistry* **279**, 45312-45321
 80. Nong, Z., González-Navarro, H., Amar, M., Freeman, L., Knapper, C., Neufeld, E. B., Paigen, B. J., Hoyt, R. F., Fruchart-Najib, J., and Santamarina-Fojo, S. (2003) Hepatic lipase expression in macrophages contributes to atherosclerosis in apoE-deficient and LCAT-transgenic mice. *The Journal of Clinical Investigation* **112**, 367-378
 81. Brown, R. J., and Rader, D. J. (2007) Lipases as modulators of atherosclerosis in murine models. *Current Drug Targets* **8**, 1307-1319
 82. Badellino, K. O., Wolfe, M. L., Reilly, M. P., and Rader, D. J. (2006) Endothelial lipase concentrations are increased in metabolic syndrome and associated with coronary atherosclerosis. *PLOS Medicine* **3**, 245
 83. Azumi, H., Hirata, K.-i., Ishida, T., Kojima, Y., Rikitake, Y., Takeuchi, S., Inoue, N., Kawashima, S., Hayashi, Y., and Itoh, H. (2003) Immunohistochemical localization of endothelial cell-derived lipase in atherosclerotic human coronary arteries. *Cardiovascular Research* **58**, 647-654
 84. Qiu, G., and Hill, J. S. (2009) Endothelial lipase promotes apolipoprotein AI-mediated cholesterol efflux in THP-1 macrophages. *Arteriosclerosis, Thrombosis, and Vascular Biology* **29**, 84-91
 85. Deeb, S. S., and Peng, R. (1989) Structure of the human lipoprotein lipase gene. *Biochemistry* **28**, 4131-4135
 86. Van Tilbeurgh, H., Roussel, A., Lalouel, J.-M., and Cambillau, C. (1994) Lipoprotein lipase. Molecular model based on the pancreatic lipase x-ray structure: consequences for heparin binding and catalysis. *The Journal of Biological Chemistry* **269**, 4626-4633
 87. Wong, H., Davis, R. C., Thuren, T., Goers, J. W., Nikazy, J., Waite, M., and Schotz, M. C. (1994) Lipoprotein lipase domain function. *The Journal of Biological Chemistry* **269**, 10319-10323

88. Lookene, A., and Bengtsson-Olivecrona, G. (1993) Chymotryptic cleavage of lipoprotein lipase. *European Journal of Biochemistry* **213**, 185-194
89. Dugi, K., Dichek, H., Talley, G., Brewer, H., and Santamarina-Fojo, S. (1992) Human lipoprotein lipase: the loop covering the catalytic site is essential for interaction with lipid substrates. *The Journal of Biological Chemistry* **267**, 25086-25091
90. Faustinella, F., Smith, L., Semenkovich, C., and Chan, L. (1991) Structural and functional roles of highly conserved serines in human lipoprotein lipase. Evidence that serine 132 is essential for enzyme catalysis. *The Journal of Biological Chemistry* **266**, 9481-9485
91. Henderson, H., Ma, Y., Liu, M., Clark-Lewis, I., Maeder, D., Kastelein, J., Brunzell, J., and Hayden, M. (1993) Structure-function relationships of lipoprotein lipase: mutation analysis and mutagenesis of the loop region. *Journal of Lipid Research* **34**, 1593-1602
92. Wong, H., Yang, D., Hill, J. S., Davis, R. C., Nikazy, J., and Schotz, M. C. (1997) A molecular biology-based approach to resolve the subunit orientation of lipoprotein lipase. *Proceedings of the National Academy of Sciences of the United States of America* **94**, 5594-5598
93. Osborne Jr, J. C., Bengtsson-Olivecrona, G., Lee, N. S., and Olivecrona, T. (1985) Studies on inactivation of lipoprotein lipase: role of the dimer to monomer dissociation. *Biochemistry* **24**, 5606-5611
94. Vannier, C., and Ailhaud, G. (1989) Biosynthesis of lipoprotein lipase in cultured mouse adipocytes. II. Processing, subunit assembly, and intracellular transport. *The Journal of Biological Chemistry* **264**, 13206-13216
95. Semb, H., and Olivecrona, T. (1989) The relation between glycosylation and activity of guinea pig lipoprotein lipase. *The Journal of Biological Chemistry* **264**, 4195-4200
96. Masuno, H., Blanchette-Mackie, E., Chernick, S., and Scow, R. (1990) Synthesis of inactive nonsecretable high mannose-type lipoprotein lipase by cultured brown adipocytes of combined lipase-deficient cld/cld mice. *The Journal of Biological Chemistry* **265**, 1628-1638
97. Ben-Zeev, O., Doolittle, M., Davis, R., Elovson, J., and Schotz, M. (1992) Maturation of lipoprotein lipase. Expression of full catalytic activity requires glucose trimming but not translocation to the cis-Golgi compartment. *The Journal of Biological Chemistry* **267**, 6219-6227
98. Péterfy, M., Ben-Zeev, O., Mao, H. Z., Weissglas-Volkov, D., Aouizerat, B. E., Pullinger, C. R., Frost, P. H., Kane, J. P., Malloy, M. J., and Reue, K. (2007) Mutations in LMF1 cause combined lipase deficiency and severe hypertriglyceridemia. *Nature Genetics* **39**, 1483-1487
99. Hosseini, M., Ehrhardt, N., Weissglas-Volkov, D., Lai, C.-M., Mao, H. Z., Liao, J.-L., Nikkola, E., Bensadoun, A., Taskinen, M.-R., and Doolittle, M. H. (2012) Transgenic expression and genetic variation of Lmf1 affect LPL activity in mice and humans. *Arteriosclerosis, Thrombosis, and Vascular Biology* **32**, 1204-1210

100. Sha, H., Sun, S., Francisco, A. B., Ehrhardt, N., Xue, Z., Liu, L., Lawrence, P., Mattijssen, F., Guber, R. D., and Panhwar, M. S. (2014) The ER-associated degradation adaptor protein Sel1L regulates LPL secretion and lipid metabolism. *Cell Metabolism* **20**, 458-470
101. Beigneux, A. P., Davies, B. S., Gin, P., Weinstein, M. M., Farber, E., Qiao, X., Peale, F., Bunting, S., Walzem, R. L., and Wong, J. S. (2007) Glycosylphosphatidylinositol-anchored high-density lipoprotein-binding protein 1 plays a critical role in the lipolytic processing of chylomicrons. *Cell Metabolism* **5**, 279-291
102. Korn, E. D. (1955) Clearing factor, a heparin-activated lipoprotein lipase I. Isolation and characterization of the enzyme from normal rat heart. *The Journal of Biological Chemistry* **215**, 1-14
103. Braun, J., and Severson, D. L. (1992) Regulation of the synthesis, processing and translocation of lipoprotein lipase. *Biochemical Journal* **287**, 337
104. Eisenberg, S., and Rachmilewitz, D. (1975) Interaction of rat plasma very low density lipoprotein with lipoprotein lipase-rich (postheparin) plasma. *Journal of Lipid Research* **16**, 341-351
105. Saxena, U., Witte, L., and Goldberg, I. (1989) Release of endothelial cell lipoprotein lipase by plasma lipoproteins and free fatty acids. *The Journal of Biological Chemistry* **264**, 4349-4355
106. Vilella, E., Joven, J., Fernandez, M., Vilaro, S., Brunzell, J., Olivecrona, T., and Bengtsson-Olivecrona, G. (1993) Lipoprotein lipase in human plasma is mainly inactive and associated with cholesterol-rich lipoproteins. *Journal of Lipid Research* **34**, 1555-1564
107. Beisiegel, U., and Heeren, J. (1997) Lipoprotein lipase (EC 3.1. 1.34) targeting of lipoproteins to receptors. *Proceedings of the Nutrition Society of the United States of America* **56**, 731-737
108. Yang, W.-S., and Deeb, S. S. (1998) Sp1 and Sp3 transactivate the human lipoprotein lipase gene promoter through binding to a CT element: synergy with the sterol regulatory element binding protein and reduced transactivation of a naturally occurring promoter variant. *Journal of Lipid Research* **39**, 2054-2064
109. Schoonjans, K., Peinado-Onsurbe, J., Lefebvre, A.-M., Heyman, R. A., Briggs, M., Deeb, S., Staels, B., and Auwerx, J. (1996) PPARalpha and PPARgamma activators direct a distinct tissue-specific transcriptional response via a PPRE in the lipoprotein lipase gene. *The EMBO Journal* **15**, 5336
110. Blanchard, P.-G., Festuccia, W. T., Houde, V. P., St-Pierre, P., Brule, S., Turcotte, V., Cote, M., Bellmann, K., Marette, A., and Deshaies, Y. (2012) Major involvement of mTOR in the PPAR γ -induced stimulation of adipose tissue lipid uptake and fat accretion. *Journal of Lipid Research* **53**, 1117-1125
111. Chawla, A., Lee, C.-H., Barak, Y., He, W., Rosenfeld, J., Liao, D., Han, J., Kang, H., and Evans, R. M. (2003) PPAR δ is a very low-density lipoprotein sensor in macrophages. *Proceedings of the National Academy of Sciences of the United States of America* **100**, 1268-1273

112. Lee, C.-H., Kang, K., Mehl, I. R., Nofsinger, R., Alaynick, W. A., Chong, L.-W., Rosenfeld, J. M., and Evans, R. M. (2006) Peroxisome proliferator-activated receptor δ promotes very low-density lipoprotein-derived fatty acid catabolism in the macrophage. *Proceedings of the National Academy of Sciences of the United States of America* **103**, 2434-2439
113. Ruby, M. A., Goldenson, B., Orasanu, G., Johnston, T. P., Plutzky, J., and Krauss, R. M. (2010) VLDL hydrolysis by LPL activates PPAR- α through generation of unbound fatty acids. *Journal of Lipid Research* **51**, 2275-2281
114. Zhang, Y., Repa, J. J., Gauthier, K., and Mangelsdorf, D. J. (2001) Regulation of lipoprotein lipase by the oxysterol receptors, LXR α and LXR β . *The Journal of Biological Chemistry* **276**, 43018-43024
115. Tengku-Muhammad, T. S., Cryer, A., and Ramji, D. P. (1998) Synergism between interferon γ and tumour necrosis factor α in the regulation of lipoprotein lipase in the macrophage J774. 2 cell line. *Cytokine* **10**, 38-48
116. Morin, C. L., Schlaepfer, I. R., and Eckel, R. H. (1995) Tumor necrosis factor- α eliminates binding of NF- κ B and an octamer-binding protein to the lipoprotein lipase promoter in 3T3-L1 adipocytes. *The Journal of Clinical Investigation* **95**, 1684-1689
117. Irvine, S. A., Foka, P., Rogers, S. A., Mead, J. R., and Ramji, D. P. (2005) A critical role for the Sp1-binding sites in the transforming growth factor- β -mediated inhibition of lipoprotein lipase gene expression in macrophages. *Nucleic Acids Research* **33**, 1423-1434
118. Kraemer, F. B., Takeda, D., Natsu, V., and Sztalryd, C. (1998) Insulin regulates lipoprotein lipase activity in rat adipose cells via wortmannin- and rapamycin-sensitive pathways. *Metabolism* **47**, 555-559
119. Ranganathan, G., Li, C., and Kern, P. A. (2000) The translational regulation of lipoprotein lipase in diabetic rats involves the 3'-untranslated region of the lipoprotein lipase mRNA. *The Journal of Biological Chemistry* **275**, 40986-40991
120. Kern, P., Ranganathan, G., Yukht, A., Ong, J., and Davis, R. (1996) Translational regulation of lipoprotein lipase by thyroid hormone is via a cytoplasmic repressor that interacts with the 3'untranslated region. *Journal of Lipid Research* **37**, 2332-2340
121. Ranganathan, G., Phan, D., Pokrovskaya, I. D., McEwen, J. E., Li, C., and Kern, P. A. (2002) The translational regulation of lipoprotein lipase by epinephrine involves an RNA binding complex including the catalytic subunit of protein kinase A. *The Journal of Biological Chemistry* **277**, 43281-43287
122. Peterson, J., Bihain, B. E., Bengtsson-Olivecrona, G., Deckelbaum, R. J., Carpentier, Y. A., and Olivecrona, T. (1990) Fatty acid control of lipoprotein lipase: a link between energy metabolism and lipid transport. *Proceedings of the National Academy of Sciences of the United States of America* **87**, 909-913
123. Ahn, J., Lee, H., Chung, C. H., and Ha, T. (2011) High fat diet induced downregulation of microRNA-467b increased lipoprotein lipase in hepatic steatosis. *Biochemical and Biophysical Research Communications* **414**, 664-669

124. Tian, G.-P., Tang, Y.-Y., He, P.-P., Lv, Y.-C., Ouyang, X.-P., Zhao, G.-J., Tang, S.-L., Wu, J.-F., Wang, J.-L., and Peng, J. (2014) The effects of miR-467b on lipoprotein lipase (LPL) expression, pro-inflammatory cytokine, lipid levels and atherosclerotic lesions in apolipoprotein E knockout mice. *Biochemical and Biophysical Research Communications* **443**, 428-434
125. Bergö, M., Wu, G., Ruge, T., and Olivecrona, T. (2002) Down-regulation of adipose tissue lipoprotein lipase during fasting requires that a gene, separate from the lipase gene, is switched on. *The Journal of Biological Chemistry* **277**, 11927-11932
126. Sukonina, V., Lookene, A., Olivecrona, T., and Olivecrona, G. (2006) Angiotensin-like protein 4 converts lipoprotein lipase to inactive monomers and modulates lipase activity in adipose tissue. *Proceedings of the National Academy of Sciences of the United States of America* **103**, 17450-17455
127. Renier, G., Skamene, E., DeSanctis, J., and Radzioch, D. (1993) High macrophage lipoprotein lipase expression and secretion are associated in inbred murine strains with susceptibility to atherosclerosis. *Arteriosclerosis, Thrombosis, and Vascular Biology* **13**, 190-196
128. Van Eck, M., Zimmermann, R., Groot, P. H., Zechner, R., and Van Berkel, T. J. (2000) Role of macrophage-derived lipoprotein lipase in lipoprotein metabolism and atherosclerosis. *Arteriosclerosis, Thrombosis, and Vascular Biology* **20**, e53-e62
129. Wu, X., Wang, J., Fan, J., Chen, M., Chen, L., Huang, W., and Liu, G. (2006) Localized vessel expression of lipoprotein lipase in rabbits leads to rapid lipid deposition in the balloon-injured arterial wall. *Atherosclerosis* **187**, 65-73
130. Wang, J., Xian, X., Huang, W., Chen, L., Wu, L., Zhu, Y., Fan, J., Ross, C., Hayden, M. R., and Liu, G. (2007) Expression of LPL in endothelial-intact artery results in lipid deposition and vascular cell adhesion molecule-1 upregulation in both LPL and ApoE-deficient mice. *Arteriosclerosis, Thrombosis, and Vascular Biology* **27**, 197-203
131. Takahashi, M., Yagyu, H., Tazoe, F., Nagashima, S., Ohshiro, T., Okada, K., Osuga, J.-i., Goldberg, I. J., and Ishibashi, S. (2013) Macrophage lipoprotein lipase modulates the development of atherosclerosis but not adiposity. *Journal of Lipid Research* **54**, 1124-1134
132. Lindqvist, P., Ostlund-Lindqvist, A., Witztum, J., Steinberg, D., and Little, J. (1983) The role of lipoprotein lipase in the metabolism of triglyceride-rich lipoproteins by macrophages. *The Journal of Biological Chemistry* **258**, 9086-9092
133. Rumsey, S., Obunike, J., Arad, Y., Deckelbaum, R., and Goldberg, I. (1992) Lipoprotein lipase-mediated uptake and degradation of low density lipoproteins by fibroblasts and macrophages. *The Journal of Clinical Investigation* **90**, 1504-1512
134. Makoveichuk, E., Lookene, A., and Olivecrona, G. (1998) Mild oxidation of lipoproteins increases their affinity for surfaces covered by heparan sulfate and lipoprotein lipase. *Biochemical and Biophysical Research Communications* **252**, 703-710

135. Esenabhalu, V. E., Cerimagic, M., Malli, R., Osibow, K., Levak-Frank, S., Frieden, M., Sattler, W., Kostner, G. M., Zechner, R., and Graier, W. F. (2002) Tissue-specific expression of human lipoprotein lipase in the vascular system affects vascular reactivity in transgenic mice. *British Journal of Pharmacology* **135**, 143-154
136. Bharadwaj, K. G., Hiyama, Y., Hu, Y., Huggins, L. A., Ramakrishnan, R., Abumrad, N. A., Shulman, G. I., Blaner, W. S., and Goldberg, I. J. (2010) Chylomicron-and VLDL-derived Lipids Enter the Heart through Different Pathways In Vivo evidence for receptor- and non-receptor-mediated fatty acid uptake. *The Journal of Biological Chemistry* **285**, 37976-37986
137. Essaji, Y., Yang, Y., Albert, C. J., Ford, D. A., and Brown, R. J. (2013) Hydrolysis products generated by lipoprotein lipase and endothelial lipase differentially impact THP-1 macrophage cell signalling pathways. *Lipids* **48**, 769-778
138. Courage, E., Fitzpatrick, M., Elliott, R., Yang, Y., and Brown, R. (2015) The Association of Lipoprotein Lipase and Phosphatidylinositol 3-Kinase with Macrophage Lipid Accumulation. *The FASEB Journal* **29**, 885.26
139. Den Hartigh, L. J., Connolly-Rohrbach, J. E., Fore, S., Huser, T. R., and Rutledge, J. C. (2010) Fatty acids from very low-density lipoprotein lipolysis products induce lipid droplet accumulation in human monocytes. *The Journal of Immunology* **184**, 3927-3936
140. Eiselein, L., Wilson, D. W., Lamé, M. W., and Rutledge, J. C. (2007) Lipolysis products from triglyceride-rich lipoproteins increase endothelial permeability, perturb zonula occludens-1 and F-actin, and induce apoptosis. *American Journal of Physiology-Heart and Circulatory Physiology* **292**, H2745-H2753
141. Eiselein, L., Nyunt, T., Lamé, M. W., Ng, K. F., Wilson, D. W., Rutledge, J. C., and Aung, H. H. (2015) TGRL Lipolysis Products Induce Stress Protein ATF3 via the TGF- β Receptor Pathway in Human Aortic Endothelial Cells. *PLoS ONE* **10**, e0145523
142. Wang, L., Sapuri-Butti, A. R., Aung, H. H., Parikh, A. N., and Rutledge, J. C. (2008) Triglyceride-rich lipoprotein lipolysis increases aggregation of endothelial cell membrane microdomains and produces reactive oxygen species. *American Journal of Physiology-Heart and Circulatory Physiology* **295**, H237-H244
143. Wang, L., Gill, R., Pedersen, T. L., Higgins, L. J., Newman, J. W., and Rutledge, J. C. (2009) Triglyceride-rich lipoprotein lipolysis releases neutral and oxidized FFAs that induce endothelial cell inflammation. *Journal of Lipid Research* **50**, 204-213
144. Augustus, A. S., Buchanan, J., Park, T.-S., Hirata, K., Noh, H.-I., Sun, J., Homma, S., D'armiento, J., Abel, E. D., and Goldberg, I. J. (2006) Loss of lipoprotein lipase-derived fatty acids leads to increased cardiac glucose metabolism and heart dysfunction. *The Journal of Biological Chemistry* **281**, 8716-8723
145. Skottova, N., Savonen, R., Lookene, A., Hultin, M., and Olivecrona, G. (1995) Lipoprotein lipase enhances removal of chylomicrons and chylomicron remnants by the perfused rat liver. *Journal of Lipid Research* **36**, 1334-1344

146. Lehner, R., and Verger, R. (1997) Purification and characterization of a porcine liver microsomal triacylglycerol hydrolase. *Biochemistry* **36**, 1861-1868
147. Griffon, N., Budreck, E. C., Long, C. J., Broedl, U. C., Marchadier, D. H., Glick, J. M., and Rader, D. J. (2006) Substrate specificity of lipoprotein lipase and endothelial lipase: studies of lid chimeras. *Journal of Lipid Research* **47**, 1803-1811
148. Rider, O. J., Holloway, C. J., Emmanuel, Y., Bloch, E., Clarke, K., and Neubauer, S. (2012) Increasing plasma free fatty acids in healthy subjects induces aortic distensibility changes seen in obesity. *Circulation: Cardiovascular Imaging* **5**, 367-375
149. Li, X., Hatanaka, K., Ishibashi-Ueda, H., Yutani, C., and Yamamoto, A. (1995) Characterization of serum amyloid P component from human aortic atherosclerotic lesions. *Arteriosclerosis, Thrombosis, and Vascular Biology* **15**, 252-257
150. Chomczynski, P., and Sacchi, N. (1987) Single-step method of RNA isolation by acid guanidinium thiocyanate-phenol-chloroform extraction. *Analytical Biochemistry* **162**, 156-159
151. Gentleman, R. C., Carey, V. J., Bates, D. M., Bolstad, B., Dettling, M., Dudoit, S., Ellis, B., Gautier, L., Ge, Y., and Gentry, J. (2004) Bioconductor: open software development for computational biology and bioinformatics. *Genome Biology* **5**, R80
152. Team, R. C. (2013) R: A language and environment for statistical computing.
153. Irizarry, R. A., Bolstad, B. M., Collin, F., Cope, L. M., Hobbs, B., and Speed, T. P. (2003) Summaries of Affymetrix GeneChip probe level data. *Nucleic Acids Research* **31**, e15-e15
154. Carvalho, B. S., and Irizarry, R. A. (2010) A framework for oligonucleotide microarray preprocessing. *Bioinformatics* **26**, 2363-2367
155. Ritchie, M. E., Phipson, B., Wu, D., Hu, Y., Law, C. W., Shi, W., and Smyth, G. K. (2015) limma powers differential expression analyses for RNA-sequencing and microarray studies. *Nucleic Acids Research*, gkv007
156. Durinck, S., Spellman, P. T., Birney, E., and Huber, W. (2009) Mapping identifiers for the integration of genomic datasets with the R/Bioconductor package biomaRt. *Nature Protocols* **4**, 1184-1191
157. Durinck, S., Moreau, Y., Kasprzyk, A., Davis, S., De Moor, B., Brazma, A., and Huber, W. (2005) BioMart and Bioconductor: a powerful link between biological databases and microarray data analysis. *Bioinformatics* **21**, 3439-3440
158. Liu, G., Loraine, A. E., Shigeta, R., Cline, M., Cheng, J., Valmееkam, V., Sun, S., Kulp, D., and Siani-Rose, M. A. (2003) NetAffx: Affymetrix probesets and annotations. *Nucleic Acids Research* **31**, 82-86
159. Mostafavi, S., Ray, D., Warde-Farley, D., Grouios, C., and Morris, Q. (2008) GeneMANIA: a real-time multiple association network integration algorithm for predicting gene function. *Genome Biology* **9**, 1
160. Brazma, A., Hingamp, P., Quackenbush, J., Sherlock, G., Spellman, P., Stoeckert, C., Aach, J., Ansorge, W., Ball, C. A., and Causton, H. C. (2001) Minimum information about a microarray experiment (MIAME)—toward standards for microarray data. *Nature Genetics* **29**, 365-371

161. Pfaffl, M. W. (2001) A new mathematical model for relative quantification in real-time RT-PCR. *Nucleic Acids Research* **29**, e45-e45
162. Lestrade, L., and Weber, M. J. (2006) snoRNA-LBME-db, a comprehensive database of human H/ACA and C/D box snoRNAs. *Nucleic Acids Research* **34**, D158-D162
163. Gordon, D., Reidy, M., Benditt, E., and Schwartz, S. (1990) Cell proliferation in human coronary arteries. *Proceedings of the National Academy of Sciences of the United States of America* **87**, 4600-4604
164. Erbay, E., Babaev, V. R., Mayers, J. R., Makowski, L., Charles, K. N., Snitow, M. E., Fazio, S., Wiest, M. M., Watkins, S. M., and Linton, M. F. (2009) Reducing endoplasmic reticulum stress through a macrophage lipid chaperone alleviates atherosclerosis. *Nature Medicine* **15**, 1383-1391
165. Korman, B. D., Huang, C.-C., Skamra, C., Wu, P., Koessler, R., Yao, D., Huang, Q. Q., Pearce, W., Sutton-Tyrrell, K., and Kondos, G. (2014) Inflammatory expression profiles in monocyte-to-macrophage differentiation in patients with systemic lupus erythematosus and relationship with atherosclerosis. *Arthritis Research & Therapy* **16**, R147
166. Kiss, T. (2002) Small nucleolar RNAs: an abundant group of noncoding RNAs with diverse cellular functions. *Cell* **109**, 145-148
167. Liu, B., Liang, X.-h., Piekna-Przybylska, D., Liu, Q., and Fournier, M. J. (2008) Mis-targeted methylation in rRNA can severely impair ribosome synthesis and activity. *RNA Biology* **5**, 249-254
168. Cohen, E., Avrahami, D., Frid, K., Canello, T., Lahad, E. L., Zeligson, S., Perlberg, S., Chapman, J., Cohen, O. S., and Kahana, E. (2013) Snord 3A: a molecular marker and modulator of prion disease progression. *PLOS ONE* **8**, e54433
169. Brandis, K. A., Gale, S., Jinn, S., Langmade, S. J., Dudley-Rucker, N., Jiang, H., Sidhu, R., Ren, A., Goldberg, A., and Schaffer, J. E. (2013) Box C/D small nucleolar RNA (snoRNA) U60 regulates intracellular cholesterol trafficking. *The Journal of Biological Chemistry* **288**, 35703-35713
170. Ganot, P., Bortolin, M.-L., and Kiss, T. (1997) Site-specific pseudouridine formation in preribosomal RNA is guided by small nucleolar RNAs. *Cell* **89**, 799-809
171. Kiss, A. M., Jády, B. E., Bertrand, E., and Kiss, T. (2004) Human box H/ACA pseudouridylation guide RNA machinery. *Molecular and Cellular Biology* **24**, 5797-5807
172. Ofengand, J., and Bakin, A. (1997) Mapping to nucleotide resolution of pseudouridine residues in large subunit ribosomal RNAs from representative eukaryotes, prokaryotes, archaeobacteria, mitochondria and chloroplasts. *Journal of Molecular Biology* **266**, 246-268
173. Turano, M., Angrisani, A., Di Maio, N., and Furia, M. (2013) Intron retention: a human DKC1 gene common splicing event. *Biochemistry and Cell Biology* **91**, 506-512
174. Michel, C. I., Holley, C. L., Scruggs, B. S., Sidhu, R., Brookheart, R. T., Listenberger, L. L., Behlke, M. A., Ory, D. S., and Schaffer, J. E. (2011) Small

- nucleolar RNAs U32a, U33, and U35a are critical mediators of metabolic stress. *Cell Metabolism* **14**, 33-44
175. Giordano, M., Danova, M., Pellicciari, C., Wilson, G. D., Mazzini, G., Conti, A. M. F., Franchini, G., Riccardi, A., and Romanini, M. G. M. (1991) Proliferating cell nuclear antigen (PCNA)/cyclin expression during the cell cycle in normal and leukemic cells. *Leukemia Research* **15**, 965-974
176. Artwohl, M., Roden, M., Waldhäusl, W., Freudenthaler, A., and Baumgartner-Parzer, S. M. (2004) Free fatty acids trigger apoptosis and inhibit cell cycle progression in human vascular endothelial cells. *The FASEB Journal* **18**, 146-148
177. Zhou, J., Lhoták, Š., Hilditch, B. A., and Austin, R. C. (2005) Activation of the unfolded protein response occurs at all stages of atherosclerotic lesion development in apolipoprotein E-deficient mice. *Circulation* **111**, 1814-1821
178. Oh, J., Riek, A. E., Weng, S., Petty, M., Kim, D., Colonna, M., Cella, M., and Bernal-Mizrachi, C. (2012) Endoplasmic reticulum stress controls M2 macrophage differentiation and foam cell formation. *The Journal of Biological Chemistry* **287**, 11629-11641
179. Myoishi, M., Hao, H., Minamino, T., Watanabe, K., Nishihira, K., Hatakeyama, K., Asada, Y., Okada, K.-i., Ishibashi-Ueda, H., and Gabbiani, G. (2007) Increased endoplasmic reticulum stress in atherosclerotic plaques associated with acute coronary syndrome. *Circulation* **116**, 1226-1233
180. Chen, B., Wolfgang, C. D., and Hai, T. (1996) Analysis of ATF3, a transcription factor induced by physiological stresses and modulated by gadd153/Chop10. *Molecular and Cellular Biology* **16**, 1157-1168
181. Aung, H. H., Lame, M. W., Gohil, K., An, C.-I., Wilson, D. W., and Rutledge, J. C. (2013) Induction of ATF3 gene network by triglyceride-rich lipoprotein lipolysis products increases vascular apoptosis and inflammation. *Arteriosclerosis, Thrombosis, and Vascular Biology* **33**, 2088-2096
182. Krogmann, A., Staiger, K., Haas, C., Gommer, N., Peter, A., Heni, M., Machicao, F., Häring, H.-U., and Staiger, H. (2011) Inflammatory response of human coronary artery endothelial cells to saturated long-chain fatty acids. *Microvascular Research* **81**, 52-59
183. Suganami, T., Yuan, X., Shimoda, Y., Uchio-Yamada, K., Nakagawa, N., Shirakawa, I., Usami, T., Tsukahara, T., Nakayama, K., and Miyamoto, Y. (2009) Activating transcription factor 3 constitutes a negative feedback mechanism that attenuates saturated Fatty acid/toll-like receptor 4 signaling and macrophage activation in obese adipose tissue. *Circulation Research* **105**, 25-32
184. Goossens, P., Gijbels, M. J., Zerneck, A., Eijgelaar, W., Vergouwe, M. N., van der Made, I., Vanderlocht, J., Beckers, L., Buurman, W. A., and Daemen, M. J. (2010) Myeloid type I interferon signaling promotes atherosclerosis by stimulating macrophage recruitment to lesions. *Cell Metabolism* **12**, 142-153
185. Yang, G., Xu, Y., Chen, X., and Hu, G. (2007) IFITM1 plays an essential role in the antiproliferative action of interferon- γ . *Oncogene* **26**, 594-603

186. Choi, H. J., Lui, A., Ogony, J., Jan, R., Sims, P. J., and Lewis-Wambi, J. (2015) Targeting interferon response genes sensitizes aromatase inhibitor resistant breast cancer cells to estrogen-induced cell death. *Breast Cancer Research* **17**, 1
187. Witztum, J. L. (2005) You are right too! *The Journal of Clinical Investigation* **115**, 2072-2075
188. Vallvé, J.-C., Uliaque, K., Girona, J., Cabré, A., Ribalta, J., Heras, M., and Masana, L. s. (2002) Unsaturated fatty acids and their oxidation products stimulate CD36 gene expression in human macrophages. *Atherosclerosis* **164**, 45-56
189. Varela, L. M., López, S., Ortega-Gómez, A., Bermúdez, B., Buers, I., Robenek, H., Muriana, F. J., and Abia, R. (2015) Postprandial triglyceride-rich lipoproteins regulate perilipin-2 and perilipin-3 lipid-droplet-associated proteins in macrophages. *The Journal of Nutritional Biochemistry* **26**, 327-336
190. Ender, C., Krek, A., Friedländer, M. R., Beitzinger, M., Weinmann, L., Chen, W., Pfeffer, S., Rajewsky, N., and Meister, G. (2008) A human snoRNA with microRNA-like functions. *Molecular Cell* **32**, 519-528

Appendix I: Supplementary methods

R-studio Scripts: Functions used to obtain a list of differentially regulated genes in LPL hydrolysis product-treated macrophage cells. # represents the purpose of using any commands

```
>setwd("~/R/nammiR/lplmicroarray") # to set working directory
>source("https://bioconductor.org/biocLite.R") # source to find packages
>biocLite("hugene20sttranscriptcluster.db") # to install the packages
>library(hugene20sttranscriptcluster.db) # package that is required analyze human gene array
>library(oligo) # command that helps to read CEL file format
>celfiles <- list.celfiles() # to load CEL files
>celfiles
>data <- read.celfiles(celfiles) # to read data in CEL file format
>data
>hist(data) # quality assessment step; histogram analyzes of raw data before normalization
>boxplot(data) # quality assessment step; boxplot analysis of raw data before normalization
>image(data) # gives image of raw data intensities
>genes <- rma(data) # normalizes the data and performs background correction
>genes
>hist(genes) # histogram analyses of data after normalization
>boxplot(genes) # boxplot analyses of data after normalization
>library(limma) # package needed for analyses of differentially regulated genes
>design <- model.matrix(~0+factor(c(1,1,1,2,2,2))) # function that creates a matrix design for 2
treatments with 3 replicates
>colnames(design) <- c("N","H") # command that assigns row or column names for matrix c, where
N represents non-hydrolysis product and H represents hydrolysis product
>design # function that helps to design a matrix
>fit <- lmFit(genes, design) # function fits probeset in designed matrix
>contrast.matrix <- makeContrasts(H-N,levels=design) # function compares LPL hydrolysis
product treatment vs non-hydrolysis product treatment
>contrast.matrix
>fit2 <- contrasts.fit(fit, contrast.matrix) # function fits probeset in contrast adjusted matrix
>fit3 <- eBayes(fit2) # eBayes function helps to rank differentially regulated genes in treatment
>write.csv(fit3, file="results.csv") # command helps to write the matrix file in new file name
'results'
>results <- decideTests(fit3, p.value=0.05) # to get differentially regulated genes with a specific P.
value 0.03
>nar <- topTable(fit3, coef=1, n=10000, adjust="fdr", p.value=0.03) # extract table of top ranked
genes linear model fit
>head(nar) # Shows top 6 genes that are differentially expressed in a file 'ttHP'
>write.csv(nar, file="nar.csv") # writes topTable transcript ID in CSV format
```

Gene Annotation

```
>getwd() # function confirms working directory
>library(biomaRt) # to use biomaRt for gene annotation
>ensembl <- useMart("ensembl")
>listDatasets(ensembl)
```

```
>ensembl = useMart("ensembl",dataset="hsapiens_gene_ensembl")
>filters = listFilters(ensembl)
>attributes = listAttributes(ensembl)
>affy<- read.csv("nar.csv",header=T)
>LPLgenes<-getBM(attributes=c('affy_hugene_2_0_st_v1', 'hgnc_symbol', 'description'), filters =
'affy_hugene_2_0_st_v1', values = affy, mart = ensembl) # to annotate genes in TopTable
>write.csv(LPLgenes, file="LPLgenes.csv")
```

Appendix II: Supplementary tables

Table S1: Product length and amplification efficiencies of select gene-primers

Gene	Product length	Efficiency (IQ SYBR)	Efficiency (Sso advanced)
<i>ACTB</i>	148	0.73	1.02
<i>ATF3</i>	127	1.09	Not calculated
<i>ADRP</i>	139	1.05	Not calculated
<i>CD36</i>	131	0.89	Not calculated
<i>PCNA</i>	125	0.95	Not calculated
<i>IFITM1</i>	145	0.98	Not calculated
<i>SNORA75</i>	135	1.08	Not calculated
<i>SNORA56</i>	104	0.97	Not calculated
<i>DKC-v3</i>	136	1.15	1.22

The amplification efficiencies of the primers are mentioned above. Except *DKC-v3* gene expression, transcript levels of other genes were measured using IQ SYBR green (Bio-Rad) after LPL hydrolysis product treatment in THP-1 macrophages. To assess the expression of *DKC1-v3*, SsoAdvanced SYBR green (Bio-Rad) was used.

Table S2: List of up-regulated transcripts in LPL hydrolysis product treatment

ID	Gene symbol	Gene Description	Log₂FC
16913572	<i>SNORA60</i>	small nucleolar RNA, H/ACA box 60 [Source:HGNC Symbol;Acc:HGNC:32654]	3.5866661
17070492	<i>ATP6V0D2</i>	ATPase, H ⁺ transporting, lysosomal 38kDa, V0 subunit d2 [Source:HGNC Symbol;Acc:HGNC:18266]	2.7880616
17038309	<i>HSPA1B/HSPA1A</i>	heat shock 70kDa protein 1B [Source:HGNC Symbol;Acc:HGNC:5233]/ heat shock 70kDa protein 1A [Source:HGNC Symbol;Acc:HGNC:5232]	2.7216879
16909520	<i>SNORA75/ SNORD20/NCL</i>	small nucleolar RNA, H/ACA box 75 [Source:HGNC Symbol;Acc:HGNC:32661]/ small nucleolar RNA, C/D box 20 [Source:HGNC Symbol;Acc:HGNC:10143]/ nucleolin [Source:HGNC Symbol;Acc:HGNC:7667]	2.7216756
17026331	<i>HSPA1A/HSPA1B</i>	heat shock 70kDa protein 1A [Source:HGNC Symbol;Acc:HGNC:5232]/ heat shock 70kDa protein 1B [Source:HGNC Symbol;Acc:HGNC:5233]	2.7068702
16700713	<i>SNORA14B</i>	small nucleolar RNA, H/ACA box 14B [Source:HGNC Symbol;Acc:HGNC:32603]	2.6892518
17006863	<i>HSPA1A/HSPA1B</i>	heat shock 70kDa protein 1A [Source:HGNC Symbol;Acc:HGNC:5232]/ heat shock 70kDa protein 1B [Source:HGNC Symbol;Acc:HGNC:5233]	2.6840046
17028007	<i>HSPA1A/HSPA1B</i>	heat shock 70kDa protein 1A [Source:HGNC Symbol;Acc:HGNC:5232]/ heat shock 70kDa protein 1B [Source:HGNC Symbol;Acc:HGNC:5233]	2.6584235
16694357	<i>SNORA80E</i>	small nucleolar RNA, H/ACA box 80E [Source:HGNC Symbol;Acc:HGNC:32635]	2.6564718
17006881	<i>HSPA1A/HSPA1B</i>	heat shock 70kDa protein 1A [Source:HGNC Symbol;Acc:HGNC:5232]/ heat shock 70kDa protein 1B [Source:HGNC Symbol;Acc:HGNC:5233]	2.6275314
17118411	---	---	2.6227777
17118415	---	---	2.6227777
17038297	<i>HSPA1B/HSPA1A</i>	heat shock 70kDa protein 1B [Source:HGNC Symbol;Acc:HGNC:5233]/ heat shock 70kDa protein 1A [Source:HGNC Symbol;Acc:HGNC:5232]	2.5986065
17026318	<i>HSPA1A/HSPA1B</i>	heat shock 70kDa protein 1A [Source:HGNC Symbol;Acc:HGNC:5232]/ heat shock 70kDa protein 1B [Source:HGNC Symbol;Acc:HGNC:5233]	2.5803337
17027994	<i>HSPA1A/HSPA1B</i>	heat shock 70kDa protein 1A [Source:HGNC Symbol;Acc:HGNC:5232]/ heat shock 70kDa protein 1B [Source:HGNC Symbol;Acc:HGNC:5233]	2.5803337

17030820	<i>HSPA1A/HSPA1B</i>	heat shock 70kDa protein 1A [Source:HGNC Symbol;Acc:HGNC:5232]/ heat shock 70kDa protein 1B [Source:HGNC Symbol;Acc:HGNC:5233]	2.5803337
17030833	<i>HSPA1A/HSPA1B</i>	heat shock 70kDa protein 1A [Source:HGNC Symbol;Acc:HGNC:5232]/ heat shock 70kDa protein 1B [Source:HGNC Symbol;Acc:HGNC:5233]	2.4877231
17046094	<i>RNU1-14P</i>	RNA, U1 small nuclear 14, pseudogene [Source:HGNC Symbol;Acc:HGNC:10139]	2.4656077
17078592	<i>FABP4</i>	fatty acid binding protein 4, adipocyte [Source:HGNC Symbol;Acc:HGNC:3559]	2.4445675
16837063	<i>SNHG25/ SNORA76C</i>	small nucleolar RNA host gene 25 [Source:HGNC Symbol;Acc:HGNC:51534]/ small nucleolar RNA, H/ACA box 76C [Source:HGNC Symbol;Acc:HGNC:32662]/ Small nucleolar RNA SNORA50 [Source:RFAM;Acc:RF00407]	2.3765251
17104049	<i>SNORA11</i>	small nucleolar RNA, H/ACA box 11 [Source:HGNC Symbol;Acc:HGNC:32599]	2.3553409
16763966	<i>SNORA2A</i>	small nucleolar RNA, H/ACA box 2A [Source:HGNC Symbol;Acc:HGNC:32584]	2.2757955
16691331	<i>SNORA42</i>	Small nucleolar RNA SNORA42/SNORA80 family [Source:RFAM;Acc:RF00406]	2.2552694
17012711	<i>SNORA33</i>	small nucleolar RNA, H/ACA box 33 [Source:HGNC Symbol;Acc:HGNC:32623]	2.2304004
17116675	---	---	2.2272587
16702705	<i>OLAH</i>	oleoyl-ACP hydrolase [Source:HGNC Symbol;Acc:HGNC:25625]	2.2220248
16846359	<i>RNU1-42P</i>	RNA, U1 small nuclear 42, pseudogene [Source:HGNC Symbol;Acc:HGNC:48384]	2.2037127
17092710	<i>SCARNA8</i>	small Cajal body-specific RNA 8 [Source:HGNC Symbol;Acc:HGNC:32564]	2.1576388
17119802	<i>DKC1/SNORA56</i>	dyskeratosis congenita 1, dyskerin [Source:HGNC Symbol;Acc:HGNC:2890]/ small nucleolar RNA, H/ACA box 56 [Source:HGNC Symbol;Acc:HGNC:32650]	2.0804498
16694359	<i>SCARNA4</i>	small Cajal body-specific RNA 4 [Source:HGNC Symbol;Acc:HGNC:32560]	2.0437777
17059955	<i>PDK4</i>	pyruvate dehydrogenase kinase, isozyme 4 [Source:HGNC Symbol;Acc:HGNC:8812]	2.0370528
16919223	<i>SNORA71B</i>	small nucleolar RNA, H/ACA box 71B [Source:HGNC Symbol;Acc:HGNC:10233]	2.0075156
16661646	<i>RNU11</i>	RNA, U11 small nuclear [Source:HGNC Symbol;Acc:HGNC:10108]	2.0064381
17100695	<i>MT-TS1</i>	mitochondrially encoded tRNA serine 1 (UCN) [Source:HGNC Symbol;Acc:HGNC:7497]	2.0015946
16878583	<i>SNORD92</i>	small nucleolar RNA, C/D box 92 [Source:HGNC Symbol;Acc:HGNC:32754]	2.000231
16696685	<i>SCARNA3</i>	small Cajal body-specific RNA 3 [Source:HGNC Symbol;Acc:HGNC:32577]	1.9633422
16650847	---	---	1.9607653
16800297	<i>RNU6-353P</i>	RNA, U6 small nuclear 353, pseudogene [Source:HGNC Symbol;Acc:HGNC:47316]	1.9267232

17119340	<i>SNORA6/ RPSA</i>	small nucleolar RNA, H/ACA box 6 [Source:HGNC Symbol;Acc:HGNC:32591]/ ribosomal protein SA [Source:HGNC Symbol;Acc:HGNC:6502]	1.9105746
16943230	<i>LINC00973</i>	long intergenic non-protein coding RNA 973 [Source:HGNC Symbol;Acc:HGNC:48868]	1.8895967
16826966	<i>SNORA46</i>	small nucleolar RNA, H/ACA box 46 [Source:HGNC Symbol;Acc:HGNC:32639]	1.8595548
17119224	<i>SNORA41/ SNORD51/ EEF1B2</i>	small nucleolar RNA, H/ACA box 41 [Source:HGNC Symbol;Acc:HGNC:32634]/ small nucleolar RNA, C/D box 51 [Source:HGNC Symbol;Acc:HGNC:10201]/ eukaryotic translation elongation factor 1 beta 2 [Source:HGNC Symbol;Acc:HGNC:3208]/ Small nucleolar RNA Z196/R39/R59 family [Source:RFAM;Acc:RF00134]	1.8408576
16734524	<i>SNORA54</i>	small nucleolar RNA, H/ACA box 54 [Source:HGNC Symbol;Acc:HGNC:32647]	1.8271199
16676682	<i>IL24</i>	interleukin 24 [Source:HGNC Symbol;Acc:HGNC:11346]	1.7993536
16837226	<i>SNORA38B</i>	small nucleolar RNA, H/ACA box 38B [Source:HGNC Symbol;Acc:HGNC:33617]	1.7666499
16992465	<i>SNORA74B/ ATP6V0E1</i>	small nucleolar RNA, H/ACA box 74B [Source:HGNC Symbol;Acc:HGNC:32660]/ ATPase, H ⁺ transporting, lysosomal 9kDa, V0 subunit e1 [Source:HGNC Symbol;Acc:HGNC:863]	1.7585149
16992466	<i>SNORA74B</i>	small nucleolar RNA, H/ACA box 74B [Source:HGNC Symbol;Acc:HGNC:32660]	1.7585149
17079434	<i>SNORA72/ RPL30</i>	small nucleolar RNA, H/ACA box 72 [Source:HGNC Symbol;Acc:HGNC:10234]/ ribosomal protein L30 [Source:HGNC Symbol;Acc:HGNC:10333]	1.7416766
17079435	<i>SNORA72/ RPL30</i>	small nucleolar RNA, H/ACA box 72 [Source:HGNC Symbol;Acc:HGNC:10234]/ ribosomal protein L30 [Source:HGNC Symbol;Acc:HGNC:10333]	1.7416766
17021510	<i>CNR1</i>	cannabinoid receptor 1 (brain) [Source:HGNC Symbol;Acc:HGNC:2159]	1.7297764
17119488	<i>SNORA20/ TCP1</i>	small nucleolar RNA, H/ACA box 20 [Source:HGNC Symbol;Acc:HGNC:32610]/ t-complex 1 [Source:HGNC Symbol;Acc:HGNC:11655]	1.7272721
16977868	<i>ABCG2</i>	ATP-binding cassette, sub-family G (WHITE), member 2 (Junior blood group) [Source:HGNC Symbol;Acc:HGNC:74]	1.713334
16837061	<i>SNORD104</i>	small nucleolar RNA, C/D box 104 [Source:HGNC Symbol;Acc:HGNC:32768]	1.7079617
17021504	<i>CNR1</i>	cannabinoid receptor 1 (brain) [Source:HGNC Symbol;Acc:HGNC:2159]	1.6914375
17016025	<i>RNU6-801P</i>	RNA, U6 small nuclear 801, pseudogene [Source:HGNC Symbol;Acc:HGNC:47764]	1.6740173
16732345	<i>RNU6-1123P</i>	RNA, U6 small nuclear 1123, pseudogene [Source:HGNC Symbol;Acc:HGNC:48086]	1.6567592

16847393	<i>SCARNA20</i>	small Cajal body-specific RNA 20 [Source:HGNC Symbol;Acc:HGNC:32578]	1.6468453
17085901	<i>ANXA1</i>	annexin A1 [Source:HGNC Symbol;Acc:HGNC:533]	1.6458665
16842237	<i>SNORD3C</i>	small nucleolar RNA, C/D box 3C [Source:HGNC Symbol;Acc:HGNC:33191]	1.6442244
16747336	<i>SCARNA10</i>	small Cajal body-specific RNA 10 [Source:HGNC Symbol;Acc:HGNC:32567]	1.6229055
16997793	<i>SCARNA18</i>	small Cajal body-specific RNA 18 [Source:HGNC Symbol;Acc:HGNC:32559]	1.6159547
16904022	<i>RNU6-580P</i>	RNA, U6 small nuclear 580, pseudogene [Source:HGNC Symbol;Acc:HGNC:47543]	1.6153682
16969988	<i>RNU1-138P/ RN7SL184P</i>	RNA, U1 small nuclear 138, pseudogene [Source:HGNC Symbol;Acc:HGNC:48480]/ RNA, 7SL, cytoplasmic 184, pseudogene [Source:HGNC Symbol;Acc:HGNC:46200]	1.6128574
16919229	<i>SNORA71D</i>	small nucleolar RNA, H/ACA box 71D [Source:HGNC Symbol;Acc:HGNC:32657]	1.6022969
17047459	<i>SNORA14A</i>	small nucleolar RNA, H/ACA box 14A [Source:HGNC Symbol;Acc:HGNC:32602]	1.5993334
16741287	<i>CPT1A</i>	carnitine palmitoyltransferase 1A (liver) [Source:HGNC Symbol;Acc:HGNC:2328]	1.5958596
16899758	<i>RNU1-38P</i>	RNA, U1 small nuclear 38, pseudogene [Source:HGNC Symbol;Acc:HGNC:48380]	1.5788866
17119236	<i>RNU1-38P</i>	RNA, U1 small nuclear 38, pseudogene [Source:HGNC Symbol;Acc:HGNC:48380]	1.5788866
16677278	<i>ATF3</i>	activating transcription factor 3 [Source:HGNC Symbol;Acc:HGNC:785]	1.5618703
17047795	<i>CD36</i>	Cluster of differentiation 36	1.5612921
16892523	<i>SCARNA6</i>	small Cajal body-specific RNA 6 [Source:HGNC Symbol;Acc:HGNC:32562]	1.5516909
17092712	<i>PLIN2</i>	Perilipin 2	1.5503564
16721732	<i>SNORA45B</i>	small nucleolar RNA, H/ACA box 45B [Source:HGNC Symbol;Acc:HGNC:32638]	1.5448671
16822904	<i>SNORA64/ SNORA10/ RPS2</i>	small nucleolar RNA, H/ACA box 64 [Source:HGNC Symbol;Acc:HGNC:10221]/ small nucleolar RNA, H/ACA box 10 [Source:HGNC Symbol;Acc:HGNC:32598]/ ribosomal protein S2 [Source:HGNC Symbol;Acc:HGNC:10404]	1.5310674
16688022	<i>RNU6-371P</i>	RNA, U6 small nuclear 371, pseudogene [Source:HGNC Symbol;Acc:HGNC:47334]	1.5209346
16808555	<i>RNU1-119P/ RNU1-78P</i>	RNA, U1 small nuclear 119, pseudogene [Source:HGNC Symbol;Acc:HGNC:48461]/ RNA, U1 small nuclear 78, pseudogene [Source:HGNC Symbol;Acc:HGNC:48420]	1.5208139
16881353	<i>DYSF</i>	dysferlin [Source:HGNC Symbol;Acc:HGNC:3097]	1.5186063
16793674	<i>HIF1A-AS2</i>	HIF1A antisense RNA 2 [Source:HGNC Symbol;Acc:HGNC:43015]	1.5170582
16855340	<i>SNORA37</i>	small nucleolar RNA, H/ACA box 37 [Source:HGNC Symbol;Acc:HGNC:32630]	1.5107854
16948967	<i>SNORD66</i>	small nucleolar RNA, C/D box 66 [Source:HGNC Symbol;Acc:HGNC:32727]	1.5060778
16985704	<i>OCLN</i>	occludin [Source:HGNC Symbol;Acc:HGNC:8104]	1.4780406
17009627	<i>RN7SK</i>	RNA, 7SK small nuclear [Source:HGNC Symbol;Acc:HGNC:10037]	1.4471638

17118690	<i>SNORA61/</i> <i>SNORA44/</i> <i>SNHG12</i>	small nucleolar RNA, H/ACA box 61 [Source:HGNC Symbol;Acc:HGNC:32655]/ small nucleolar RNA, H/ACA box 44 [Source:HGNC Symbol;Acc:HGNC:32637]/ small nucleolar RNA host gene 12 [Source:HGNC Symbol;Acc:HGNC:30062]	1.4452369
16725908	<i>METTL12/</i> <i>SNORA57</i>	methyltransferase like 12 [Source:HGNC Symbol;Acc:HGNC:33113]/ small nucleolar RNA, H/ACA box 57	1.4413508
16726880	<i>NEAT1</i>	nuclear paraspeckle assembly transcript 1 (non-protein coding) [Source:HGNC Symbol;Acc:HGNC:30815]	1.4348734
16756078	<i>MIR3652/</i> <i>HSP90B1</i>	microRNA 3652 [Source:HGNC Symbol;Acc:HGNC:38894]/ heat shock protein 90kDa beta (Grp94),member 1[Acc: HGNC: 12028]	1.4287571
17057422	<i>SNORA9/ SNHG15</i>	small nucleolar RNA, H/ACA box 9 [Source:HGNC Symbol;Acc:HGNC:32597]/ small nucleolar RNA host gene 15 [Source:HGNC Symbol;Acc:HGNC:27797]	1.4272427
16745561	<i>SNORD14E/</i> <i>HSPA8</i>	small nucleolar RNA, C/D box 14E [Source:HGNC Symbol;Acc:HGNC:30354]/ heat shock 70kDa protein 8 [Source:HGNC Symbol;Acc:HGNC:5241]	1.4184116
16892521	<i>SCARNA5</i>	small Cajal body-specific RNA 5 [Source:HGNC Symbol;Acc:HGNC:32561]	1.4166707
16650739	---	---	1.4156
17118778	<i>SNORA52/ RPLP2</i>	small nucleolar RNA, H/ACA box 52 [Source:HGNC Symbol;Acc:HGNC:32645]/ ribosomal protein, large, P2 [Source:HGNC Symbol;Acc:HGNC:10377]	1.411497
16849274	<i>ST6GALNAC2</i>	ST6 (alpha-N-acetyl-neuraminy-2,3-beta-galactosyl-1,3)-N-acetylgalactosaminide alpha-2,6-sialyltransferase 2 [Source:HGNC Symbol;Acc:HGNC:10867]	1.4111302
16989863	<i>SNORA74A</i>	small nucleolar RNA, H/ACA box 74A [Source:HGNC Symbol;Acc:HGNC:10119]	1.4061698
16984408	---	---	1.3952916
16917849	<i>THBD</i>	thrombomodulin [Source:HGNC Symbol;Acc:HGNC:11784]	1.3641165
16984689	<i>ITGA2</i>	integrin, alpha 2 (CD49B, alpha 2 subunit of VLA-2 receptor) [Source:HGNC Symbol;Acc:HGNC:6137]	1.356986
16914741	<i>SNORD12C</i>	small nucleolar RNA, C/D box 12C [Source:HGNC Symbol;Acc:HGNC:10105]	1.3563469
17059087	<i>RNU6-530P</i>	RNA, U6 small nuclear 530, pseudogene [Source:HGNC Symbol;Acc:HGNC:47493]	1.3500675
17021489	---	---	1.348503
16798665	<i>GOLGA8J</i>	golgin A8 family, member J [Source:HGNC Symbol;Acc:HGNC:38650]	1.3450867
16655929	---	---	1.3410729
16892075	<i>ARMC9</i>	armadillo repeat containing 9 [Source:HGNC Symbol;Acc:HGNC:20730]	1.3246787

16777185	<i>GJB2</i>	gap junction protein, beta 2, 26kDa [Source:HGNC Symbol;Acc:HGNC:4284]	1.3239012
16752024	<i>COPZ1</i>	Coatomer Protein Complex, Subunit Zeta 1 [Source:HGNC Symbol;Acc:HGNC:2243]	1.3238051
17119260	<i>SNORA51/ NOP56/ SNORD110</i>	small nucleolar RNA, H/ACA box 51 [Source:HGNC Symbol;Acc:HGNC:32644]/ NOP56 ribonucleoprotein [Source:HGNC Symbol;Acc:HGNC:15911]/ small nucleolar RNA, C/D box 110 [Source:HGNC Symbol;Acc:HGNC:32775]/ Small nucleolar RNA SNORA51 [Source:RFAM;Acc:RF00432]	1.3226882
16654979	---	---	1.2894301
16867349	<i>SEMA6B</i>	sema domain, transmembrane domain (TM), and cytoplasmic domain, (semaphorin) 6B [Source:HGNC Symbol;Acc:HGNC:10739]	1.270519
17020608	<i>ERVH-3</i>	endogenous retrovirus group H member 3 [Source:HGNC Symbol;Acc:HGNC:39055]	1.2634586
17126140	---	---	1.2619936
16878674	<i>SNORA64/ SNORA10</i>	Small nucleolar RNA SNORA64/SNORA10 family [Source:RFAM;Acc:RF00264]	1.2599949
16852666	<i>SEC11C</i>	SEC11 homolog C (<i>S. cerevisiae</i>) [Source:HGNC Symbol;Acc:HGNC:23400]	1.2522244
17124336	---	---	1.2491668
17099678	<i>RNU6ATAC2P/ RNU6ATAC</i>	RNA, U6atac small nuclear 2, pseudogene [Source:HGNC Symbol;Acc:HGNC:34092]/ RNA, U6atac small nuclear (U12-dependent splicing) [Source:HGNC Symbol;Acc:HGNC:34017]	1.2425555
16832031	<i>SNORD3D/ SNORD3B-2/ SNORD3B-1/ SNORD3C/ SNORD3A</i>	small nucleolar RNA, C/D box 3D [Source:HGNC Symbol;Acc:HGNC:33192]/ small nucleolar RNA, C/D box 3B-2 [Source:HGNC Symbol;Acc:HGNC:33190]/ small nucleolar RNA, C/D box 3B-1 [Source:HGNC Symbol;Acc:HGNC:10168]/ small nucleolar RNA, C/D box 3C [Source:HGNC Symbol;Acc:HGNC:33191]/ small nucleolar RNA, C/D box 3A [Source:HGNC Symbol;Acc:HGNC:33189]	1.2419421
16832005	<i>SNORD3C/ SNORD3A/ SNORD3D/ SNORD3B-1/ SNORD3B-2</i>	small nucleolar RNA, C/D box 3C [Source:HGNC Symbol;Acc:HGNC:33191]/ small nucleolar RNA, C/D box 3A [Source:HGNC Symbol;Acc:HGNC:33189]/ small nucleolar RNA, C/D box 3D [Source:HGNC Symbol;Acc:HGNC:33192]/ small nucleolar RNA, C/D box 3B-1 [Source:HGNC Symbol;Acc:HGNC:10168]/ small nucleolar RNA, C/D box 3B-2 [Source:HGNC Symbol;Acc:HGNC:33190]	1.2397501
16842215	<i>SNORD3D/ SNORD3B-2/</i>	small nucleolar RNA, C/D box 3D [Source:HGNC Symbol;Acc:HGNC:33192]/ small nucleolar RNA, C/D box 3A [Source:HGNC Symbol;Acc:HGNC:33189]/ small	1.2397501

	<i>SNORD3B-1/</i> <i>SNORD3A</i>	nucleolar RNA, C/D box 3B-1 [Source:HGNC Symbol;Acc:HGNC:10168]/ small nucleolar RNA, C/D box 3B-2 [Source:HGNC Symbol;Acc:HGNC:33190]	
16661149	<i>CD52</i>	CD52 molecule [Source:HGNC Symbol;Acc:HGNC:1804]	1.2345235
16917529	<i>SNORD17</i>	small nucleolar RNA, C/D box 17 [Source:HGNC Symbol;Acc:HGNC:32713]	1.2270778
17009661	<i>RNU1-136P</i>	RNA, U1 small nuclear 136, pseudogene [Source:HGNC Symbol;Acc:HGNC:48478]	1.2262186
16988913	<i>RNU6ATAC10P</i>	RNA, U6atac small nuclear 10, pseudogene [Source:HGNC Symbol;Acc:HGNC:46909]	1.2178176
16778713	<i>TPT1</i>	tumor protein, translationally-controlled 1 [Source:HGNC Symbol;Acc:HGNC:12022]/ Small nucleolar RNA SNORA31 [Acc: RF00322]	1.2157673
17118780	<i>SNORA45A/</i> <i>RPL27A</i>	small nucleolar RNA, H/ACA box 45A [Source:HGNC Symbol;Acc:HGNC:32586]/ ribosomal protein L27a [Source:HGNC Symbol;Acc:HGNC:10329]	1.2108397
16874643	<i>SNORD88A</i>	small nucleolar RNA, C/D box 88A [Source:HGNC Symbol;Acc:HGNC:32747]	1.2094201
16972249	<i>PALLD</i>	palladin, cytoskeletal associated protein [Source:HGNC Symbol;Acc:HGNC:17068]	1.2077975
17015472	<i>SCARNA27</i>	small Cajal body-specific RNA 27 [Source:HGNC Symbol;Acc:HGNC:33614]	1.2047601
16996347	<i>RNU6ATAC2P/</i> <i>RNU6ATAC</i>	RNA, U6atac small nuclear 2, pseudogene [Source:HGNC Symbol;Acc:HGNC:34092]/ RNA, U6atac small nuclear (U12-dependent splicing) [Source:HGNC Symbol;Acc:HGNC:34017]	1.2032134
16763964	<i>SNORA34</i>	small nucleolar RNA, H/ACA box 34 [Source:HGNC Symbol;Acc:HGNC:32624]	1.1952417
16732807	<i>VWA5A</i>	von Willebrand factor A domain containing 5A [Source:HGNC Symbol;Acc:HGNC:6658]	1.1886058
17118694	<i>SNORA16A/</i> <i>SNHG12</i>	small nucleolar RNA, H/ACA box 16A [Source:HGNC Symbol;Acc:HGNC:32605]/ small nucleolar RNA host gene 12 [Source:HGNC Symbol;Acc:HGNC:30062]	1.1865771
17064135	<i>PDIA4</i>	protein disulfide isomerase family A, member 4 [Source:HGNC Symbol;Acc:HGNC:30167]	1.1839374
17027880	<i>SNORA38</i>	small nucleolar RNA, H/ACA box 38 [Source:HGNC Symbol;Acc:HGNC:32631]	1.1837403
17033410	<i>SNORA38</i>	small nucleolar RNA, H/ACA box 38 [Source:HGNC Symbol;Acc:HGNC:32631]	1.1837403
17038203	<i>SNORA38</i>	small nucleolar RNA, H/ACA box 38 [Source:HGNC Symbol;Acc:HGNC:32631]	1.1837403
17040798	<i>SNORA38</i>	small nucleolar RNA, H/ACA box 38 [Source:HGNC Symbol;Acc:HGNC:32631]	1.1837403
17098411	<i>HSPA5</i>	heat shock 70kDa protein 5 (glucose-regulated protein, 78kDa) [Source:HGNC Symbol;Acc:HGNC:5238]	1.1779852

16929562	<i>HMOX1</i>	heme oxygenase 1 [Source:HGNC Symbol;Acc:HGNC:5013]	1.1458621
16684581	<i>SPOCD1</i>	SPOC domain containing 1 [Source:HGNC Symbol;Acc:HGNC:26338]	1.1432937
16961947	<i>RNA5SP150</i>	RNA, 5S ribosomal pseudogene 150 [Source:HGNC Symbol;Acc:HGNC:43050]	1.1322181
17120056	<i>PDE4DIP</i>	phosphodiesterase 4D interacting protein [Source:HGNC Symbol;Acc:HGNC:15580]	1.1314978
16961037	<i>SCARNA7</i>	small Cajal body-specific RNA 7 [Source:HGNC Symbol;Acc:HGNC:32563]	1.1314575
16651537	---	---	1.1265227
17054328	<i>ZFAND2A</i>	zinc finger, AN1-type domain 2A [Source:HGNC Symbol;Acc:HGNC:28073]	1.1047416
17118848	<i>SNORA25/ TAF1D/ SNORD6/ SNORA32</i>	small nucleolar RNA, H/ACA box 25 [Source:HGNC Symbol;Acc:HGNC:32615]/ TATA box binding protein (TBP)-associated factor, RNA polymerase I, D, 41kDa [Source:HGNC Symbol;Acc:HGNC:28759]/ small nucleolar RNA, C/D box 6 [Source:HGNC Symbol;Acc:HGNC:32703]/ small nucleolar RNA, H/ACA box 32 [Source:HGNC Symbol;Acc:HGNC:32622]	1.0932321
16685702	<i>SNORA55</i>	small nucleolar RNA, H/ACA box 55 [Source:HGNC Symbol;Acc:HGNC:32649]	1.0832591
16930066	<i>KDELRL3</i>	KDEL (Lys-Asp-Glu-Leu) endoplasmic reticulum protein retention receptor 3 [Source:HGNC Symbol;Acc:HGNC:6306]	1.0729487
16970894	<i>RNU6-1214P</i>	RNA, U6 small nuclear 1214, pseudogene [Source:HGNC Symbol;Acc:HGNC:48177]	1.0618682
16889629	<i>SNORD11B/ NOP58</i>	small nucleolar RNA, C/D box 11B [Source:HGNC Symbol;Acc:HGNC:33571]/ NOP58 ribonucleoprotein [Source:HGNC Symbol;Acc:HGNC:29926]	1.0576988
16948561	<i>SNORA63</i>	Small nucleolar RNA, H/ACA box 63 [Source:RFAM;Acc:RF00092]	1.0531162
17010354	<i>CD109</i>	CD109 molecule [Source:HGNC Symbol;Acc:HGNC:21685]	1.0490491
16869653	<i>DNAJB1</i>	DnaJ (Hsp40) homolog, subfamily B, member 1 [Source:HGNC Symbol;Acc:HGNC:5270]	1.0209808
16891082	<i>CYP27A1</i>	cytochrome P450, family 27, subfamily A, polypeptide 1 [Source:HGNC Symbol;Acc:HGNC:2605]	1.01658
16830302	<i>ACADVL</i>	acyl-CoA dehydrogenase, very long chain [Source:HGNC Symbol;Acc:HGNC:92]	1.0048522
17100967	---	---	0.9936192
16889631	<i>SNORD11</i>	small nucleolar RNA, C/D box 11 [Source:HGNC Symbol;Acc:HGNC:32707]	0.986239
16829683	---	---	0.9832682
16815807	<i>ATF7IP2</i>	activating transcription factor 7 interacting protein 2 [Source:HGNC Symbol;Acc:HGNC:20397]	0.9825237

16997399	<i>SNORA47</i>	small nucleolar RNA, H/ACA box 47 [Source:HGNC Symbol;Acc:HGNC:32640]	0.9789526
16655723	---	---	0.9788117
17118876	<i>SNORA53/</i> <i>SLC25A3</i>	small nucleolar RNA, H/ACA box 53 [Source:HGNC Symbol;Acc:HGNC:32646]/ solute carrier family 25 (mitochondrial carrier; phosphate carrier), member 3 [Source:HGNC Symbol;Acc:HGNC:10989]	0.9605636
16931569	<i>CRELD2</i>	cysteine-rich with EGF-like domains 2 [Source:HGNC Symbol;Acc:HGNC:28150]	0.9579686
16808296	<i>RNU6-354P/</i> <i>RNU6-610</i>	RNA, U6 small nuclear 354, pseudogene [Source:HGNC Symbol;Acc:HGNC:47317]/ RNA, U6 small nuclear 610, pseudogene [Source:HGNC Symbol;Acc:HGNC:47573]	0.9538288
16808338	<i>RNU6-354P/</i> <i>RNU6-610</i>	RNA, U6 small nuclear 354, pseudogene [Source:HGNC Symbol;Acc:HGNC:47317]/ RNA, U6 small nuclear 610, pseudogene [Source:HGNC Symbol;Acc:HGNC:47573]	0.9538288
16745186	<i>HYOU1</i>	hypoxia up-regulated 1 [Source:HGNC Symbol;Acc:HGNC:16931]	0.9466647
17006743	<i>SNORA38</i>	small nucleolar RNA, H/ACA box 38 [Source:HGNC Symbol;Acc:HGNC:32631]	0.9447982
17121352	<i>SNX29P1/</i> <i>SNX29/</i> <i>SNX29P2</i>	sorting nexin 29 pseudogene 1 [Source:HGNC Symbol;Acc:HGNC:31913]/ sorting nexin 29 [Source:HGNC Symbol;Acc:HGNC:30542]/ sorting nexin 29 pseudogene 2 [Source:HGNC Symbol;Acc:HGNC:31914]	0.9433485
16795394	<i>SEL1L</i>	sel-1 suppressor of lin-12-like (C. elegans) [Source:HGNC Symbol;Acc:HGNC:10717]	0.9421456
16858118	<i>SNORD105</i>	small nucleolar RNA, C/D box 105 [Source:HGNC Symbol;Acc:HGNC:32769]	0.94159
16886564	<i>FMNL2</i>	formin-like 2 [Source:HGNC Symbol;Acc:HGNC:18267]	0.9222717
16656633	---	---	0.9221184
16737841	<i>SNORD67</i>	small nucleolar RNA, C/D box 67 [Source:HGNC Symbol;Acc:HGNC:32728]	0.9132485
17076220	<i>LOC100507403</i>	uncharacterized LOC100507403[Source:HGNC Symbol;Acc:HGNC:100507403]	0.9100782
16670210	<i>RNVU1-19</i>	RNA, variant U1 small nuclear 19 [Source:HGNC Symbol;Acc:HGNC:48324]	0.9084498
16953753	<i>SLC25A20</i>	solute carrier family 25 (carnitine/acylcarnitine translocase), member 20 [Source:HGNC Symbol;Acc:HGNC:1421]	0.9064836
16748788	<i>MGST1</i>	Microsomal Glutathione S-Transferase 1[Source:HGNC Symbol;Acc:HGNC:7061]	0.8992862
16780929	<i>COL4A1</i>	collagen, type IV, alpha 1 [Source:HGNC Symbol;Acc:HGNC:2202]	0.8972641
16980051	<i>CLGN</i>	calmegin [Source:HGNC Symbol;Acc:HGNC:2060]	0.8671733
16890473	<i>SNORA70</i>	Small nucleolar RNA 70 [Source:RFAM;Acc:RF00156]	0.8153768
16878585	<i>SNORD53</i>	small nucleolar RNA, C/D box 53 [Source:HGNC Symbol;Acc:HGNC:10203]	0.8056947

16689752	<i>GCLM</i>	glutamate-cysteine ligase, modifier subunit [Source:HGNC Symbol;Acc:HGNC:4312]	0.7862908
17025659	<i>RPS6KA2-IT1</i>	RPS6KA2 intronic transcript 1 [Source:HGNC Symbol;Acc:HGNC:41378]	0.77634
16947850	<i>GPR160</i>	G protein-coupled receptor 160 [Source:HGNC Symbol;Acc:HGNC:23693]	0.7666492
16700456	<i>FAM89A</i>	family with sequence similarity 89, member A [Source:HGNC Symbol;Acc:HGNC:25057]	0.7651809
17088124	<i>HSDL2</i>	hydroxysteroid dehydrogenase like 2 [Source:HGNC Symbol;Acc:HGNC:18572]	0.7485383

THP-1 macrophages were incubated with LPL hydrolysis products or non-hydrolysis products for 18 h. RNA from the treated cells were subjected to human gene 2.0ST array (n=3). Using R studio, a top list of up-regulated genes in LPL hydrolysis product treated macrophages were obtained at FDR ≤ 0.03 . Log₂FC represents 2-fold change of modulated transcript in macrophages treated with LPL hydrolysis products compared to control.

Table S3: List of down-regulated transcripts in LPL hydrolysis product treatment

ID	Gene symbol	Gene Description	Log₂FC
16666485	<i>IFI44L</i>	interferon-induced protein 44-like	-3.40455
17011886	---	---	-2.84948
17002328	<i>IL12B</i>	interleukin 12B [Source:HGNC Symbol;Acc:HGNC:5970]	-2.70207
16651207	---	---	-2.36415
16826634	<i>RP11-212I21.2</i>	Novel transcript	-2.34831
16977052	<i>CXCL10</i>	chemokine (C-X-C motif) ligand 10 [Source:HGNC Symbol;Acc:HGNC:10637]	-2.18077
16799739	<i>CHAC1</i>	ChaC glutathione-specific gamma-glutamylcyclotransferase 1 [Source:HGNC Symbol;Acc:HGNC:28680]	-2.17631
16720085	<i>IFITM1</i>	interferon induced transmembrane protein 1 [Source:HGNC Symbol;Acc:HGNC:5412]	-2.17551
17055786	<i>AC073072.5</i>	Novel transcript	-1.9856
16978779	<i>DKK2</i>	dickkopf WNT signaling pathway inhibitor 2 [Source:HGNC Symbol;Acc:HGNC:2892]	-1.95953
17031178	<i>HLA-DQA2</i>	major histocompatibility complex, class II, DQ alpha 2 [Source:HGNC Symbol;Acc:HGNC:4943]	-1.90379
17033646	<i>HLA-DQA2</i>	major histocompatibility complex, class II, DQ alpha 2 [Source:HGNC Symbol;Acc:HGNC:4943]	-1.89539
17038629	<i>HLA-DQA2</i>	major histocompatibility complex, class II, DQ alpha 2 [Source:HGNC Symbol;Acc:HGNC:4943]	-1.88352
17007292	<i>HLA-DQA2</i>	major histocompatibility complex, class II, DQ alpha 2 [Source:HGNC Symbol;Acc:HGNC:4943]	-1.87547
17028345	<i>HLA-DQA2</i>	major histocompatibility complex, class II, DQ alpha 2 [Source:HGNC Symbol;Acc:HGNC:4943]	-1.84619
16725041	<i>FAM111B</i>	family with sequence similarity 111, member B [Source:HGNC Symbol;Acc:HGNC:24200]	-1.81466
16843309	<i>CCL1</i>	chemokine (C-C motif) ligand 1 [Source:HGNC Symbol;Acc:HGNC:10609]	-1.8101

17041260	<i>HLA-DQA2</i>	major histocompatibility complex, class II, DQ alpha 2 [Source:HGNC Symbol;Acc:HGNC:4943]	-1.80845
17035918	<i>HLA-DQA2</i>	major histocompatibility complex, class II, DQ alpha 2 [Source:HGNC Symbol;Acc:HGNC:4943]	-1.78535
17044177	<i>IL6</i>	interleukin 6 [Source:HGNC Symbol;Acc:HGNC:6018]	-1.72362
17013694	<i>PLEKHG1</i>	pleckstrin homology domain containing, family G (with RhoGef domain) member 1 [Source:HGNC Symbol;Acc:HGNC:20884]	-1.68931
16677201	<i>DTL</i>	denticleless E3 ubiquitin protein ligase homolog (Drosophila) [Source:HGNC Symbol;Acc:HGNC:30288]	-1.68798
16767306	<i>RP11-81H14.2</i>	Novel transcript	-1.68462
16757373	<i>OAS2</i>	2'-5'-oligoadenylate synthetase 2, 69/71kDa [Source:HGNC Symbol;Acc:HGNC:8087]	-1.66236
16771535	<i>KDM2B</i>	Lysine (K)-Specific Demethylase 2B [Source:HGNC Symbol;Acc:HGNC:13610]	-1.66136
17012959	<i>RP11-240M16.1</i>	Novel transcript	-1.60761
16852312	<i>SKA1</i>	spindle and kinetochore associated complex subunit 1 [Source:HGNC Symbol;Acc:HGNC:28109]	-1.59535
16988441	<i>CTC-546K23.1</i>	Novel transcript	-1.56669
16691327	<i>NGF</i>	nerve growth factor (beta polypeptide) [Source:HGNC Symbol;Acc:HGNC:7808]	-1.5156
16965346	<i>NCAPG</i>	non-SMC condensin I complex, subunit G [Source:HGNC Symbol;Acc:HGNC:24304]	-1.50886
16979515	<i>CCNA2</i>	cyclin A2 [Source:HGNC Symbol;Acc:HGNC:1578]	-1.48705
16877019	<i>RRM2</i>	ribonucleotide reductase M2 [Source:HGNC Symbol;Acc:HGNC:10452]	-1.4867
16990138	<i>IK/ MIR3655</i>	IK cytokine/ down-regulator of HLA 2 MIR3655	-1.48067
16716371	<i>CH25H</i>	cholesterol 25-hydroxylase [Source:HGNC Symbol;Acc:HGNC:1907]	-1.47679
17121988	---	---	-1.46159
16912379	<i>TPX2</i>	TPX2, microtubule-associated [Source:HGNC Symbol;Acc:HGNC:1249]	-1.44848
16830202	<i>XAF1</i>	XIAP associated factor 1 [Source:HGNC Symbol;Acc:HGNC:30932]	-1.4443
17014361	<i>MAS1</i>	MAS1 proto-oncogene, G protein-coupled receptor [Source:HGNC Symbol;Acc:HGNC:6899]	-1.43399
16757347	<i>OAS3</i>	2'-5'-oligoadenylate synthetase 3, 100kDa [Source:HGNC Symbol;Acc:HGNC:8088]	-1.43037

16922959	<i>MX2</i>	MX Dynamin-Like GTPase 2 [Source:HGNC Symbol;Acc:HGNC:7533]	-1.40598
16916605	<i>CPXM1</i>	carboxypeptidase X (M14 family), member 1 [Source:HGNC Symbol;Acc:HGNC:15771]	-1.37974
16844312	<i>TOP2A</i>	topoisomerase (DNA) II alpha 170kDa [Source:HGNC Symbol;Acc:HGNC:11989]	-1.36849
16757324	<i>OAS1</i>	2'-5'-oligoadenylate synthetase 1, 40/46kDa [Source:HGNC Symbol;Acc:HGNC:8086]	-1.34118
16850477	<i>TYMS</i>	thymidylate synthetase [Source:HGNC Symbol;Acc:HGNC:12441]	-1.32701
17067332	<i>ESCO2</i>	establishment of sister chromatid cohesion N-acetyltransferase 2 [Source:HGNC Symbol;Acc:HGNC:27230]	-1.31974
16799598	<i>CASC5</i>	cancer susceptibility candidate 5 [Source:HGNC Symbol;Acc:HGNC:24054]	-1.30174
17079293	<i>CCNE2</i>	cyclin E2 [Source:HGNC Symbol;Acc:HGNC:1590]	-1.2966
17012804	<i>MYB</i>	v-myb avian myeloblastosis viral oncogene homolog [Source:HGNC Symbol;Acc:HGNC:7545]	-1.27778
16894127	<i>CMPK2</i>	cytidine monophosphate (UMP-CMP) kinase 2, mitochondrial [Source:HGNC Symbol;Acc:HGNC:27015]	-1.27582
16976891	<i>RP11-44F21.5</i>	Novel transcript	-1.27541
16962022	<i>LAMP3</i>	lysosomal-associated membrane protein 3 [Source:HGNC Symbol;Acc:HGNC:14582]	-1.26724
16719515	<i>MKI67</i>	marker of proliferation Ki-67 [Source:HGNC Symbol;Acc:HGNC:7107]	-1.26063
16665083	---	---	-1.25446
16707196	<i>IFIT1</i>	interferon-induced protein with tetratricopeptide repeats 1 [Source:HGNC Symbol;Acc:HGNC:5407]	-1.25149
16832429	<i>TMEM97</i>	transmembrane protein 97 [Source:HGNC Symbol;Acc:HGNC:28106]	-1.24236
16799724	<i>DLL4</i>	delta-like 4 (Drosophila) [Source:HGNC Symbol;Acc:HGNC:2910]	-1.23867
16882975	<i>NCAPH</i>	non-SMC condensin I complex, subunit H [Source:HGNC Symbol;Acc:HGNC:1112]	-1.23766
16901755	<i>BUB1</i>	BUB1 mitotic checkpoint serine/threonine kinase [Source:HGNC Symbol;Acc:HGNC:1148]	-1.22838
17080595	<i>DSCC1</i>	DNA replication and sister chromatid cohesion 1 [Source:HGNC Symbol;Acc:HGNC:24453]	-1.21952
17073259	<i>LY6E</i>	lymphocyte antigen 6 complex, locus E [Source:HGNC Symbol;Acc:HGNC:6727]	-1.2134

16911212	<i>MCM8</i>	minichromosome maintenance complex component 8 [Source:HGNC Symbol;Acc:HGNC:16147]	-1.21168
16869588	<i>ASF1B</i>	anti-silencing function 1B histone chaperone [Source:HGNC Symbol;Acc:HGNC:20996]	-1.20891
17014358	<i>RPI-249F5.3</i>	Novel transcript	-1.20702
16900441	<i>DUSP2</i>	dual specificity phosphatase 2 [Source:HGNC Symbol;Acc:HGNC:3068]	-1.20217
16777278	<i>SKA3</i>	spindle and kinetochore associated complex subunit 3 [Source:HGNC Symbol;Acc:HGNC:20262]	-1.20129
16686796	<i>STIL</i>	SCL/TAL1 interrupting locus [Source:HGNC Symbol;Acc:HGNC:10879]	-1.19581
16679411	<i>EXO1</i>	exonuclease 1 [Source:HGNC Symbol;Acc:HGNC:3511]	-1.1886
16741501	<i>DHCR7</i>	7-dehydrocholesterol reductase [Source:HGNC Symbol;Acc:HGNC:2860]	-1.18506
16802838	<i>RP11-272D12.1</i>	Novel transcript	-1.18468
16852858	<i>SERPINB7</i>	serpin peptidase inhibitor, clade B (ovalbumin), member 7 [Source:HGNC Symbol;Acc:HGNC:13902]	-1.18131
16962632	<i>P3H2</i>	prolyl 3-hydroxylase 2 [Source:HGNC Symbol;Acc:HGNC:19317]	-1.17795
17016499	<i>HIST1H1B</i>	histone cluster 1, H1b [Source:HGNC Symbol;Acc:HGNC:4719]	-1.1738
16800355	<i>WDR76</i>	WD repeat domain 76 [Source:HGNC Symbol;Acc:HGNC:25773]	-1.15908
16687618	<i>DHCR24</i>	24-dehydrocholesterol reductase [Source:HGNC Symbol;Acc:HGNC:2859]	-1.15263
16799637	<i>RAD51</i>	RAD51 recombinase [Source:HGNC Symbol;Acc:HGNC:9817]	-1.15118
16804559	<i>FANCI</i>	Fanconi anemia, complementation group I [Source:HGNC Symbol;Acc:HGNC:25568]	-1.15065
16799793	<i>NUSAP1</i>	nucleolar and spindle associated protein 1 [Source:HGNC Symbol;Acc:HGNC:18538]	-1.1438
17080749	<i>ATAD2</i>	ATPase family, AAA domain containing 2 [Source:HGNC Symbol;Acc:HGNC:30123]	-1.11597
16903090	<i>MCM6</i>	minichromosome maintenance complex component 6 [Source:HGNC Symbol;Acc:HGNC:6949]	-1.11384
17067231	<i>PTK2B</i>	protein tyrosine kinase 2 beta [Source:HGNC Symbol;Acc:HGNC:9612]	-1.10854
16763926	---	---	-1.09536
17121990	<i>ZNF730</i>	zinc finger protein 730 [Source:HGNC Symbol;Acc:HGNC:32470]	-1.08445

16689400	<i>GBP5</i>	guanylate binding protein 5 [Source:HGNC Symbol;Acc:HGNC:19895]	-1.08386
17020019	<i>MCM3</i>	minichromosome maintenance complex component 3 [Source:HGNC Symbol;Acc:HGNC:6945]	-1.07626
16970563	<i>PLK4</i>	polo-like kinase 4 [Source:HGNC Symbol;Acc:HGNC:11397]	-1.07621
16743686	<i>MMP8</i>	matrix metalloproteinase 8 [Source:HGNC Symbol;Acc:HGNC:7175]	-1.06327
16968735	<i>HERC6</i>	HECT and RLD domain containing E3 ubiquitin protein ligase family member 6 [Source:HGNC Symbol;Acc:HGNC:26072]	-1.06251
17105401	<i>CENPI</i>	centromere protein I [Source:HGNC Symbol;Acc:HGNC:3968]	-1.05133
16725742	<i>FADS2</i>	Fatty Acid Desaturase 2[Source:HGNC Symbol;Acc:HGNC:3575]	-1.04559
16743721	<i>MMP1</i>	matrix metalloproteinase 1 [Source:HGNC Symbol;Acc:HGNC:7155]	-1.03982
17057946	<i>PSPH</i>	phosphoserine phosphatase [Source:HGNC Symbol;Acc:HGNC:9577]	-1.03575
16996813	<i>CD180</i>	CD180 molecule [Source:HGNC Symbol;Acc:HGNC:6726]	-1.03128
16736638	<i>E2F8</i>	E2F transcription factor 8 [Source:HGNC Symbol;Acc:HGNC:24727]	-1.02866
17014309	<i>ACAT2</i>	acetyl-CoA acetyltransferase 2 [Source:HGNC Symbol;Acc:HGNC:94]	-1.02657
16768923	<i>SLC9A7P1</i>	solute carrier family 9, subfamily A (NHE7, cation proton antiporter 7), member 7 pseudogene 1 [Source:HGNC Symbol;Acc:HGNC:32679]	-1.02643
17068782	<i>MCM4</i>	minichromosome maintenance complex component 4 [Source:HGNC Symbol;Acc:HGNC:6947]	-1.00873
16897026	<i>ZFP36L2</i>	ZFP36 ring finger protein-like 2 [Source:HGNC Symbol;Acc:HGNC:1108]	-0.99468
16850107	<i>FASN</i>	fatty acid synthase [Source:HGNC Symbol;Acc:HGNC:3594]	-0.9922
16913957	<i>MYBL2</i>	v-myb avian myeloblastosis viral oncogene homolog-like 2 [Source:HGNC Symbol;Acc:HGNC:7548]	-0.99002
16916958	<i>PCNA</i>	proliferating cell nuclear antigen [Source:HGNC Symbol;Acc:HGNC:8729]	-0.98979
16995890	<i>HMGCS1</i>	3-hydroxy-3-methylglutaryl-CoA synthase 1 (soluble) [Source:HGNC Symbol;Acc:HGNC:5007]	-0.98191
16733104	<i>CHEK1</i>	checkpoint kinase 1 [Source:HGNC Symbol;Acc:HGNC:1925]	-0.97452
16900090	---	---	-0.95088
16723662	<i>FJX1</i>	four jointed box 1 [Source:HGNC Symbol;Acc:HGNC:17166]	-0.94352

16957951	<i>POLQ</i>	polymerase (DNA directed), theta [Source:HGNC Symbol;Acc:HGNC:9186]	-0.94286
16671738	<i>FDPS</i>	farnesyl diphosphate synthase [Source:HGNC Symbol;Acc:HGNC:3631]	-0.93997
16758052	<i>P2RX7</i>	purinergic receptor P2X, ligand gated ion channel, 7 [Source:HGNC Symbol;Acc:HGNC:8537]	-0.9363
16821174	<i>VATIL</i>	vesicle amine transport 1-like [Source:HGNC Symbol;Acc:HGNC:29315]	-0.928
17060412	<i>MCM7</i>	minichromosome maintenance complex component 7 [Source:HGNC Symbol;Acc:HGNC:6950]	-0.92716
16700699	<i>RP11-443B7.3</i>	uncharacterized	-0.92035
16978568	<i>CENPE</i>	centromere protein E, 312kDa [Source:HGNC Symbol;Acc:HGNC:1856]	-0.92017
16996722	<i>CENPK</i>	centromere protein K [Source:HGNC Symbol;Acc:HGNC:29479]	-0.91942
16971737	<i>GUCY1B3</i>	guanylate cyclase 1, soluble, beta 3 [Source:HGNC Symbol;Acc:HGNC:4687]	-0.90563
16792615	<i>C14orf182</i>	Chromosome 14 Open Reading Frame 182 [Source:HGNC Symbol;Acc:HGNC:27503]	-0.90269
16988703	<i>LMNB1</i>	lamin B1 [Source:HGNC Symbol;Acc:HGNC:6637]	-0.90146
16729557	<i>DDIAS</i>	DNA damage-induced apoptosis suppressor [Source:HGNC Symbol;Acc:HGNC:26351]	-0.88615
16760889	<i>C3AR1</i>	complement component 3a receptor 1 [Source:HGNC Symbol;Acc:HGNC:1319]	-0.87944
16721835	<i>WEE1</i>	WEE1 G2 checkpoint kinase [Source:HGNC Symbol;Acc:HGNC:12761]	-0.84931
16787814	<i>IFI27</i>	interferon, alpha-inducible protein 27 [Source:HGNC Symbol;Acc:HGNC:5397]	-0.8247
16923549	<i>LOC102725378</i>	uncharacterized	-0.82168
16953279	<i>CDC25A</i>	cell division cycle 25A [Source:HGNC Symbol;Acc:HGNC:1725]	-0.81485
16917183	<i>JAG1</i>	jagged 1 [Source:HGNC Symbol;Acc:HGNC:6188]	-0.80423
17030627	<i>LST1</i>	leukocyte specific transcript 1 [Source:HGNC Symbol;Acc:HGNC:14189]	-0.7952
17035425	<i>LST1</i>	leukocyte specific transcript 1 [Source:HGNC Symbol;Acc:HGNC:14189]	-0.7952
17027801	<i>LST1</i>	leukocyte specific transcript 1 [Source:HGNC Symbol;Acc:HGNC:14189]	-0.78947
17033344	<i>LST1</i>	leukocyte specific transcript 1 [Source:HGNC Symbol;Acc:HGNC:14189]	-0.78947
16675794	<i>NAVI</i>	neuron navigator 1 [Source:HGNC Symbol;Acc:HGNC:15989]	-0.76481

16858386	<i>LDLR</i>	low density lipoprotein receptor [Source:HGNC Symbol;Acc:HGNC:6547]	-0.75917
16794966	<i>C14orf1</i>	chromosome 14 open reading frame 1 [Source:HGNC Symbol;Acc:HGNC:1187]	-0.75121
16739132	<i>FADS1</i>	fatty acid desaturase 1 [Source:HGNC Symbol;Acc:HGNC:3574]	-0.73089
17124612	<i>AC003092.1</i>	putative novel transcript	-0.7298
16662648	<i>CDCA8</i>	cell division cycle associated 8 [Source:HGNC Symbol;Acc:HGNC:14629]	-0.71305
17120696	<i>RP11-705C15.2</i>	uncharacterized	-0.70986

THP-1 macrophages were incubated with LPL hydrolysis products or non-hydrolysis products for 18 h. RNA from the treated cells were subjected to human gene 2.0ST array (n=3). Using R studio, a top list of up-regulated genes in LPL hydrolysis product treated macrophages were obtained at FDR ≤ 0.03 . Log₂FC represents 2-fold change of modulated transcript in macrophages treated with LPL hydrolysis products compared to control.

Figure S4: Enrichment analysis on biological processes modulated by LPL hydrolysis products

GO biological process	GO term ID	FDR	Genes in list	Gene in genome
<u>Cell cycle</u>				
DNA replication*	GO:0006260	7×10^{-7}	16	222
DNA-dependent DNA replication	GO:0006261	7×10^{-5}	10	102
DNA strand elongation involved in DNA replication	GO:0006271	6×10^{-4}	6	34
DNA strand elongation	GO:0022616	9×10^{-4}	6	37
MCM complex	GO:0042555	7×10^{-5}	5	11
chromosome segregation	GO:0007059	3×10^{-4}	10	128
sister chromatid segregation	GO:0000819	0.006	6	54
mitotic sister chromatid segregation	GO:0000070	0.024	5	49
chromosome condensation*	GO:0030261	0.012	4	19
mitotic chromosome condensation	GO:0007076	0.047	3	12
condensed chromosome	GO:0000793	1×10^{-4}	9	86
chromosome, centromeric region	GO:0000775	0.012	7	98
condensed chromosome kinetochore	GO:0000777	0.017	4	22
condensed chromosome outer kinetochore	GO:0000940	0.036	3	11
DNA packaging	GO:0006323	0.008	7	88
DNA conformation change	GO:0071103	0.012	8	135
nuclear division	GO:0000280	0.008	11	257
organelle fission	GO:0048285	0.014	11	282
G2 DNA damage checkpoint	GO:0031572	0.033	4	28
protein-DNA complex	GO:0032993	0.001	10	158
G1/S transition of mitotic cell cycle	GO:0000082	0.001	11	201
<u>Antiviral response</u>				

cellular response to type I interferon	GO:0071357	4×10^{-4}	8	74
response to type I interferon*	GO:0034340	4×10^{-4}	8	75
type I interferon signaling pathway	GO:0060337	4×10^{-4}	8	74
response to virus	GO:0009615	0.024	9	205
<u>Stress response</u>				
response to unfolded protein*	GO:0006986	0.003	8	106
cellular response to unfolded protein	GO:0034620	0.024	6	79
response to topologically incorrect protein	GO:0035966	0.005	8	113
cellular response to topologically incorrect protein	GO:0035967	0.03	6	84
activation of signaling protein activity involved in unfolded protein response	GO:0006987	0.012	6	65
response to endoplasmic reticulum stress	GO:0034976	0.023	7	113
endoplasmic reticulum unfolded protein response	GO:0030968	0.024	6	78
ER-nucleus signaling pathway	GO:0006984	0.033	6	86
<u>Ion homeostasis</u>				
cellular metal ion homeostasis*	GO:0006875	0.01	11	264
cellular cation homeostasis	GO:0030003	0.015	11	284
metal ion homeostasis	GO:0055065	0.016	11	288
cellular ion homeostasis	GO:0006873	0.017	11	292
<u>Lipid metabolic process</u>				
sterol metabolic process*	GO:0016125	0.024	6	80
<u>Hydrolase activity</u>				
regulation of nuclease activity*	GO:0032069	7×10^{-5}	9	73

positive regulation of nuclease activity	GO:0032075	0.002	7	67
<u>Viral life cycle</u>				
regulation of viral genome replication	GO:0045069	0.028	5	51

Microarray data analysis showed that several genes were differentially regulated by lipoprotein hydrolysis products liberated by LPL. To understand the functions of modulated genes, enrichment analysis on biological processes was performed using the GeneMANIA database (158). My data revealed that several biological processes were significantly enriched (with FDR<0.05) following LPL hydrolysis product treatment. Each biological process term is derived from a root process (parent term) that possesses sub-categories (child terms), in addition to their relationship with other GO terms (co-occurring terms). The relationship between each and every biological process that was significantly over-represented in the list were carefully considered and grouped all child terms and co-occurring terms under their parent term. The underlined processes are parent terms. *, represent child terms that were selected for gene validation